Distribution Agreement

In presenting this thesis or dissertation as a partial fulfillment of the requirements for an advanced degree from Emory University, I hereby grant to Emory University and its agents the non-exclusive license to archive, make accessible, and display my thesis or dissertation in whole or in part in all forms of media, now or hereafter known, including display on the world wide web. I understand that I may select some access restrictions as part of the online submission of this thesis or dissertation. I retain all ownership rights to the copyright of the thesis or dissertation. I also retain the right to use in future works (such as articles or books) all or part of this thesis or dissertation.

Signature:

_____ _____

Jeffrey Meisner Date

A Junction between Differentiating Bacterial Cells

By

Jeffrey Meisner
Doctor of Philosophy

Graduate Division of Biological and Biomedical Sciences
Microbiology and Molecular Genetics

Charles Moran Jr., Ph.D.
Advisor

Gordon Churchward, Ph.D.
Committee Member

Philip Rather, Ph.D.
Committee Member

William Shafer, Ph.D.
Committee Member

June Scott, Ph.D.
Committee Member

Accepted:

Lisa A. Tedesco, Ph.D.
Dean of the James T. Laney School of Graduate Studies

Date

A Junction between Differentiating Bacterial Cells

By

Jeffrey Meisner
B.S., University of California, Santa Barbara, 2001

Advisor: Charles Moran, Jr., Ph.D.

An abstract of
A dissertation submitted to the Faculty of the
James T. Laney School of Graduate Studies of Emory University
in partial fulfillment of the requirements for the degree of
Doctor of Philosophy

In

Graduate Division of Biological and Biomedical Sciences
Microbiology and Molecular Genetics

2011

Abstract

A Junction between Differentiating Bacterial Cells
By Jeffrey Meisner

When nutrient availability is insufficient to sustain growth, *Bacillus subtilis* can form a metabolically dormant and environmentally resistant cell type called an endospore. Endospore formation involves the differentiation of two adjacent daughter cells, the mother cell and forespore. The differentiation of these two cells involves an ordered series of morphological changes governed by parallel and interlocked transcriptional programs. The transition from the early to late transcription programs is thought to be controlled by a junction composed of the eight SpoIIIA proteins in the mother cell and SpoIIQ in the forespore. Based on remote homology between SpoIIIAH and the YscJ family of ring-forming proteins, we hypothesized that SpoIIIAH and SpoIIQ form a channel through which the mother cell and forespore communicate. In support of this hypothesis, we demonstrated that the extracellular domains of SpoIIIAH and SpoIIQ are accessible to modification by an enzyme produced in the forespore. To begin to understand molecular basis for the assembly of the putative channel, we examined the interaction of the purified extracellular domains of these proteins. We demonstrated that the putative ring-forming YscJ domain of SpoIIIAH recognizes the degenerate LytM domain of SpoIIQ. By analogy with YscJ proteins, we hypothesized that putative SpoIIIAH channel serves as a structural scaffold for the assembly of a specialized export apparatus consisting of the other seven SpoIIIA proteins. Consistent with this hypothesis, we showed that SpoIIIAA is homologous to the superfamily of

ATP hydrolases that provide the energy for various types of protein secretion systems. We also analyzed the predicted membrane topology of SpoIIIAB, SpoIIIAC, SpoIIIAD, and SpoIIIAE, and identified important residues in each. Together, these data support a new model for understanding the mechanisms that control the differentiation of the mother cell and forespore during endospore formation.

A Junction between Differentiating Bacterial Cells

By

Jeffrey Meisner
B.S., University of California, Santa Barbara, 2001

Advisor: Charles Moran, Jr., Ph.D.

A dissertation submitted to the Faculty of the
James T. Laney School of Graduate Studies of Emory University
in partial fulfillment of the requirements for the degree of
Doctor of Philosophy

In

Graduate Division of Biological and Biomedical Sciences
Microbiology and Molecular Genetics

2011

ACKNOWLEDGEMENTS

I would like to thank Charlie Moran for providing invaluable guidance and allowing me the liberty to express my own intellectual creativity. I also appreciate the helpful comments and suggestions from the members of my dissertation committee. In addition, I am grateful for stimulating interactions with Christine Dunham and Graeme Conn. Finally, I would like to thank Kyle Frantz for assistance in improving my writing.

TABLE OF CONTENTS

LIST OF FIGURES AND TABLES

Chapter 1

Chapter 2

Chapter 3

Chapter 4

Chapter 5

CHAPTER 1. General Introduction

Bacillus subtilis, a ubiquitous soil-dwelling Gram-positive bacterium, is among the best understood organisms. Its genetic amenability and the development of cytological techniques provide powerful tools for the investigation of numerous bacterial behaviors. In particular, its ability to display a variety of adaptive responses, engage in social interactions (cell-cell communication), and differentiate into distinct cell types makes *B. subtilis* an important model organism. Together, molecular and cellular biology provide insight into how this model bacterium processes information about itself and its environment, and how it chooses the appropriate behavioral response. Generally, these choices are governed by regulatory networks that dictate which genes need to be transcribed in order for the cell to exhibit a specific behavior.

To ensure growth and survival, bacteria respond and adapt to diverse environmental conditions such as changes in temperature, pH, osmolarity, and nutrient availability. When nutrient availability is inadequate to sustain growth (i.e. during stationary phase), *B. subtilis* employs responses such as production of extracellular degradative enzymes and antibiotics to scavenge and compete for scarce nutrients, chemotaxis and motility to seek out new nutrient sources, genetic competence to acquire new genes, biofilm formation to construct multicellular communities, and sporulation to form metabolically dormant, environmentally resistant cells. Sporulation is likely the response of last resort, undertaken only when other attempts to grow have been exhausted.

When nutrients are abundant, a growing (vegetative) cell replicates its chromosome, doubles in length, and divides at midcell to produce two identical daughter cells. Once the cell decides to initiate sporulation, it undergoes a series of morphological changes that distinguish it from a vegetative cell (Figure 1) (22, 28, 50, 54). First, the replicated chromosomes are remodeled and segregated, one to each of the two cell poles. Then, the cell divides near one of the cell poles, producing two dissimilar-sized daughter cells. Although the two cells initially lie side-by side, the larger mother cell is wrapped around the smaller forespore, in a process termed forespore engulfment, until it is released into the mother cell cytoplasm. After engulfment, the forespore is endowed with a second membrane layer, an outer membrane derived from the mother cell. Next, coat proteins are deposited on the outer forespore membrane and specialized peptidoglycan called spore cortex is synthesized in the space between the inner and outer membranes. The forespore cytoplasm is then dehydrated and its chromosome is condensed. Finally, the mother cell lyses and the mature endospore is released. The spore is metabolically dormant and resistant to environmental damage, but retains the ability to sense nutrient availability, germinate, and resume vegetative growth.

Because sporulation is an energy-intensive and time-consuming process (about 8 hours at 37°C under laboratory conditions), the cell must make the decision to initiate this response based on an understanding of environmental conditions and its physiological status (57). Cells that inappropriately initiate sporulation, under conditions that support growth, will be at a competitive disadvantage compared to cells that continue to grow. Conversely, cells that fail to initiate sporulation will be unable to

survive when nutrients are exhausted. *B. subtilis* uses a complex regulatory network to integrate environmental and cellular information, and to determine whether sporulation should be initiated.

The decision to initiate sporulation is controlled by a phosphorelay that culminates in the activation of the master transcriptional regulator Spo0A (Figure 2) (11, 48). Five different kinases (KinA, KinB, KinC, KinD, and KinE) sense environmental changes and respond by autophosphorylation of a histidine residue (3, 31, 63). The phosphoryl group is transferred from the kinases to an aspartate residue of Spo0F, then to a histidine of phosphotransferase Spo0B, and finally to an aspartate of Spo0A. Phosphorylated Spo0A binds to specific DNA sequences and represses or activates transcription of its target genes. The phosphorelay is modulated by phosphatases (Rap and Spo0E) that remove the phosphoryl group from Spo0F or Spo0A, as well as proteins that inhibit the sensor kinases. The activity of the Rap phosphatases is inhibited by peptides (Phr pentapeptides) that are first exported and subsequently reimported and serve as cell density signals (34, 47). When these peptides are present in sufficiently high amounts, i.e. cell density is sufficiently high, Rap phosphatases are inhibited and Spo0A activity is increased. When defects in chromosome replication are encountered, Sda inhibits KinA activity, thereby decreasing Spo0A activity (12, 52). The phosphorelay and its modulators control Spo0A activity, allowing the cell to process numerous environmental and cellular signal inputs and integrate them into a single regulatory output, the initiation of sporulation.

Once activated by phosphorylation, Spo0A directly or indirectly activates or represses transcription of many genes (44). These genes are distinguished by the threshold level of Spo0A activity necessary for their regulation; in other words, some genes are regulated by a low-level of Spo0A activity while others are regulated by a high-level of activity (25). A low-level of Spo0A activity serves two basic functions for when available nutrients can no longer sustain growth: it opens a window of opportunity to engage in the adaptive responses described above and increases the capacity of the phosphorelay to promote a high-level of Spo0A activity. In two different ways a low-level of Spo0A activity inhibits AbrB, a transcriptional repressor of many adaptive response genes: first, it represses the *abrB* gene and second, it activates *abbA* which encodes an inhibitor of the AbrB protein (5, 60, 61). Therefore, low-level Spo0A activity removes the transcriptional block applied to adaptive response genes during vegetative growth, when they are not needed for survival (62). Further, a low-level of Spo0A activity directly activates several adaptive response genes, notably those involved in scavenging and competing for scarce nutrients. A low-level of Spo0A activity also directly and indirectly activates genes that encode components of the phosphorelay, providing positive feedback on Spo0A activity. AbrB represses the *sigH* gene which encodes an RNA polymerase sigma factor (σ^H) necessary for the initiation of sporulation (65). Thus, low-level Spo0A activity indirectly activates *sigH*. σ^H directs transcription of several genes that function at the transition from vegetative (exponential) growth to stationary phase, including the *phr* genes which encode the Phr peptides (9). Acting together, Spo0A-P and σ^H activate transcription of *kinA*, *spo0F*, and

spo0A (51). This positive feedback regulation increases the capacity of the phosphorelay to activate Spo0A. Additionally, low-level Spo0A activity activates *sinI* which encodes an inhibitor of the transcriptional regulator SinR (4). Because SinR represses the σ^H-dependent *spo0A* promoter, SinI indirectly activates *spo0A* and contributes to the positive feedback on Spo0A activity (39). SinR also controls genes involved in motility, biofilm formation, and genetic competence (26, 27, 33, 55). Therefore, the intersection of Spo0A and SinR activities may constitute an important decision-making process, whereby the cell chooses between mutually exclusive responses. Low-level Spo0A activity activates *rapA* (Spo0F-P phosphatase) and indirectly activates (AbrB represses) *spo0E* (Spo0A-P phosphatase), however, exerting negative feedback on Spo0A activity. This negative feedback may slow the progression from low- to high-level Spo0A activity to allow the cell to attempt alternative adaptive responses and postpone the initiation of sporulation.

Once a high-level of Spo0A activity is reached, the cell initiates sporulation because low-level Spo0A responses were insufficient to sustain growth. A high-level of Spo0A activity activates transcription of genes involved in the early stages of sporulation, such as *racA* and *spoIIE* (25). RacA helps remodel and segregate the replicated chromosomes to guarantee that one of them is captured in the forespore following asymmetric cell division (7, 66). SpoIIE aids in the repositioning of the cell division apparatus necessary for asymmetric cell division (6). Furthermore, high-level Spo0A activity activates transcription of *spoIIA* and *spoIIG* which encode the alternative RNA polymerase sigma factors σ^F and σ^E, respectively. After asymmetric cell division,

these transcriptional regulators govern the differentiation of the forespore and mother cell, as will be discussed later. High-level Spo0A activity also represses *rapA* which encodes the RapA phosphatase, creating positive feedback on Spo0A activity. This positive feedback may ensure that the level of Spo0A activity remains high and sporulation is initiated.

At the onset of sporulation, asymmetric cell division produces two dissimilar sized daughter cells which differentiate into distinct cell types, the forespore and mother cell. Underlying the differentiation of these two cell types are two parallel and compartmentalized transcriptional programs, one in the forespore and the other in the mother cell (21, 49, 59, 64). Both programs are divided into two temporal classes (early and late), each of which is further subdivided. Each of the four classes (early forespore, early mother cell, late forespore and late mother cell) is controlled by a specific RNA polymerase sigma factor. The activities of these sigma factors are organized into a hierarchical cascade, whereby the activity of one sigma factor gives rise to the activity of the next (Figure 3) (37, 58). The transcriptional programs governing differentiation of the two cell types are not free-running. Instead, they are interlocked by a series of cell-cell signaling pathways that keep the differentiation of the two cells in register (38).

After the completion of asymmetric cell division, σ^F is activated in the forespore and directs the transcription of early forespore genes. One of these genes, *spoIIR*, encodes a secreted protein that signals the activation of σ^E in the mother cell (29, 36). σ^E directs the transcription of early mother cell genes, including those that mediate forespore engulfment (*spoIIM*, *spoIIP*, and *spoIID*) (1, 45). σ^E also directs the transcription

of the eight genes of the *spoIIIA* locus (*spoIIIAA*, *spoIIIAB*, *spoIIIAC*, *spoIIIAD*, *spoIIIAF*, *spoIIAG*, and *spoIIIAH*), each of which is necessary to signal the activation of σ^G in the forespore (30). σ^G directs the transcription of late forespore genes, such as those involved in dehydration of the cytoplasm and condensation of the chromosome. Additionally, σ^G directs the transcription of *spoIVB* which encodes a secreted protease that signals the activation of σ^K in the mother cell (15, 17). σ^K directs the transcription of late mother cell genes, including those responsible for the synthesis of the spore coat and cortex that endows the endospore with its resistant properties, as well as the germination receptors that allow the spore to resume vegetative growth when nutrients are available once again. Therefore, differentiation of the forespore and mother cell is organized into a dependent series of events, i.e. late events occur only after the successful completion of early events. One or more genes associated with one event are responsible for activation of those genes associated with the next event.

Each pair of temporal classes is responsible for specific morphological changes. The early forespore and mother cell transcriptional classes control forespore engulfment, while the late forespore and mother cell transcriptional classes govern development of the spore coat, cortex and core, collectively referred to here as forespore maturation. To ensure that one morphological change finishes before the next one begins, the early and late transcriptional classes are further regulated by morphological signals. For example, σ^F activity appears in the forespore only after asymmetric cell division is completed (40). Prior to asymmetric cell division, σ^F is held inactive by its inhibitor SpoIIAB (20). σ^F activation is controlled by a partner-switching mechanism, whereby SpoIIAA interacts

with SpoIIAB, displacing and activating σ^F (2, 19). SpoIIAB is a serine kinase that phosphorylates, and thereby inactivates, SpoIIAA (43). Prior to asymmetric cell division, SpoIIAA is phosphorylated and unable to free σ^F from inhibition by SpoIIAB. As mentioned above, SpoIIE helps redeploy the cell division machinery for asymmetric cell division. In addition to being an integral membrane protein that localizes to the asymmetric cell division septum, it is also a phosphatase which removes the phosphoryl group from SpoIIAA (18). After asymmetric cell division, SpoIIE is sufficiently concentrated in the forespore to offset the kinase activity of SpoIIAB (14). Thus, dephosphorylated SpoIIAA can productively interact with SpoIIAB and activate σ^F. Consequently, early forespore transcription is coupled to the successful completion of asymmetric cell division. Because early forespore transcription signals the activation of σ^E, early mother cell transcription is indirectly coupled to asymmetric cell division. The ultimate effect of this type of morphological regulation is to control the transition between asymmetric cell division and forespore engulfment, ensuring that engulfment does not begin until cell division gives rise to the forespore and mother cell.

The late transcriptional classes, controlled by σ^G in the forespore and σ^K in the mother cell, are coupled to the completion of forespore engulfment. As is the case for the early transcriptional classes, the morphological signal activates late forespore transcription, which in turn signals the activation of late mother cell transcription. Together, the late transcriptional classes govern forespore maturation. Thus, the morphological signal that controls the transition from forespore engulfment to forespore maturation is processed at the level of σ^G activation. Compared to our understanding of

the regulation of σ^F activity, however, we know very little about the regulation of σ^G activity.

Unlike σ^F activity, σ^G activity is regulated by a morphological signal which is transmitted from the mother cell to the forespore. Mutations that block the activation of σ^G fall into two categories; those that prevent forespore engulfment and block σ^G activation (*spoIIB*, *spoIIM*, *spoIIP*, and *spoIID*), and those that allow engulfment to be completed but do not permit σ^G activation (*spoIIIA*, *spoIIQ*, and *spoIIIJ*) (24, 32, 41, 46). The former prevent the morphological signal due to the completion of engulfment, while the latter disrupt the transmission of the signal from the mother cell to the forespore. As stated earlier, the *spoIIIA* genes are transcribed early in the mother cell under the control of σ^E and, thus, contribute to a cell-cell signaling pathway. The eight-gene *spoIIIA* locus encodes a cytoplasmic protein (SpoIIIAA) and seven predicted integral membrane proteins (SpoIIIAB, SpoIIIAC, SpoIIIAD, SpoIIIAE, SpoIIIAF, SpoIIIAG, and SpoIIIAH). *spoIIQ* is transcribed early in the forespore under the control of σ^F (35). It encodes an integral membrane protein that interacts with SpoIIIAH and is thought to complete the mother cell-to-forespore signaling pathway. Finally, *spoIIIJ* is transcribed during vegetative growth and encodes an integral membrane protein chaperone which is thought to facilitate the proper membrane insertion of SpoIIIAE (13, 23, 56). Presumably the proteins encoded by *spoIIIA* and *spoIIQ* monitor forespore engulfment, and upon its completion, transmit a cell-cell signal that triggers the activation of σ^G. The mechanisms by which these proteins accomplish their functions are

unknown. This signaling pathway controls the late transcriptional classes and, ultimately, the transition from forespore engulfment to forespore maturation.

What little is known about the proteins encoded by *spoIIIA* and *spoIIQ* derives from cytological analyses of their subcellular localization. SpoIIQ is inserted into the forespore membrane at the cell division septum, tracks the adjacent engulfing mother cell membrane around the forespore, and then forms discrete foci around the forespore (53). In mutants defective in engulfment (*spoIIM*, *spoIID*, and *spoIIP* mutants), SpoIIQ remains at the division septum. In a mutant defective in mother cell gene expression (*sigE* mutant), SpoIIQ is uniformly distributed in the forespore membrane. Thus, a protein or proteins produced in the mother cell are necessary for the dynamic localization of SpoIIQ.

SpoIIIAH also localizes to the cell division septum and tracks the engulfing mother cell membrane around the forespore. In a *spoIIQ* mutant, SpoIIIAH is uniformly distributed in the mother cell membrane (8, 16). SpoIIIAH localization is defective in engulfment mutants. In partially defective engulfment mutants that result in bulging of the forespore into the mother cell (*spoIIP* and *spoIID* mutants), SpoIIIAH localizes to the bulges. In a completely defective mutant (*spoIIP spoIID* double mutant), SpoIIIAH is uniformly distributed. These data were interpreted to indicate that the SpoIIIAH-SpoIIQ complex is inhibited by septal peptidoglycan. Once it is removed by hydrolysis (catalyzed by SpoIIP and SpoIID), SpoIIIAH and SpoIIQ interact across the intermembrane space between the mother cell and forespore. When septal peptidoglyan is removed by lysozyme in a *spoIIP spoIID* double mutant, the SpoIIIAH-SpoIIQ complex

functions as a thermal ratchet that drives forespore engulfment (10). Peptidoglycan synthesis occurs in the intermembrane during forespore engulfment. In fact this synthesis is proposed to contribute to the mechanical force that drives engulfment (42). Compounds that block peptidoglycan precursor synthesis or polymerization prevent engulfment in a *spoIIQ* mutant. In a *spoIIIAH* mutant, however, SpoIIQ is retained at the sporulation septum (8). Thus, the localization of SpoIIQ and SpoIIIAH is not completely reciprocal. An additional mother cell protein is necessary for proper SpoIIQ localization.

The work presented here describes several important advances in our understanding of how the late transcriptional classes are controlled during sporulation. Based on a bioinformatics observation of remote homology between SpoIIIAH and ring-forming domains of protein secretion channels, we provide evidence supporting a model whereby SpoIIIAH and SpoIIQ form a channel connecting the mother cell and forespore. Then, we determine the biochemical parameters that define the SpoIIIAH-SpoIIQ complex. We show that the complex is formed by the putative ring-forming domain of SpoIIIAH and the degenerate peptidoglycan hydrolase domain of SpoIIQ. Next, we present bioinformatics and genetic analyses arguing that the cytoplasmic protein encoded by the first *spoIIIA* gene, SpoIIIAA, is a secretion superfamily ATP hydrolase. In conjunction with the SpoIIIAH-SpoIIQ channel, this ATPase may provide the energy necessary for cell-cell signal transmission. Finally, we report extensive site-directed mutagenesis of *spoIIAB*, *spoIIAC*, *spoIIIAD*, and *spoIIIAE*. These mutations identify important residues of the encoded proteins and may provide a basis for functional characterization. In conclusion, we discuss these findings in the context of a

cell-cell junction that controls an important morphological transition during sporulation, the transition between forespore engulfment and forespore maturation.

FIGURES

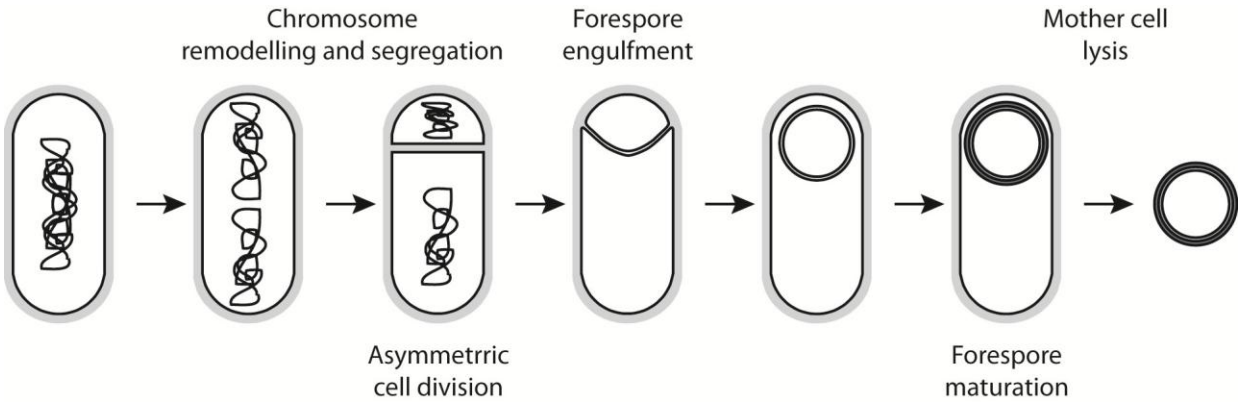

Figure 1. Morphological changes during sporulation. First, the replicated chromosomes are remodeled and segregated to the each of the cells poles. Then, the cell divides near one of the poles, giving to two dissimilar-sized cells. Although the cells initially lie side-by-side, the larger mother cell wraps itself around the smaller forespore in a process called forespore engulfment. When engulfment is complete, the forespore is released into the mother cell cytoplasm bearing an outer membrane derived from the mother cell. Next, coat proteins are deposited in the surface of this outer, specialized peptidoglycan is synthesized in the space between the outer and inner membranes, and the forespore cytoplasm is dehydrated and its chromosome is condensed. Collectively, these processes are called forespore maturation. Finally, the mother cell lyses and the mature spore is released.

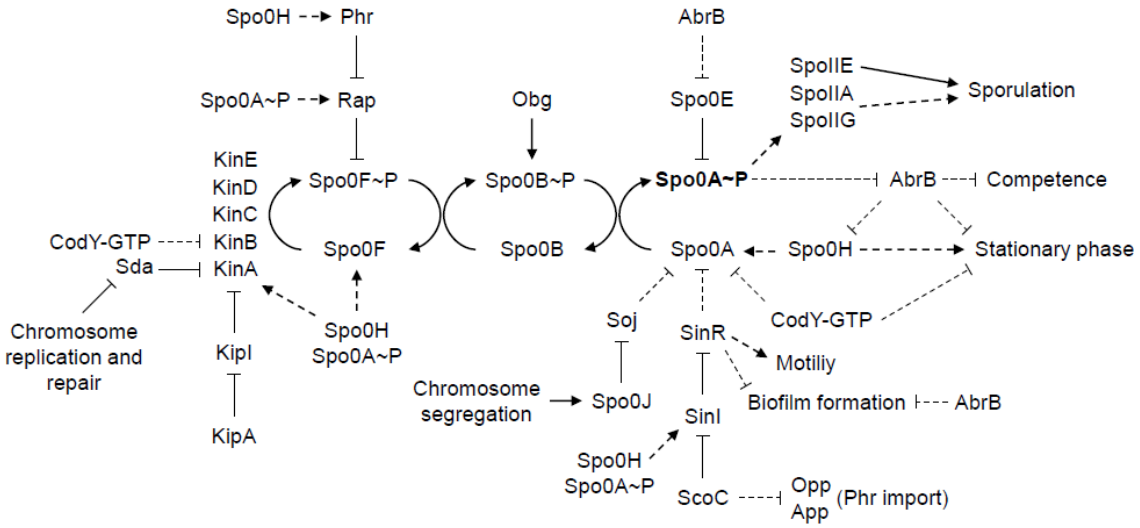

Figure 2. Regulatory network controlling the decision to initiate sporulation. Transcriptional regulation is indicated by dotted lines and post-translational regulation is indicated by solid lines. Lines with arrowheads represent positive regulation and lines with blunt ends represent negative regulation. Phosphorylated Spo0A (Spo0A-P), the master transcriptional regulator of sporulation, is shown in bold letters.

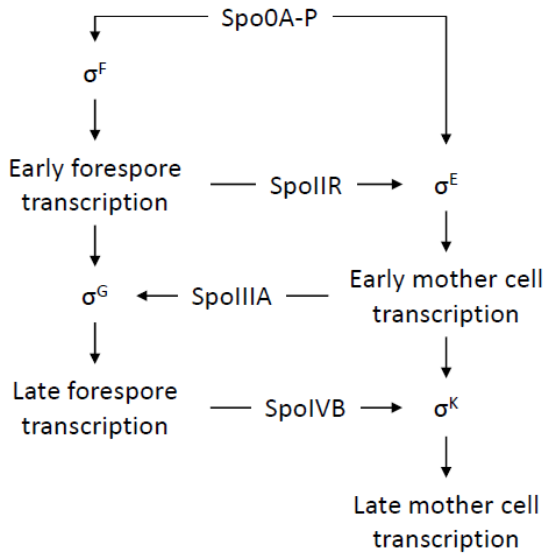

Figure 3. Parallel and interlocked transcriptional programs governing the differentiation of the forespore and mother cell. Phosphorylated Spo0A activates transcription of the genes that encode σ^F and σ^E. σ^F directs early transcription in the forespore, including the genes that encode SpoIIR and σ^G. SpoIIR is secreted from the forespore and triggers σ^E activity in the mother cell. σ^E directs early mother cell transcription, including the genes that encode the eight SpoIIIA proteins. The SpoIIIA proteins activate σ^G in the forespore. σ^G directs late forespore transcription, including the gene that encodes SpoIVB. SpoIVB is secreted from the forespore and triggers the activation of σ^K in the mother cell. σ^K directs late mother cell transcription.

REFERENCES

1. **Abanes-De Mello, A., Y. L. Sun, S. Aung, and K. Pogliano.** 2002. A cytoskeleton-like role for the bacterial cell wall during engulfment of the Bacillus subtilis forespore. Genes Dev **16:**3253-3264.

2. **Alper, S., L. Duncan, and R. Losick.** 1994. An adenosine nucleotide switch controlling the activity of a cell type-specific transcription factor in B. subtilis. Cell **77:**195-205.

3. **Antoniewski, C., B. Savelli, and P. Stragier.** 1990. The spoIIJ gene, which regulates early developmental steps in Bacillus subtilis, belongs to a class of environmentally responsive genes. J Bacteriol **172:**86-93.

4. **Bai, U., I. Mandic-Mulec, and I. Smith.** 1993. SinI modulates the activity of SinR, a developmental switch protein of Bacillus subtilis, by protein-protein interaction. Genes Dev **7:**139-148.

5. **Banse, A. V., A. Chastanet, L. Rahn-Lee, E. C. Hobbs, and R. Losick.** 2008. Parallel pathways of repression and antirepression governing the transition to stationary phase in Bacillus subtilis. Proc Natl Acad Sci U S A **105:**15547-15552.

6. **Ben-Yehuda, S., and R. Losick.** 2002. Asymmetric cell division in B. subtilis involves a spiral-like intermediate of the cytokinetic protein FtsZ. Cell **109:**257-266.

7. **Ben-Yehuda, S., D. Z. Rudner, and R. Losick.** 2003. RacA, a bacterial protein that anchors chromosomes to the cell poles. Science **299:**532-536.

8. **Blaylock, B., X. Jiang, A. Rubio, C. P. Moran, Jr., and K. Pogliano.** 2004. Zipper-like interaction between proteins in adjacent daughter cells mediates protein localization. Genes Dev **18:**2916-2928.

9. **Britton, R. A., P. Eichenberger, J. E. Gonzalez-Pastor, P. Fawcett, R. Monson, R. Losick, and A. D. Grossman.** 2002. Genome-wide analysis of the stationary-phase sigma factor (sigma-H) regulon of Bacillus subtilis. J Bacteriol **184:**4881-4890.

10. **Broder, D. H., and K. Pogliano.** 2006. Forespore engulfment mediated by a ratchet-like mechanism. Cell **126:**917-928.

11. **Burbulys, D., K. A. Trach, and J. A. Hoch.** 1991. Initiation of sporulation in B. subtilis is controlled by a multicomponent phosphorelay. Cell **64:**545-552.

12. **Burkholder, W. F., I. Kurtser, and A. D. Grossman.** 2001. Replication initiation proteins regulate a developmental checkpoint in Bacillus subtilis. Cell **104:**269-279.

13. **Camp, A. H., and R. Losick.** 2008. A novel pathway of intercellular signalling in Bacillus subtilis involves a protein with similarity to a component of type III secretion channels. Mol Microbiol **69:**402-417.

14. **Carniol, K., P. Eichenberger, and R. Losick.** 2004. A threshold mechanism governing activation of the developmental regulatory protein sigma F in Bacillus subtilis. J Biol Chem **279:**14860-14870.

15. **Cutting, S., A. Driks, R. Schmidt, B. Kunkel, and R. Losick.** 1991. Forespore-specific transcription of a gene in the signal transduction pathway that governs Pro-sigma K processing in Bacillus subtilis. Genes Dev **5:**456-466.

16. **Doan, T., K. A. Marquis, and D. Z. Rudner.** 2005. Subcellular localization of a sporulation membrane protein is achieved through a network of interactions along and across the septum. Mol Microbiol **55:**1767-1781.

17. **Dong, T. C., and S. M. Cutting.** 2003. SpoIVB-mediated cleavage of SpoIVFA could provide the intercellular signal to activate processing of Pro-sigmaK in Bacillus subtilis. Mol Microbiol **49:**1425-1434.

18. **Duncan, L., S. Alper, F. Arigoni, R. Losick, and P. Stragier.** 1995. Activation of cell-specific transcription by a serine phosphatase at the site of asymmetric division. Science **270:**641-644.

19. **Duncan, L., S. Alper, and R. Losick.** 1996. SpoIIAA governs the release of the cell-type specific transcription factor sigma F from its anti-sigma factor SpoIIAB. J Mol Biol **260:**147-164.

20. **Duncan, L., and R. Losick.** 1993. SpoIIAB is an anti-sigma factor that binds to and inhibits transcription by regulatory protein sigma F from Bacillus subtilis. Proc Natl Acad Sci U S A **90:**2325-2329.

21. **Eichenberger, P., M. Fujita, S. T. Jensen, E. M. Conlon, D. Z. Rudner, S. T. Wang, C. Ferguson, K. Haga, T. Sato, J. S. Liu, and R. Losick.** 2004. The program of gene transcription for a single differentiating cell type during sporulation in Bacillus subtilis. PLoS Biol **2:**e328.

22. **Errington, J.** 1993. Bacillus subtilis sporulation: regulation of gene expression and control of morphogenesis. Microbiol Rev **57:**1-33.

23. **Errington, J., L. Appleby, R. A. Daniel, H. Goodfellow, S. R. Partridge, and M. D. Yudkin.** 1992. Structure and function of the spoIIIJ gene of Bacillus subtilis: a vegetatively expressed gene that is essential for sigma G activity at an intermediate stage of sporulation. J Gen Microbiol **138:**2609-2618.

24. **Frandsen, N., and P. Stragier.** 1995. Identification and characterization of the Bacillus subtilis spoIIP locus. J Bacteriol **177:**716-722.

25. **Fujita, M., J. E. Gonzalez-Pastor, and R. Losick.** 2005. High- and low-threshold genes in the Spo0A regulon of Bacillus subtilis. J Bacteriol **187:**1357-1368.

26. **Gaur, N. K., E. Dubnau, and I. Smith.** 1986. Characterization of a cloned Bacillus subtilis gene that inhibits sporulation in multiple copies. J Bacteriol **168:**860-869.

27. **Hahn, J., L. Kong, and D. Dubnau.** 1994. The regulation of competence transcription factor synthesis constitutes a critical control point in the regulation of competence in Bacillus subtilis. J Bacteriol **176:**5753-5761.

28. **Hilbert, D. W., and P. J. Piggot.** 2004. Compartmentalization of gene expression during Bacillus subtilis spore formation. Microbiol Mol Biol Rev **68:**234-262.

29. **Hofmeister, A. E., A. Londono-Vallejo, E. Harry, P. Stragier, and R. Losick.** 1995. Extracellular signal protein triggering the proteolytic activation of a developmental transcription factor in B. subtilis. Cell **83:**219-226.

30. **Illing, N., and J. Errington.** 1991. The spoIIIA operon of Bacillus subtilis defines a new temporal class of mother-cell-specific sporulation genes under the control of the sigma E form of RNA polymerase. Mol Microbiol **5:**1927-1940.

31. **Jiang, M., W. Shao, M. Perego, and J. A. Hoch.** 2000. Multiple histidine kinases regulate entry into stationary phase and sporulation in Bacillus subtilis. Mol Microbiol **38:**535-542.

32. **Karmazyn-Campelli, C., C. Bonamy, B. Savelli, and P. Stragier.** 1989. Tandem genes encoding sigma-factors for consecutive steps of development in Bacillus subtilis. Genes Dev **3:**150-157.

33. **Kearns, D. B., F. Chu, S. S. Branda, R. Kolter, and R. Losick.** 2005. A master regulator for biofilm formation by Bacillus subtilis. Mol Microbiol **55:**739-749.

34. **Lazazzera, B., T. Palmer, T. Quisel, and A. Grossman.** 1999. Cell density control of gene expression and development in Bacillus subtilis, p. 47-65. *In* G. Dunny and S. Winans (ed.), Cell-Cell Signaling in Bacteria. American Society for Microbiology, Washington, DC.

35. **Londono-Vallejo, J. A., C. Frehel, and P. Stragier.** 1997. SpoIIQ, a forespore-expressed gene required for engulfment in Bacillus subtilis. Mol Microbiol **24:**29-39.

36. **Londono-Vallejo, J. A., and P. Stragier.** 1995. Cell-cell signaling pathway activating a developmental transcription factor in Bacillus subtilis. Genes Dev **9:**503-508.

37. **Losick, R., and J. Pero.** 1981. Cascades of Sigma factors. Cell **25:**582-584.

38. **Losick, R., and P. Stragier.** 1992. Crisscross regulation of cell-type-specific gene expression during development in B. subtilis. Nature **355:**601-604.

39. **Mandic-Mulec, I., L. Doukhan, and I. Smith.** 1995. The Bacillus subtilis SinR protein is a repressor of the key sporulation gene spo0A. J Bacteriol **177:**4619-4627.

40. **Margolis, P., A. Driks, and R. Losick.** 1991. Establishment of cell type by compartmentalized activation of a transcription factor. Science **254:**562-565.

41. **Mason, J. M., P. Fajardo-Cavazos, and P. Setlow.** 1988. Levels of mRNAs which code for small, acid-soluble spore proteins and their LacZ gene fusions in sporulating cells of Bacillus subtilis. Nucleic Acids Res **16:**6567-6583.

42. **Meyer, P., J. Gutierrez, K. Pogliano, and J. Dworkin.** 2010. Cell wall synthesis is necessary for membrane dynamics during sporulation of Bacillus subtilis. Mol Microbiol **76:**956-970.

43. **Min, K. T., C. M. Hilditch, B. Diederich, J. Errington, and M. D. Yudkin.** 1993. Sigma F, the first compartment-specific transcription factor of B. subtilis, is regulated by an anti-sigma factor that is also a protein kinase. Cell **74:**735-742.

44. **Molle, V., M. Fujita, S. T. Jensen, P. Eichenberger, J. E. Gonzalez-Pastor, J. S. Liu, and R. Losick.** 2003. The Spo0A regulon of Bacillus subtilis. Mol Microbiol **50:**1683-1701.

45. **Morlot, C., T. Uehara, K. A. Marquis, T. G. Bernhardt, and D. Z. Rudner.** 2010. A highly coordinated cell wall degradation machine governs spore morphogenesis in Bacillus subtilis. Genes Dev **24:**411-422.

46. **Partridge, S. R., and J. Errington.** 1993. The importance of morphological events and intercellular interactions in the regulation of prespore-specific gene expression during sporulation in Bacillus subtilis. Mol Microbiol **8:**945-955.

47. **Perego, M.** 1999. Self-signaling by Phr peptides modulates Bacillus subtilis development, p. 243-258. *In* G. Dunny and S. Winans (ed.), Cell-Cell Signaling in Bacteria. American Society for Microbiology, Washington, DC.

48. **Perego, M., and J. Hoch.** 2002. Two-component systems, phosphorelays, and regulation of their activities by phosphatases, p. 473-481. *In* A. Sonenshein, J. Hoch, and R. Losick (ed.), Bacillus subtilis and its Closest Relatives: From Genes to Cells. American Society for Microbiology, Washington, DC.

49. **Piggot, P., and R. Losick.** 2002. Sporulation genes and intercompartmental regulation, p. 483-517. *In* A. Sonenshein, J. Hoch, and R. Losick (ed.), Bacillus subtilis and its Closest Relatives: From Genes to Cells. American Society for Microbiology, Washington, DC.

50. **Piggot, P. J., and J. G. Coote.** 1976. Genetic aspects of bacterial endospore formation. Bacteriol Rev **40:**908-962.

51. **Predich, M., G. Nair, and I. Smith.** 1992. Bacillus subtilis early sporulation genes kinA, spo0F, and spo0A are transcribed by the RNA polymerase containing sigma H. J Bacteriol **174:**2771-2778.

52. **Rowland, S. L., W. F. Burkholder, K. A. Cunningham, M. W. Maciejewski, A. D. Grossman, and G. F. King.** 2004. Structure and mechanism of action of Sda,

an inhibitor of the histidine kinases that regulate initiation of sporulation in Bacillus subtilis. Mol Cell **13:**689-701.

53. **Rubio, A., and K. Pogliano.** 2004. Septal localization of forespore membrane proteins during engulfment in Bacillus subtilis. EMBO J **23:**1636-1646.

54. **Ryter, A.** 1965. [Morphologic Study of the Sporulation of Bacillus Subtilis.]. Ann Inst Pasteur (Paris) **108:**40-60.

55. **Sekiguchi, J., B. Ezaki, K. Kodama, and T. Akamatsu.** 1988. Molecular cloning of a gene affecting the autolysin level and flagellation in Bacillus subtilis. J Gen Microbiol **134:**1611-1621.

56. **Serrano, M., F. Vieira, C. P. Moran, Jr., and A. O. Henriques.** 2008. Processing of a membrane protein required for cell-to-cell signaling during endospore formation in Bacillus subtilis. J Bacteriol **190:**7786-7796.

57. **Sonenshein, A. L.** 2000. Control of sporulation initiation in Bacillus subtilis. Curr Opin Microbiol **3:**561-566.

58. **Stragier, P., and R. Losick.** 1990. Cascades of sigma factors revisited. Mol Microbiol **4:**1801-1806.

59. **Stragier, P., and R. Losick.** 1996. Molecular genetics of sporulation in Bacillus subtilis. Annu Rev Genet **30:**297-241.

60. **Strauch, M.** 1993. AbrB, a transition state regulator, p. 757-764. *In* A. Sonenshein, J. Hoch, and R. Losick (ed.), Bacillus subtilis and Other Gram-Positive Bacteria: Biochemistry, Physiology, and Molecular Genetics. American Society for Microbiology, Washington, DC.

61. **Strauch, M., V. Webb, G. Spiegelman, and J. A. Hoch.** 1990. The SpoOA protein of Bacillus subtilis is a repressor of the abrB gene. Proc Natl Acad Sci U S A **87:**1801-1805.

62. **Strauch, M. A., and J. A. Hoch.** 1993. Transition-state regulators: sentinels of Bacillus subtilis post-exponential gene expression. Mol Microbiol **7:**337-342.

63. **Trach, K. A., and J. A. Hoch.** 1993. Multisensory activation of the phosphorelay initiating sporulation in Bacillus subtilis: identification and sequence of the protein kinase of the alternate pathway. Mol Microbiol **8:**69-79.

64. **Wang, S. T., B. Setlow, E. M. Conlon, J. L. Lyon, D. Imamura, T. Sato, P. Setlow, R. Losick, and P. Eichenberger.** 2006. The forespore line of gene expression in Bacillus subtilis. J Mol Biol **358:**16-37.

65. **Weir, J., M. Predich, E. Dubnau, G. Nair, and I. Smith.** 1991. Regulation of spo0H, a gene coding for the Bacillus subtilis sigma H factor. J Bacteriol **173:**521-529.

66. **Wu, L. J., and J. Errington.** 2003. RacA and the Soj-Spo0J system combine to effect polar chromosome segregation in sporulating Bacillus subtilis. Mol Microbiol **49:**1463-1475.

CHAPTER 2. A channel connecting the mother cell and forespore

The data presented in this chapter were published in the following manuscript:

Meisner, J., X. Wang, M. Serrano, A.O. Henriques, and C.P. Moran, Jr. 2008. A channel connecting the mother cell and forespore during bacterial endospore formation. Proc Natl Acad Sci U S A **105:**15100-15105.

J.M., X.W., M.S., A.O.H., and C.P.M. designed the experiments. J.M. and X.W. performed the experiments. J.M. and C.P.M wrote the manuscript.

INTRODUCTION

Endospore formation in the Gram-positive bacterium *Bacillus subtilis* involves a series of morphological changes that culminate in the production of a dormant spore (reviewed in 15, 27, 28). In response to nutrient depletion, vegetative cells undergo an asymmetric cell division that yields two dissimilar progeny cells, the mother cell and forespore. Remarkably, the mother cell engulfs the forespore and nurtures it to maturity. Ultimately, the mother cell lyses, releasing the mature spore. The differentiation of these two cell types is governed by two parallel programs of gene expression controlled by a cascade of alternative RNA polymerase sigma (σ) factors. To synchronize the differentiation of the mother cell and forespore, the two programs of gene expression are coordinated through a series of intercellular signaling pathways. Following asymmetric cell division, σ^F is activated in the forespore. σ^F then signals the activation of σ^E in the mother cell. Together, σ^F and σ^E control expression of the genes responsible for forespore engulfment. After the completion of forespore engulfment, σ^G is activated in the forespore and signals the activation of σ^K in the mother cell. σ^G and σ^K control expression of the genes necessary for forespore maturation. While the intercellular signaling pathways that trigger the activation of σ^E and σ^K in the mother cell are well understood, the mechanisms that trigger the activation of σ^G in the forespore are not known.

In addition to the completion of forespore engulfment, the eight-gene *spoIIIA* locus (*spoIIIAA-AH*) is also necessary for the activation of σ^G. The *spoIIIA* locus is expressed under the control of σ^E in the mother cell. With the exception of *spoIIIAA*, each of the *spoIIIA* genes (*spoIIIAB-AH*) encodes a predicted integral membrane protein.

SpoIIIAH contains an N-terminal transmembrane segment (TMS) and a C-terminal extracellular domain. Although SpoIIIAH is inserted randomly into the mother cell membrane, it is targeted to the sporulation septum, separating the mother cell and forespore, through an interaction of its C-terminal domain with the forespore integral membrane protein SpoIIQ (3, 9). SpoIIIAH and SpoIIQ colocalize along the engulfing membrane and form discrete foci surrounding the forespore. However, it is unclear why SpoIIIAH is necessary for σ^G activity in the forespore.

In this study, we identified a homologous relationship between SpoIIIAH and the proteins that form the export channel and structural scaffold of type III secretion and flagellar export systems. We hypothesized that if SpoIIIAH also forms a channel, then its C-terminal extracellular domain may be accessible to modification by an enzyme produced in the forespore. To test this hypothesis, we developed a compartmentalized biotinylation assay. Using this assay, we demonstrated that the C-terminal domain of SpoIIIAH is accessible to biotin ligase produced in the forespore. These and other results suggest that SpoIIIAH and SpoIIQ may form a channel between the mother cell and forespore.

MATERIALS AND METHODS

Bioinformatics

The *B. subtilis* SpoIIIAH amino acid sequence was submitted to the HHpred server for protein homology detection and structure prediction (39, 40). An alignment of homologs was built by multiple iterations of PSI-BLAST searches against the NCBI non-

redundant database and annotated with predicted secondary structure and confidence values from PSIPRED. Next, a profile hidden Markov model (HMM) was constructed that included the information about predicted secondary structure. The query HMM was then compared with HMMs from various databases by the HHsearch software. HHsearch used position-specific gap penalties and scored for secondary structure similarity to construct local alignments with the query sequence and the matching database sequences.

Growth conditions

B. subtilis strains were grown in Luria broth (LB) and sporulation was induced by nutrient exhaustion in Difco sporulation medium (DSM). Genetic competence was developed and transformations were performed as described previously. The antibiotic concentrations used for selection were as follows: 5 μg/ml chloramphenicol, 1 μg/ml neomycin, 10 μg/ml kanamycin, 1 μg/ml erythromycin, 20 μg/ml tetracylcine and 100 μg/ml spectinomycin. *Escherichia coli* strain DH5α was grown in LB and 100 μg/ml ampicillin was used for selection.

Bacterial strains and plasmids

The strains used in this study are shown in Tables 1. The plasmids and oligonucleotide primers are shown in Tables 2 and 3, respectively. Plasmids were purified from *E.coli* strain DH5α. Each plasmid was confirmed by DNA sequencing.

To construct *B. subtilis* strains expressing *E. coli birA* in the mother cell and forespore, C-terminal His-tagged *E. coli birA* was amplified by PCR from strain MG1655 chromosomal DNA with a reverse primer containing the hexahistidine (His_6) coding

sequence and the *spoIID* and *spoIIQ* promoters were amplified from *B. subtilis* strain JH642 chromosomal DNA. P_{spoIID}-*birA*-*his*$_6$ and P_{spoIIQ}-*birA*-*his*$_6$ were constructed by overlapping PCR, digested with BamHI and PstI, and ligated into the *amyE* gene replacement vector pDG1662. *B. subtilis* strain JH642 transformants were selected for chloramphenicol resistance and double-crossover recombinants were screened for spectinomycin sensitivity.

To construct strains expressing biotin acceptor peptide (BAP)-tagged alleles, the 3′ end of each coding sequence was amplified using gene-specific primers. Each reverse primer contained the BAP coding sequence followed by a stop codon. The *spoIIID-BAP*, *sigG-BAP*, *spoIIIAH-BAP*, *spoIID-BAP*, and *spoIIQ-BAP* fragments were digested with the appropriate restriction enzymes and ligated into the integration vector pBEST501 or pDG1515. *B. subtilis* transformants were selected for neomycin and tetracycline resistance, respectively. These strains contain the BAP-tagged alleles integrated at the native loci by Campbell recombination. *spoIVFA*-BAP was cloned into *thrC* gene replacement vector pDG1664 and *B. subtilis* transformants were selected for erythromycin resistance and double-crossover recombinants were screened for spectinomycin sensitivity.

Compartmentalized biotinylation assay

B. subtilis strains expressing different combinations of BAP-tagged alleles and *E. coli birA* in the mother cell, the forespore, or not at all were grown in LB overnight. The following morning, 25 ml DSM cultures were inoculated with 250 μl of each overnight culture. Growth of each strain was monitored by measuring OD_{600} hourly. The onset of

sporulation (t_0) was defined as the transition between exponential and stationary growth phases. Since BirA acts as a repressor of biotin biosynthesis genes, the cultures were supplemented with 2 μg/ml biotin at t_0. 5 ml of each culture was collected at the indicated times during sporulation. The cells were washed once with cold PBS and stored at -80°C.

Western blots

Cell pellets were resuspended in 250 μl of PBS containing 2 mg/ml lysozyme, 10 μg/ml DNase, and Complete Mini EDTA-free protease inhibitor cocktail (Roche). Cells were lysed at 37°C for 10 min. Each lysate was mixed with an equal volume of SDS-PAGE loading buffer, heated at 95°C for 5 min, and centrifuged at 15,000 X *g* for 1 min. 10 μl of each lysate was subjected to SDS-PAGE. 25 μl of each σ^G-BAP lysate was used. 15% SDS-PAGE gels were used for SpoIIID-BAP lysates and 10% SDS-PAGE gels for σ^G-BAP, SpoIIIAH-BAP, SpoIID-BAP, SpoIVFA-BAP, and SpoIIQ-BAP lysates. Proteins were then transferred from the gels to nitrocellulose membranes.

To detect biotinylation of BAP-tagged fusion proteins, the nitrocellulose membranes were blocked with PBS containing 3% BSA and 0.05% Tween 20 at 4°C overnight. After washing 3 times with PBS containing 0.05%Tween 20 for 10 minutes each, the membranes were incubated with a streptavidin-HRP conjugate diluted 1:10,000 in PBS containing 0.05% Tween 20 at room temperature for 1 hour. Membranes were incubated with SuperSignal West Pico Chemiluminescent Substrate (Pierce) at room temperature for 5 minutes, dripped dry, wrapped in saran wrap, and exposed to CL-XPosure film (Pierce).

To detect BirA, membranes were incubated with chicken anti-BirA polyclonal antibody diluted 1:5,000 and HRP-conjugated rabbit anti-chicken polyclonal antibody (Abcam) diluted 1:10,000. Rabbit anti-SpoIIIAH polyclonal antibody (Sigma) diluted 1:10,000 and goat anti-rabbit polyclonal antibody diluted 1:10,000 were used to detect SpoIIIAH. Rabbit anti-SpoIVFA polyclonal antibody diluted 1:10,000 and goat anti-rabbit polyclonal antibody diluted 1:10,000 were used to detect SpoIVFA. Purified rabbit anti-σ^G polyclonal antibody diluted 1:750 and HRP-goat anti-rabbit polyclonal antibody diluted 1:5,000 were used to detect σ^G.

RESULTS

C-terminal extracellular domain of SpoIIIAH is homologous to the YscJ/FliF protein family

Although no significant relationship to a protein of known function could be established using conventional search methods, the HHpred server (39, 40) identified a homologous relationship between the C-terminal extracellular domain of SpoIIIAH and the YscJ/FliF protein family (PF01514) based on pairwise comparisons of profile hidden Markov models (HMMs). In addition to weighting HMMs with amino acid frequencies, the HHpred searcher includes position-specific insertion and deletion probabilities and scores predicted secondary structure. This method of aligning profile HMMs instead of simple sequence profiles improves protein homology detection sensitivity and alignment quality. This comparison revealed sequence and secondary structure similarity between the SpoIIIAH and the YscJ/FliF family proteins (Figure 1A). The

sequence similarity covers a 78-amino acid stretch with 23% identity, corresponding to the C-terminal domain of the YscJ proteins and the central domain of the FliF proteins. The members of the YscJ family are involved in type III secretion of virulence factors in Gram-negative bacteria (12). The structure of a representative member, the enteropathogenic *E. coli* EscJ protein, indicated that these proteins probably form ring structures with a central channel that is 75Å in diameter (46). The dimensions of the 24-subunit EscJ ring were similar to those estimated by electron microscopy (37). The YscJ ring is thought to form the inner membrane channel of the type III secretion system (Figure 1B) (19). The FliF protein forms the bacterial flagellar protein export channel and the structural scaffold for flagellar assembly (Figure 1C) (43). Therefore, we hypothesized that the C-terminal extracellular domain of SpoIIIAH forms a large, hollow ring with the N-terminal TMS anchored in the mother cell membrane (Figure 1D). The SpoIIIAH ring may be part of a channel between the mother cell and forespore. The similarity of SpoIIIAH with the YscJ/FliF protein family and the hypothesis that SpoIIIAH forms a channel were independently proposed by Camp and Losick (4).

Compartmentalized biotinylation assay

If SpoIIIAH forms part of a channel between the mother cell and forespore, then the C-terminal extracellular domain may be accessible to modification by an enzyme produced in the forespore. To test this prediction, we developed a compartmentalized biotinylation assay, involving the biotinylation of target proteins by the *Escherichia coli* biotin ligase, BirA, produced in either the mother cell or forespore (Figures 2A and B). BirA transfers biotin to a specific lysine in biotin-accepting proteins (8). Biotinylated

proteins can then be detected by western blot with a streptavidin-horseradish peroxidase (HRP) conjugate (44). We tagged proteins with a 14-amino acid biotin acceptor peptide (BAP), defined as the minimal substrate required for *E. coli* BirA-catalyzed biotinylation (2). Then we tested whether the fusion proteins were biotinylated in *B. subtilis* strains producing the *E. coli* BirA in either the mother cell or forespore, under the control of the *spoIID* and *spoIIQ* promoters, respectively (11, 22). Western blot analysis of BirA indicated that similar amounts of BirA accumulated after the onset of sporulation in both the mother cell- and forespore-producing strains (Figure 3).

To test whether BirA activity was compartmentalized in these strains, we analyzed the biotinylation of BAP-tagged SpoIIID and σ^G, produced exclusively in the mother cell and forespore, respectively (20, 41). The biotinylated BAP-tagged fusion proteins were detected by western blot with a streptavidin-HRP conjugate. SpoIIID-BAP was only biotinylated in the strain that produced BirA in the mother cell and not in the strain that produced BirA in the forespore (Figure 2C, lanes 4 and 5). Conversely, σ^G-BAP was biotinylated only in the strain that produced BirA in the forespore and not the strain that produced BirA in the mother cell (Figure 2D, lanes 4 and 5). Neither biotinyl-SpoIIID-BAP nor biotinyl-σ^G-BAP was detected in the control strains that produced BirA or the BAP-tagged fusion proteins alone (Figures 2C and 2D, lanes 1-3). *B. subtilis* BirA-catalyzed biotinylation of the biotin carboxyl carrier protein (24) served as an internal control, showing that each lane contained similar amounts of protein (Figures 2C and 2D, bottom panels). Each of the strains was sporulation proficient, indicating that the

BAP tag did not interfere with normal protein function (Table 4). These results demonstrate that the compartmentalized biotinylation assay can be used to determine if a protein is accessible to either the mother cell or forespore cytoplasm.

C-terminal domain of SpoIIIAH is accessible to forespore-produced BirA

To test whether the C-terminal extracellular domain of SpoIIIAH is accessible to the forespore cytoplasm, we assessed compartmentalized biotinylation in strains producing a C-terminal BAP-tagged SpoIIIAH. The SpoIIIAH-BAP fusion protein was biotinylated when BirA was produced in the forespore (Figure 4, lane 5). Biotinyl-SpoIIIAH-BAP was not detected in the absence of *E. coli* BirA (Figure 4, lane 3) or when it was produced in the mother cell (Figure 4, lane 4). Immuno-blots with anti-SpoIIIAH antiserum showed that SpoIIIAH-BAP accumulated to levels similar to that of wild-type SpoIIIAH in each of the strains (Figure 4, bottom panel). Furthermore, these strains supported the production of heat-resistant spores similar to that of the wild-type strain, indicating that the BAP-tagged fusion protein was functional (Table 4). These results suggest that the C-terminal extracellular domain of the mother cell protein SpoIIIAH is accessible to the forespore cytoplasm.

Alternative explanations for the apparent forespore-accessibility of the C-terminal BAP-tagged SpoIIIAH include noncompartmentalized production of SpoIIIAH-BAP in the forespore or noncompartmentalized BirA activity in the mother cell or intermembrane space. To test whether SpoIIIAH-BAP was produced in the forespore, we measured SpoIIIAH-BAP biotinylation in a mutant (*sigE*) that is defective in mother cell but not forespore gene expression. If SpoIIIAH-BAP were produced in the forespore

under the control of σ^F, then its expression would not be dependent on the mother cell specific activity of σ^E and therefore would be biotinylated even in a *sigE* mutant. However, we found that biotinyl-SpoIIIAH-BAP was not detected in the *sigE* mutant strain (Figure 5A, top panel). BirA production was unaffected in the mutant as expected, indicating that forespore gene expression was intact (Figure 5A, bottom panel). We also found that production of biotinyl-SpoIIIAH-BAP was not dependent on σ^G, the late forespore-specific factor (Figure 6). Thus, SpoIIIAH-BAP production was completely dependent on σ^E and therefore restricted to the mother cell. To test for BirA activity in the mother cell in the strain that expressed BirA in the forespore, we analyzed biotinylation of SpoIIIAH-BAP and the mother cell protein SpoIIID-BAP in the same strain. As expected, SpoIIID-BAP was biotinylated only when BirA was produced in the mother cell but not in the strain that produced BirA in the forespore (Figure 5B, bottom panel). Conversely, SpoIIIAH-BAP was biotinylated only when BirA was produced in the forespore and not in the strain that produced BirA in the mother cell (Figure 5B, top panel). These results eliminate the possibility that biotinylation of SpoIIIAH-BAP occurred in the mother cell when BirA was produced in the forespore.

To test whether BirA produced in the forespore exhibited activity in the intermembrane space, we assessed biotinylation of C-terminal BAP-tagged control septal proteins SpoIID and SpoIVFA. SpoIID contains an extracellular peptidoglycan hydrolase domain that is necessary for septal thinning during forespore engulfment (1). SpoIVFA contains an extracellular domain that regulates late mother cell gene expression in response to a forespore protein that is secreted into the intermembrane

space following engulfment (35). Neither SpoIID-BAP nor SpoIVFA-BAP was biotinylated (data not shown), while both supported the production of heat-resistant spores similar to wild type, indicating the fusion proteins were functional (Table 4). Therefore, BirA produced in the forespore is not active in the intermembrane space. This was not surprising because BirA-catalyzed biotinylation requires ATP (21), which is expected to be absent from the intermembrane space. Together these results indicate that SpoIIIAH-BAP is produced exclusively in the mother cell and accessible to biotinylation by BirA produced in the forespore cytoplasm. We note that the central diameter of the EscJ ring is large enough to accommodate BirA (45, 46). Therefore, these results are consistent with the hypothesis that SpoIIIAH forms a channel.

C-terminal extracellular domain of SpoIIQ is also accessible to forespore-produced BirA

In order for the SpoIIIAH extracellular domain to be accessible to the forespore cytoplasm, it may interact with an integral membrane protein that forms a channel across the forespore membrane. Since SpoIIIAH interacts with the forespore protein SpoIIQ (3, 9), we tested whether the C-terminal extracellular domain of SpoIIQ was also accessible to the forespore cytoplasm. We introduced a C-terminal BAP-tagged *spoIIQ* allele into the compartmentalized biotinylation strains. These strains produced heat-resistant spores similar to wild type, indicating that the fusion protein was functional (Table 4). SpoIIQ-BAP was biotinylated only when BirA was produced in the forespore, suggesting that the C-terminus of SpoIIQ is accessible to the forespore cytoplasm (Figure 7A). After the completion of engulfment, SpoIIQ is degraded by SpoIVB, a protease

produced in the forespore and secreted into the intermembrane space, releasing the 30 kDa C-terminal domain from the full-length protein (17). To confirm that SpoIIQ-BAP was properly inserted into the membrane, we tested whether the biotinylated C-terminal proteolytic product accumulated after engulfment. Engulfment typically begins 2 hours after the onset of sporulation (t_2) and completes within 60 minutes (t_3) (30, 38). We detected the expected 30 kDa biotinylated product beginning at about t_3 (Figure 7B), indicating that the biotinyl-SpoIIQ-BAP was correctly inserted in the membrane with the C-terminal domain in the intermembrane space. Since the insertion of bacterial integral membrane proteins is cotranslational (reviewed in 32), it is unlikely that C-terminal BAP-tagged SpoIIQ is biotinylated in the cytoplasm prior to membrane insertion. These results are consistent with the idea that SpoIIIAH and SpoIIQ form a channel that is open on the forespore end and closed (or gated) on the mother cell end (Figure 7C).

Degradation of the putative channel after engulfment

The interaction with SpoIIQ is necessary for the septal localization and stability of SpoIIIAH (3, 6, 9). This suggests that SpoIIQ should be necessary for the forespore accessibility and stability of SpoIIIAH-BAP. As expected, SpoIIIAH-BAP failed to accumulate in a *spoIIQ* mutant (data not shown). Septal thinning is necessary for the interaction of SpoIIIAH and SpoIIQ (3, 9). SpoIIIAH-BAP was undetectable (data not shown) in a mutant (*spoIIP spoIID*) that is completely defective in septal thinning (1). Because the interaction with SpoIIQ was necessary for SpoIIIAH-BAP stability, we hypothesized that biotinyl-SpoIIIAH-BAP would be degraded upon the completion of engulfment and initiation of SpoIIQ proteolysis. We found that biotinyl-SpoIIIAH-BAP

accumulated until t_3 and was degraded at t_4 (Figure 8, top panel). To confirm that the degradation of biotinyl-SpoIIIAH correlated with the completion of engulfment, we analyzed the control proteins SpoIVFA and σ^G. SpoIVB cleaves SpoIVFA after engulfment, resulting in SpoIVFA degradation (and activation of pro-σ^K processing) (5, 10). After engulfment, σ^G activates expression of its own gene, promoting the accumulation of σ^G. While SpoIVFA was present at t_2-t_3 and lost at t_4 (Figure 8, middle panel), σ^G was detected by t_4 (Figure 8, bottom panel). These results suggest that the channel forms during engulfment and is degraded shortly after its completion.

DISCUSSION

We identified a homologous relationship between the C-terminal extracellular domain of SpoIIIAH and the YscJ and FliF proteins, involved in type III secretion of virulence factors and flagellar protein export apparatus, respectively. We developed an *in vivo* compartmentalized biotinylation assay and showed that the C-terminal extracellular domain of the mother cell protein SpoIIIAH is accessible to biotinylation by BirA produced in the forespore. This result supports the hypothesis that SpoIIIAH forms a channel, analogous to those formed by YscJ and FliF, in the engulfing mother cell membrane. An alternative explanation is that the C-terminus of SpoIIIAH extends across the forespore membrane. This is unlikely, however, because the C-terminus of SpoIIIAH does not contain a predicted transmembrane segment or amphipathic α-helix. Furthermore, the C-terminus of SpoIIIAH is predicted to form a globular mixed α/β domain that is topologically similar to the YscJ/FliF domain and unlikely to extend

across the forespore membrane (46). The fraction of SpoIIIAH that is biotinylated is unknown. Therefore, we don't know whether all molecules of SpoIIIAH participate in channel formation, or whether only a fraction of the SpoIIIAH C-termini within a channel is accessible to BirA. We also showed that the C-terminal extracellular domain of the forespore protein SpoIIQ, with which SpoIIIAH interacts, is accessible to BirA produced in the forespore. Therefore, we propose that SpoIIIAH and SpoIIQ form a channel that is open on the forespore end and closed (or gated) on the mother cell end.

The core components of the flagellar protein export apparatus, including three soluble proteins (ATPase regulator FliH, ATPase FliI, and chaperone FliJ) and six integral membrane proteins (FlhA, FlhB, FliO, FliP, FliQ, and FliR), are homologous to the type III secretion system (7, 23). FlhA, FlhB, FliO, FliP, FliQ, and FliR are thought to be located within the FliF ring (25, 26). In the type III secretion system, the YscJ ring is thought to be functionally analogous to the FliF ring, providing a scaffold for the assembly of YscR, YscS, YscT, YscU, and YscV. FlhA and FlhB (YscV and YscU) act as a docking platform for the FliI (YscN) ATPase (18, 25, 26, 33). Although the functions of FliO, FliP, FliQ, and FliR (YscR, YscS, and YscT) are unknown, together with FlhA and FlhB, they are thought to form a protein-conducting channel (25).

By analogy with the type III secretion system and flagellar protein export apparatus, we propose that SpoIIIAH acts as a scaffold upon which the components of a novel export apparatus is assembled and, together with SpoIIQ, forms the channel through which substrate translocation between the mother cell and forespore occurs. In addition to SpoIIIAH, the *spoIIIA* locus is predicted to encode a cytoplasmic protein

(SpoIIIAA) and six integral membrane proteins (SpoIIIAB-AG), several of which share similarity with the components of several protein secretion systems (data not shown). SpoIIIAA is similar to the secretion superfamily ATPases involved in type II secretion, type IV pilus assembly, type IV secretion, DNA uptake, and archaeal flagellar assembly systems (29). The predicted cytoplasmic domain of SpoIIIAB is similar to the type II secretion system protein GspF, a component of the inner membrane platform to which the ATPase docks (33). Although SpoIIIAC and SpoIIIAD do not share similarity with proteins of known function, they resemble FliQ and FliP (YscS and YscR), respectively, in size, and number and orientation of transmembrane segments. SpoIIIAE is similar to various electrochemical potential-driven transporters. SpoIIIAF shows similarity with FlhB (YscU), while SpoIIIAG has weak similarity to YscJ and FliF. Therefore, we hypothesize that SpoIIIAB-AG are assembled within the SpoIIIAH ring and form a novel export apparatus that gates the SpoIIIAH-SpoIIQ channel at the mother cell end. SpoIIIAB, and possibly SpoIIIAF, provide a docking platform for SpoIIIAA which couples substrate translocation with ATP hydrolysis. Although the roles of SpoIIIAA-AG are not known, our preliminary results indicate that SpoIIIAA is not required for formation of the SpoIIIAH-SpoIIQ channel (data not shown). This result is consistent with those of Camp and Losick in which they identified a mutation that partially bypasses the requirement for *spoIIIAA-AG*, but not *spoIIIAH* and *spoIIQ*, for σ^G activation (4). They postulated that, under certain conditions, SpoIIIAH and SpoIIQ can constitute a minimal pathway for σ^G activation. However, in an otherwise wild-type strain SpoIIIAA-AG are necessary for efficient σ^G activation via the SpoIIIAH-SpoIIQ channel.

The export apparatus model predicts that a substrate(s) is produced in the mother cell and translocated into the forespore, where it triggers the activation of σ^G. The nature of the substrate is unclear. Based on the similarities of the SpoIIIA proteins to various protein secretion systems, we suspect that the substrate is a protein. If this were the case, then a mutation in the gene encoding the protein substrate would block σ^G activation. No such mutant has been isolated in decades of selection and screening. As noted by Camp and Losick, it is possible that the gene is essential for viability or necessary for a process earlier in sporulation (4). The substrate may also be a peptide encoded by a small open reading frame missed by mutagenesis and overlooked in microarray analyses. Another possibility is that the substrate is a small molecule or metabolite, without which the forespore cannot sustain essential processes such as transcription or translation (4). While we acknowledge that the substrate might be a metabolite, this model does not account for the fact that, prior to engulfment, σ^G remains inactive while σ^F is active in the forespore. This argues that σ^G inactivity is not due exclusively to a general metabolic deficiency but rather a specific inhibition of σ^G that must also be relieved. Although the function of the SpoIIIAH-SpoIIQ channel remains to be elucidated, all of the SpoIIIA-encoded products are highly conserved among evolutionarily diverse endospore-forming *Bacillus* and *Clostridium* species (data not shown). Therefore, this novel hybrid secretion system may be an ancient, but specialized and essential structure for mother cell-forespore communication.

FIGURES

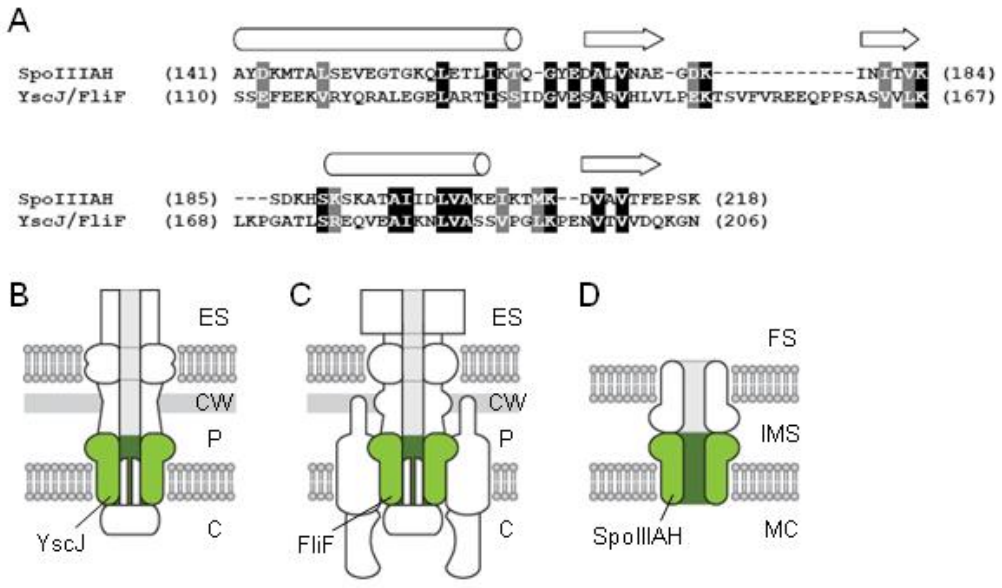

Figure 1. Similarity between SpoIIIAH and YscJ/FliF protein family. HHpred alignment of SpoIIIAH and YscJ/FliF family. Identical (black boxes) and similar (grey boxes) amino acids are highlighted. Predicted secondary structure is indicated above the alignment. Cartoon representations of the (B) type III secretion system, (C) flagellar basal body, and (D) SpoIIIAH channel model. YscJ, FliF, and SpoIIIAH are labeled and colored green. The extracellular space (ES), cell wall (CW), periplasm (P), and cytoplasm (C) of Gram-negative bacteria, as well as mother cell (MC), intermembrane space (IMS), and forespore (FS) of bacterial endospores are indicated in each panel.

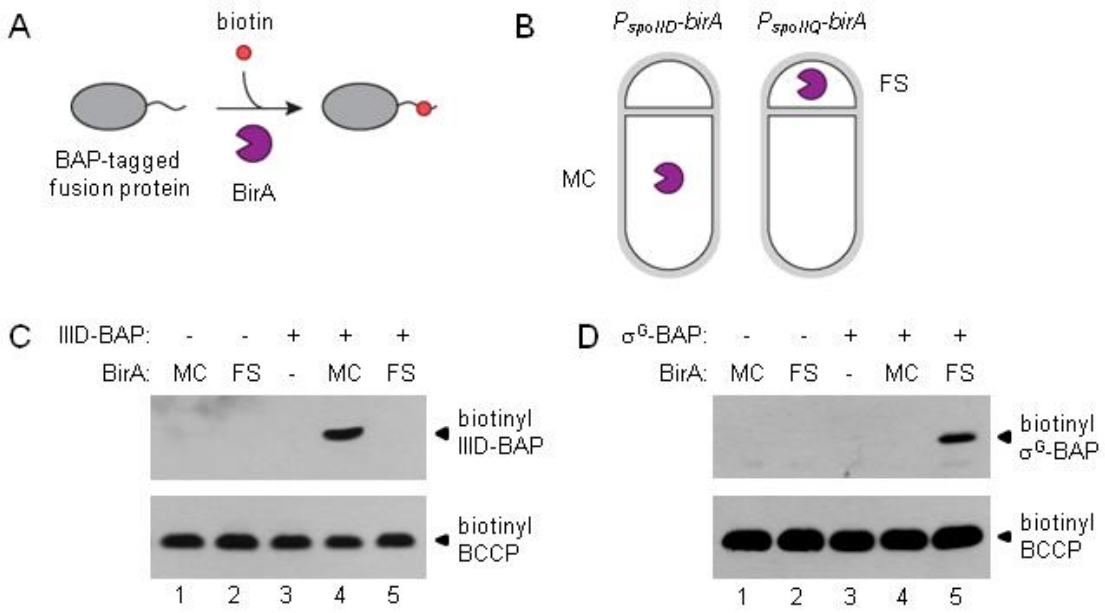

Figure 2. Compartmentalized biotinylation assay. Cartoon representations of (A) BirA-catalyzed transfer of biotin to biotin acceptor peptide (BAP)-tagged fusion proteins, and (B) strains producing *E.coli* BirA in the mother cell (MC) and the forespore (FS). Compartmentalized biotinylation of SpoIIID-BAP (C) and σ^G-BAP (D). Top panels of (C) and (D) are streptavidin-HRP western blots with lysates prepared at t_3 (SpoIIID-BAP) and t_4 (σ^G-BAP). Lysates were prepared from strains producing different combinations of the indicated BAP-tagged fusion protein and BirA in the mother cell, the forespore, or not at all. Bottom panels are streptavidin western blots, with the same lysates as the top panels, comparing levels of biotinyl-biotin carboxyl carrier protein (BCCP).

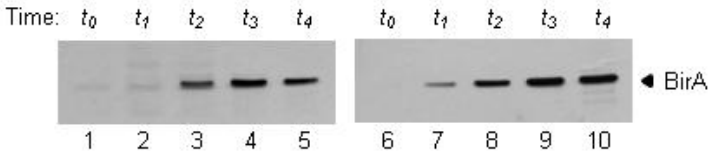

Figure 3. Western blot analysis of BirA accumulation. Anti-BirA antiserum was used in western blots to detect BirA accumulation at hourly intervals after the onset of sporulation in a P_{spoIID}-*birA* (lanes 1 -5) or P_{spoIIQ}-*birA* expressing strain (lanes 6 - 10).

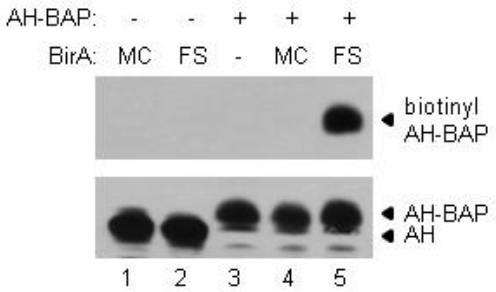

Figure 4. Forespore-specific biotinylation of C-terminal BAP-tagged SpoIIIAH. Top panel is a streptavidin-HRP western blot with lysates prepared at t_3 from strains producing combinations of SpoIIIAH-BAP and BirA produced in the mother cell, the forespore, or not at all. Bottom panel is an anti-SpoIIIAH western blot with the same lysates as the top panel.

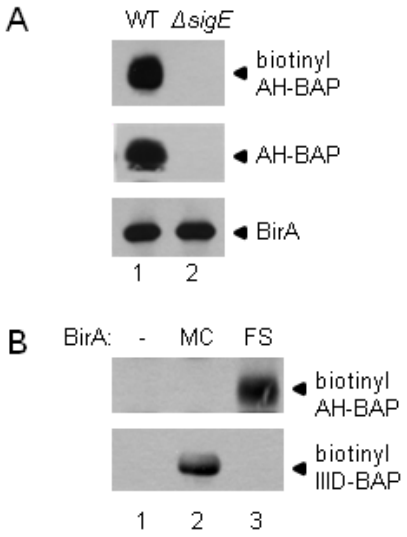

Figure 5. Compartmentalization of SpoIIIAH-BAP production and BirA activity. (A) SpoIIIAH-BAP biotinylation in WT (lane 1) and *sigE* (lane 2) strains producing BirA in the forespore. Streptavidin-HRP (top panel), anti-SpoIIIAH (middle panel), and anti-BirA (bottom panel) western blots with lysates prepared at t_3. (B) Compartmentalized biotinylation of SpoIIIAH-BAP (top panel) and SpoIIID-BAP (bottom panel) in the same strains. Lysates were prepared at t_3 and analyzed by streptavidin-HRP western blots.

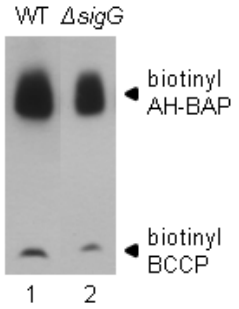

Figure 6. Forespore-specific biotinylation of SpoIIIAH-BAP in a *sigG* mutant. SpoIIIAH-BAP biotinylation in WT (lane 1) and *sigG* (lane 2) strains producing BirA in the forespore. Streptavidin-HRP western blot with lysates prepared at t_3.

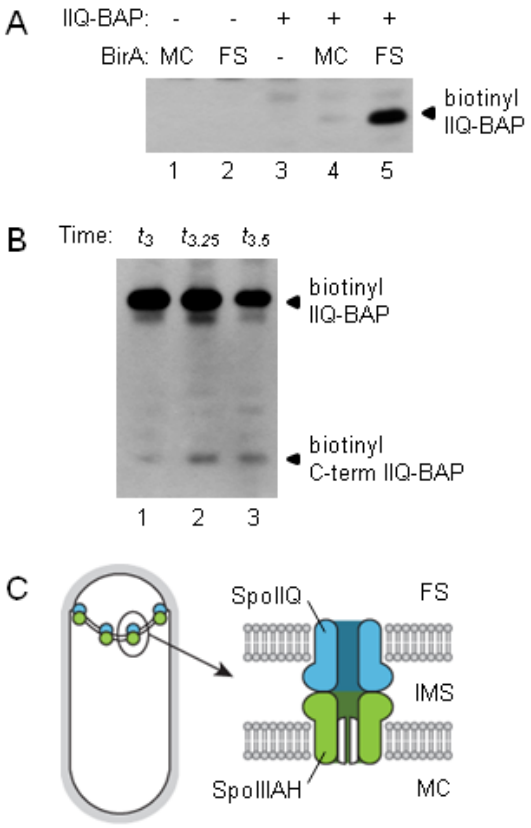

Figure 7. Forespore-specific biotinylation of C-terminal BAP-tagged SpoIIQ.

(A) Streptavidin-HRP western blot with lysates prepared at t_3 from strains producing combinations of SpoIIQ-BAP and BirA produced in the mother cell, the forespore, or not at all. (B) Biotinyl-SpoIIQ-BAP proteolysis. Lysates prepared at t_3 (lane 1), $t_{3.25}$ (lane 2), and $t_{3.5}$ (lane 3). (C) SpoIIIAH-SpoIIQ channel model. (Left) SpoIIIAH and SpoIIQ track along the engulfing membrane and colocalize in discrete foci surrounding the forespore. (Right) The C-terminal extracellular domains of SpoIIIAH and SpoIIQ interact in the intermembrane space and form a channel that is open at the forespore end and closed (or gated) at the mother cell end.

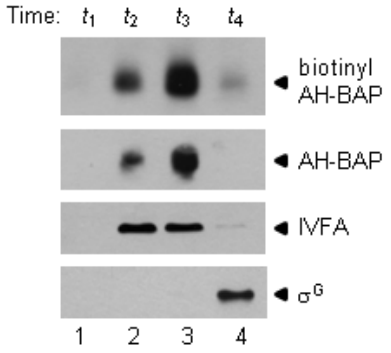

Figure 8. Degradation of biotinyl-SpoIIIAH-BAP after engulfment. Lysates prepared hourly between t_1 and t_4 were analyzed by streptavidin-HRP (top panel), anti-SpoIIIAH antibody (second panel from top), anti-SpoIVFA (third panel), and anti-σ^G (bottom panel) western blot.

TABLES

Table 1. Bacterial strains

Strain	Relevant genotype	Source or Reference
JH642	*trpC2 pheA1*	J. Hoch
XWB11	*amyE::P$_{spoIID}$-birA*	This study
XWB10	*amyE::P$_{spoIIQ}$-birA*	This study
XWB13	*spoIIID-BAP*	This study
XWB15	*amyE::P$_{spoIID}$-birA spoIIID-BAP*	This study
XWB16	*amyE::P$_{spoIIQ}$-birA spoIIID-BAP*	This study
XWB27	*sigG-BAP*	This study
XWB29	*amyE::P$_{spoIID}$-birA sigG-BAP*	This study
XWB28	*amyE::P$_{spoIIQ}$-birA sigG-BAP*	This study
XWB49	*spoIIIAH-BAP*	This study
XWB50	*amyE::P$_{spoIID}$-birA spoIIIAH-BAP*	This study
XWB51	*amyE::P$_{spoIIQ}$-birA spoIIIAH-BAP*	This study
CGB182	*sigE::spc*	C. Guillot
JMB233	*amyE::P$_{spoIIQ}$-birA spoIIIAH-BAP sigE::spc*	This study
XWB91	*spoIIIAH-BAP spoIIID-BAP*	This study
XWB92	*amyE::P$_{spoIIQ}$-birA spoIIIAH-BAP spoIIID-BAP*	This study
XWB93	*amyE::P$_{spoIIQ}$-birA spoIIIAH-BAP spoIIID-BAP*	This study
XWB88	*spoIID-BAP*	This study
XWB89	*amyE::P$_{spoIID}$-birA spoIID-BAP*	This study
XWB90	*amyE::P$_{spoIIQ}$-birA spoIID-BAP*	This study
BDR364	PY79 *spoIVFAΔ91*	(36)
JMB311	*spoIVFAΔ91 thrC::spoIVFA-BAP*	This study
BMA2	PY79 *spoIVFA::spc*	(31)
JMB264	*spoIVF::spc thrC::spoIVFA-BAP*	This study
JMB265	*amyE::P$_{spoIID}$-birA spoIVF::spc thrC::spoIVFA-BAP*	This study
JMB266	*amyE::P$_{spoIIQ}$-birA spoIVF::spc thrC::spoIVFA-BAP*	This study
XWB46	*spoIIQ-BAP*	This study
XWB48	*amyE::P$_{spoIID}$-birA spoIIQ-BAP*	This study
XWB47	*amyE::P$_{spoIIQ}$-birA spoIIQ-BAP*	This study
KP575	*spoIIQ::spc*	(42)

XWB69	*amyE::P$_{spoIIQ}$-birA spoIIIAH-BAP spoIIQ::spc*	This study
KP719	PY79 *spoIIP::tet*	(1)
RL826	PY79 *spoIID::Tn917ΩHU298*	(34)
JMB325	*amyE::P$_{spoIIQ}$-birA spoIIIAH-BAP spoIIP::tet spoIID::Tn917ΩHU298*	This study

Table 2. Plasmids

Plasmid	Description/genotype	Source or Reference
pDG1662	Integration of cloned insert and chloramphenicol resistance cassette at *amyE* locus	(13)
pBEST501	Integration of neomycin resistance cassette at cloned locus	(16)
pDG1515	Integration of tetracycline resistance cassette at cloned locus	(14)
pDG1664	Integration of cloned insert and erythromycin resistance cassette at *thrC* locus	(13)
pIIDbirA	pDG1662 P_{spoIID}-*birA-his*$_6$	This study
pIIQbirA	pDG1662 P_{spoIIQ}-*birA-his*$_6$	This study
pIIIDBAP	pBEST501 *'spoIIID-BAP*	This study
pIIIGBAP	pBEST501 *'sigG-BAP*	This study
pAHBAP	pBEST501 *'spoIIIAH-BAP*	This study
pIIIDBAPtet	pDG1515 *'spoIIID-BAP*	This study
pIIDBAP	pBEST501 *'spoIID-BAP*	This study
pIVFABAP	pDG1664 *spoIVFA-BAP*	This study
pIIQBAP	pBEST501 *'spoIIQ-BAP*	This study

Table 3. Oligonucleotide primers

Primer	Sequence
IIQFW	CGGGATCCCGGCCATAAGTGAGCGGATGCCAAG
IIQRV	TGTTATCCTTCATTGTTTCATCACCTCAGCA
QbirAFW	ATGAAACAATGAAGGATAACACCGTGCCACTG
birAhisRV	GGAATTCCTTAATGATGATGATGATGATGTTTTTCTGCACTACGCAGGGATA
IIDFW	CGGGATCCCGCCGCCGTATGAATGGTGATA
IIDRV	CGGTGTTATCCTTCATATTCAGCTGCCTCCTGCTCG
DbirAFW	GGAGGCAGCTGAATATGAAGGATAACACCGTGCCACTG
IIIDFW	ACATGCATGCTTTTACAGGAGCGATCAATA
IIIDBAPRV	CGATTTTTTGAGCTTCGAAGATGTCGTTAAGTCCCGATTGCTGAACAGGCTCTC
BAPRV1	CCAATGCATTGGTTCTGCAGTTAATGCCATTCGATTTTTTGAGCTTCGAAGATGTCG
IIIGFW	ACCTCCAAATTACCAGTACT
IIIGBAPRV	TTTTGAGCTTCGAAGATGTCGTTAAGTCCTTGATGAATATTTTTATTCA
BAPRV3	ACATGCATGCTTAATGCCATTCGATTTTTTGAGCTTCGAAGATGTCGTTAAG
spoIIIAHF1	CCCAAGCTTCTATATCATGTCGCCGGAAAGC
spoIIIAHR2	CGATTTTTTGAGCTTCGAAGATGTCGTTAAGTCCTTTAGAGGGTTCAAATGTGACAGCG
IIDFW1	ACATGCATGCAGCCGATTGAAGCATCCTTT
IIDBAPRV	TTTTGAGCTTCGAAGATGTCGTTAAGTCCCTTTTTCGCCATATATTTAT
IVFAFW1	CGGGATCCCTGACCGTATTATAGGACTG
IVFARV2	TTTTGAGCTTCGAAGATGTCGTTAAGTCCTTCAAATGAAATCA
BAPRV2	GGAATTCTTAATGCCATTTCGATTTTTTGAGCTTCGAAGATGTCGTTAAG
spoIIQF4	ACATGCATGCTCGCAATGCCGGTTGTTGATTCTG
spoIIQR2	CGATTTTTTGAGCTTCGAAGATGTCGTTAAGTCCAGACTGTTCAGTGTCTTCTGTTGTGC

Table 4. Sporulation efficiencies of strains carrying BAP-tagged alleles

Relevant genotype	Sporulation efficiency
Wild-type	0.65
ΔspoIIIAH	0.013
spoIIIAH-BAP	0.35
ΔspoIIQ::tet	1.0×10^{-6}
spoIIQ-BAP	0.28
ΔspoIID::Tn917ΩHU298	4.6×10^{-6}
spoIID-BAP	0.23
spoIVFAΔ91	0.07
spoIVFAΔ91 thrC::spoIVFA-BAP	0.6

REFERENCES

1. **Abanes-De Mello, A., Y. L. Sun, S. Aung, and K. Pogliano.** 2002. A cytoskeleton-like role for the bacterial cell wall during engulfment of the Bacillus subtilis forespore. Genes Dev **16:**3253-3264.

2. **Beckett, D., E. Kovaleva, and P. J. Schatz.** 1999. A minimal peptide substrate in biotin holoenzyme synthetase-catalyzed biotinylation. Protein Sci **8:**921-929.

3. **Blaylock, B., X. Jiang, A. Rubio, C. P. Moran, Jr., and K. Pogliano.** 2004. Zipper-like interaction between proteins in adjacent daughter cells mediates protein localization. Genes Dev **18:**2916-2928.

4. **Camp, A. H., and R. Losick.** 2008. A novel pathway of intercellular signalling in Bacillus subtilis involves a protein with similarity to a component of type III secretion channels. Mol Microbiol **69:**402-417.

5. **Campo, N., and D. Z. Rudner.** 2006. A branched pathway governing the activation of a developmental transcription factor by regulated intramembrane proteolysis. Mol Cell **23:**25-35.

6. **Chiba, S., K. Coleman, and K. Pogliano.** 2007. Impact of membrane fusion and proteolysis on SpoIIQ dynamics and interaction with SpoIIIAH. J Biol Chem **282:**2576-2586.

7. **Cornelis, G. R.** 2006. The type III secretion injectisome. Nat Rev Microbiol **4:**811-825.

8. **Cronan, J. E., Jr.** 1989. The E. coli bio operon: transcriptional repression by an essential protein modification enzyme. Cell **58:**427-429.

9. **Doan, T., K. A. Marquis, and D. Z. Rudner.** 2005. Subcellular localization of a sporulation membrane protein is achieved through a network of interactions along and across the septum. Mol Microbiol **55:**1767-1781.

10. **Dong, T. C., and S. M. Cutting.** 2003. SpoIVB-mediated cleavage of SpoIVFA could provide the intercellular signal to activate processing of Pro-sigmaK in Bacillus subtilis. Mol Microbiol **49:**1425-1434.

11. **Driks, A., and R. Losick.** 1991. Compartmentalized expression of a gene under the control of sporulation transcription factor sigma E in Bacillus subtilis. Proc Natl Acad Sci U S A **88:**9934-9938.

12. **Galan, J. E., and A. Collmer.** 1999. Type III secretion machines: bacterial devices for protein delivery into host cells. Science **284:**1322-1328.

13. **Guerout-Fleury, A. M., N. Frandsen, and P. Stragier.** 1996. Plasmids for ectopic integration in Bacillus subtilis. Gene **180:**57-61.

14. **Guerout-Fleury, A. M., K. Shazand, N. Frandsen, and P. Stragier.** 1995. Antibiotic-resistance cassettes for Bacillus subtilis. Gene **167:**335-336.

15. **Hilbert, D. W., and P. J. Piggot.** 2004. Compartmentalization of gene expression during Bacillus subtilis spore formation. Microbiol Mol Biol Rev **68:**234-262.

16. **Itaya, M., K. Kondo, and T. Tanaka.** 1989. A neomycin resistance gene cassette selectable in a single copy state in the Bacillus subtilis chromosome. Nucleic Acids Res **17:**4410.

17. **Jiang, X., A. Rubio, S. Chiba, and K. Pogliano.** 2005. Engulfment-regulated proteolysis of SpoIIQ: evidence that dual checkpoints control sigma activity. Mol Microbiol **58:**102-115.

18. **Kihara, M., T. Minamino, S. Yamaguchi, and R. M. Macnab.** 2001. Intergenic suppression between the flagellar MS ring protein FliF of Salmonella and FlhA, a membrane component of its export apparatus. J Bacteriol **183:**1655-1662.

19. **Kimbrough, T. G., and S. I. Miller.** 2002. Assembly of the type III secretion needle complex of Salmonella typhimurium. Microbes Infect **4:**75-82.

20. **Kunkel, B., L. Kroos, H. Poth, P. Youngman, and R. Losick.** 1989. Temporal and spatial control of the mother-cell regulatory gene spoIIID of Bacillus subtilis. Genes Dev **3:**1735-1744.

21. **Lane, M. D., D. L. Young, and F. Lynen.** 1964. The Enzymatic Synthesis of Holotranscarboxylase from Apotranscarboxylase and (+)-Biotin. I. Purification of the Apoenzyme and Synthetase; Characteristics of the Reaction. J Biol Chem **239:**2858-2864.

22. **Londono-Vallejo, J. A., C. Frehel, and P. Stragier.** 1997. SpoIIQ, a forespore-expressed gene required for engulfment in Bacillus subtilis. Mol Microbiol **24:**29-39.

23. **Macnab, R. M.** 2003. How bacteria assemble flagella. Annu Rev Microbiol **57:**77-100.

24. **Marini, P., S. J. Li, D. Gardiol, J. E. Cronan, Jr., and D. de Mendoza.** 1995. The genes encoding the biotin carboxyl carrier protein and biotin carboxylase

subunits of Bacillus subtilis acetyl coenzyme A carboxylase, the first enzyme of fatty acid synthesis. J Bacteriol **177:**7003-7006.

25. **Minamino, T., and R. M. Macnab.** 1999. Components of the Salmonella flagellar export apparatus and classification of export substrates. J Bacteriol **181:**1388-1394.

26. **Minamino, T., and R. M. MacNab.** 2000. Interactions among components of the Salmonella flagellar export apparatus and its substrates. Mol Microbiol **35:**1052-1064.

27. **Piggot, P. J., and J. G. Coote.** 1976. Genetic aspects of bacterial endospore formation. Bacteriol Rev **40:**908-962.

28. **Piggot, P. J., and D. W. Hilbert.** 2004. Sporulation of Bacillus subtilis. Curr Opin Microbiol **7:**579-586.

29. **Planet, P. J., S. C. Kachlany, R. DeSalle, and D. H. Figurski.** 2001. Phylogeny of genes for secretion NTPases: identification of the widespread tadA subfamily and development of a diagnostic key for gene classification. Proc Natl Acad Sci U S A **98:**2503-2508.

30. **Pogliano, J., N. Osborne, M. D. Sharp, A. Abanes-De Mello, A. Perez, Y. L. Sun, and K. Pogliano.** 1999. A vital stain for studying membrane dynamics in bacteria: a novel mechanism controlling septation during Bacillus subtilis sporulation. Mol Microbiol **31:**1149-1159.

31. **Prince, H., R. Zhou, and L. Kroos.** 2005. Substrate requirements for regulated intramembrane proteolysis of Bacillus subtilis pro-sigmaK. J Bacteriol **187:**961-971.

32. **Pugsley, A. P.** 1993. The complete general secretory pathway in gram-negative bacteria. Microbiol Rev **57:**50-108.

33. **Py, B., L. Loiseau, and F. Barras.** 2001. An inner membrane platform in the type II secretion machinery of Gram-negative bacteria. EMBO Rep **2:**244-248.

34. **Resnekov, O., S. Alper, and R. Losick.** 1996. Subcellular localization of proteins governing the proteolytic activation of a developmental transcription factor in Bacillus subtilis. Genes Cells **1:**529-542.

35. **Rudner, D. Z., and R. Losick.** 2001. Morphological coupling in development: lessons from prokaryotes. Dev Cell **1:**733-742.

36. **Rudner, D. Z., and R. Losick.** 2002. A sporulation membrane protein tethers the pro-sigmaK processing enzyme to its inhibitor and dictates its subcellular localization. Genes Dev **16:**1007-1018.

37. **Sekiya, K., M. Ohishi, T. Ogino, K. Tamano, C. Sasakawa, and A. Abe.** 2001. Supermolecular structure of the enteropathogenic Escherichia coli type III secretion system and its direct interaction with the EspA-sheath-like structure. Proc Natl Acad Sci U S A **98:**11638-11643.

38. **Sharp, M. D., and K. Pogliano.** 1999. An in vivo membrane fusion assay implicates SpoIIIE in the final stages of engulfment during Bacillus subtilis sporulation. Proc Natl Acad Sci U S A **96:**14553-14558.

39. **Soding, J.** 2005. Protein homology detection by HMM-HMM comparison. Bioinformatics **21:**951-960.

40. **Soding, J., A. Biegert, and A. N. Lupas.** 2005. The HHpred interactive server for protein homology detection and structure prediction. Nucleic Acids Res **33:**W244-248.

41. **Sun, D. X., R. M. Cabrera-Martinez, and P. Setlow.** 1991. Control of transcription of the Bacillus subtilis spoIIIG gene, which codes for the forespore-specific transcription factor sigma G. J Bacteriol **173:**2977-2984.

42. **Sun, Y. L., M. D. Sharp, and K. Pogliano.** 2000. A dispensable role for forespore-specific gene expression in engulfment of the forespore during sporulation of Bacillus subtilis. J Bacteriol **182:**2919-2927.

43. **Suzuki, H., K. Yonekura, K. Murata, T. Hirai, K. Oosawa, and K. Namba.** 1998. A structural feature in the central channel of the bacterial flagellar FliF ring complex is implicated in type III protein export. J Struct Biol **124:**104-114.

44. **Tian, H., D. Boyd, and J. Beckwith.** 2000. A mutant hunt for defects in membrane protein assembly yields mutations affecting the bacterial signal recognition particle and Sec machinery. Proc Natl Acad Sci U S A **97:**4730-4735.

45. **Wilson, K. P., L. M. Shewchuk, R. G. Brennan, A. J. Otsuka, and B. W. Matthews.** 1992. Escherichia coli biotin holoenzyme synthetase/bio repressor crystal structure delineates the biotin- and DNA-binding domains. Proc Natl Acad Sci U S A **89:**9257-9261.

46. **Yip, C. K., T. G. Kimbrough, H. B. Felise, M. Vuckovic, N. A. Thomas, R. A. Pfuetzner, E. A. Frey, B. B. Finlay, S. I. Miller, and N. C. Strynadka.** 2005.

Structural characterization of the molecular platform for type III secretion system assembly. Nature **435:**702-707.

CHAPTER 3. A LytM domain dictates the localization of proteins to the mother cell-forespore interface

The data presented in this chapter were published in the following manuscript:

Meisner, J., and C.P. Moran, Jr. 2010. A LytM domain dictates the localization of proteins to the mother cell-forespore interface during bacterial endospore formation. J Bacteriol, in press.

J.M. and C.P.M. designed the experiments. J.M. performed the experiments. J.M. and C.P.M wrote the manuscript.

INTRODUCTION

The assembly of bacterial proteins at specific subcellular locations is important for numerous behaviors including motility and chemotaxis, cell division, cell differentiation, multicellularity and cell-cell interactions (reviewed in 25). Elucidation of the mechanisms that determine the subcellular localization of proteins is a fundamental issue in biology. Generally, a so-called founder protein recognizes a subcellular location and then other proteins are anchored there through interactions (either direct or indirect) with the founder protein (reviewed in 23). One of the principle challenges is to understand what positional cues dictate the localization of founder proteins.

SpoIIIAH is an example of a founder protein that localizes to a cell-cell interface by interacting with a protein in the adjacent cell during endospore formation in the Gram positive bacterium *Bacillus subtilis*. During sporulation, cells divide asymmetrically, giving rise to two adjacent daughter cells of dissimilar size, called the mother cell and forespore. As the peptidoglycan within the division septum is hydrolyzed, the mother cell septal membrane is wrapped around the forespore in a process called forespore engulfment. Once this process is completed, the forespore is released into the mother cytoplasm where it matures into a dormant and resistant spore. The mother cell produces several membrane proteins that localize to the mother cell–forespore interface and control the transition from forespore engulfment to maturation. The mother cell membrane protein SpoIIIAH recognizes this location through the interaction of its extracellular domain with that of the forespore membrane protein SpoIIQ (5, 10). Although SpoIIIAH is inserted randomly into the mother cell membrane,

it diffuses laterally and is captured at the mother cell-forespore interface by SpoIIQ (Figure 1A). The SpoIIIAH-SpoIIQ complex then helps to anchor three mother cell protein sub-complexes. The first sub-complex (SpoIIIAB, SpoIIIAC, SpoIIIAD, SpoIIIAE, SpoIIIAF, and SpoIIIAG) is required for the activation of late forespore gene expression, whereas the second (SpoIVFA, SpoIVFB, and BofA) controls the activation of late mother cell gene expression (Figure 1B) (3, 10, 11, 24). SpoIIQ-SpoIIIAH and SpoIVFA-SpoIVFB provide a secondary pathway to anchor the third sub-complex (SpoIIM, SpoIIP, and SpoIID) which mediates septal peptidoglycan hydrolysis (3, 10, 11, 24). Since the SpoIIIAH-SpoIIQ complex defines the mother cell-forespore interface and controls forespore development, we sought to understand the molecular basis of the SpoIIIAH-SpoIIQ interaction.

SpoIIIAH is an integral membrane protein containing an N-terminal transmembrane segment and a C-terminal extracellular domain. The extracellular domain (residues 25-218) shares similarity with YscJ-FliF family proteins (PF01514) that form the inner membrane structures of the protein export apparatuses of type III secretion systems and flagella in Gram negative bacteria (7, 15, 19, 29). The YscJ domain contains a mixed α/β fold with two α-helices packed on one side of a three-stranded β-sheet (31). Since this fold is conserved in the other core component of the inner membrane structure (YscD), it was proposed to be a structural motif for the assembly of symmetric ring structures (27). In addition to a C-terminal YscJ domain (residues 132-218), the extracellular domain has an N-terminal region (residues 25-95) lacking any

predicted secondary structure followed by a predicted β-strand (residues 96-99) and α-helix (residues 102-128) (Figure 1C).

SpoIIQ is also an integral membrane protein containing an N-terminal transmembrane segment and a C-terminal extracellular domain. The extracellular domain (residues 43-283) consists of a predicted LytM domain (residues 89-220) with a degenerate active site and extensions at both the N- and C-termini (residues 43-88 and 221-283, respectively) (Figure 1D) (7, 17, 19, 28). Bacterial LytM proteins are typically metalloendopeptidases (peptidase M23 family) that cleave the peptide cross-bridges of the peptidoglycan cell wall (12). LytM domains consist of a core six-stranded β-sheet with four loops that form two walls that line either side of a central groove extending the length of the domain (13, 22). The LytM active site is organized around a divalent metal cation (Zn^{2+}). The three Zn^{2+} ligands, two histidines and an aspartate (H210, D214, and H293 by *S. aureus* LytM numbering) occur in two short sequence motifs, HXXXD and HXH (where X is any amino acid). These residues allow Zn^{2+} to polarize the carbonyl carbon of the substrate for susceptibility to nucleophilic attack. A hydroxyl nucleophile generated by His247-mediated deprotonation of water was proposed to facilitate hydrolysis because His247 is close to the carbonyl group and in the same plane, while His291 is farther from the carbonyl group and off axis compared with His247 (*S. aureus* LytM numbering) (9). SpoIIQ contains only two of the three Zn^{2+} ligands (D123 and H204 by *B. subtilis* SpoIIQ numbering) and lacks the proposed catalytic His (Figures 1D and 2). Therefore, SpoIIQ contains a degenerate and probably catalytically inactive LytM domain.

Recently, an alternative function for degenerate LytM proteins was proposed. *Escherichia coli* produces two degenerate LytM proteins (EnvC and NlpD) that regulate peptidoglycan hydrolases (amidases AmiA, AmiB, and AmiC) (30). Although the LytM-amidase regulatory mechanism is unknown, a protein-protein interaction could either anchor the amidases at the cell division site or allosterically activate the amidase. A well-characterized example of a LytM domain that engages in a protein-protein interaction is the lysostaphin-type enzyme, *Staphylococcus aureus* LytM. Lysostaphin-type enzymes are produced in a latent form that is held inactive by their N-terminal segments. In the X-ray crystal structure of latent *S. aureus* LytM, the Zn^{2+} is tetrahedrally coordinated by the three residues mentioned above and an asparagine (N117) in the inhibitory segment, rendering the metal center catalytically inactive (22). The protein structure also shows that the inhibitory segment binds within the central LytM groove. Thus, degenerate LytM proteins may use their central grooves for protein-protein interactions similar to latent lystostaphin-type enzymes.

In this study, we used purified proteins to test the hypothesis that the extracellular domains of SpoIIIAH and SpoIIQ interact and form a complex through the interaction of their YscJ and LytM domains, respectively.

MATERIALS AND METHODS

Protein expression and purification

Various regions from *spoIIIAH* and *spoIIQ* were amplified by polymerase chain reaction (PCR) from *B. subtilis* strain JH642 chromosomal DNA and ligated into pET14b

(Novagen) at *NdeI*/*BamHI* or *NdeI*/*XhoI* restriction sites. The oligonucleotide primers and plasmids used in this work are shown in Tables 1 and 2. Each plasmid contained a coding sequence with an N-terminal hexahistidine (His) tag and thrombin cleavage site. SpoIIQ and SpoIIIAH expression was induced with 0.5 mM isopropyl-1-thio-β-D-galactopyranoside (IPTG) in *Escherichia coli* BL21 Star (DE3) (Invitrogen) cultures grown at 37°C in LB medium supplemented with ampicillin (100 μg/ml). The strains are shown in Table 3. Cells were disrupted by passage through a French press (15,000 lb/in^2) and the resulting lysates were centrifuged at 10,000 X g for 10 minutes. His-tagged proteins were purified on a 1 ml HisTrap FF column (GE Healthcare) using an AKTAexplorer 10 (GE Healthcare). His-tagged proteins were dialyzed at 4°C in 50 mM Tris, 100 mM NaCl, 2 mM β-mercaptoethanol (βME), pH 7.5. Proteins were then incubated with 100 units of thrombin protease (GE Healthcare) at room temperature for 2 hours to remove the His tags. Untagged proteins were purified on 1 ml HiTrap Benzamidine FF and 1 ml HisTrap columns (GE Healthcare), followed by a HiLoad 16/60 Superdex 75 prep grade gel filtration column (GE Healthcare). Protein concentrations were measured using a Bradford assay (Bio-Rad). The identity of each purified protein was confirmed by tryptic peptide fingerprint generated by matrix-assisted laser desorption ionization mass spectrometry (Targeted Metabolomics and Proteomics Laboratory, University of Alabama, Birmingham).

Gel filtration chromatography

Proteins were concentrated to 100-200 μM using Amicon Ultra centrifugal filters (Millipore). 200 μl of each test protein were mixed or diluted into 200 μl of 50 mM Tris,

100 mM NaCl, 2 mM βME, pH 7.5 and incubated on ice for 1 hour. Proteins were then loaded into a 100 µl sample loop and injected onto a Superdex 200 10/300 GL high resolution gel filtration column (GE Healthcare) in 50 mM Tris, 100 mM NaCl, 2 m βME, pH 7.5. Elution of the proteins was monitored by UV absorbance at 280 and 230 nm. 500 µl fractions were collected and analyzed by SDS-polyacrylamide gel electrophoresis (PAGE) and Coomassie blue staining.

Isothermal titration calorimetry (ITC)

ITC experiments were performed with a VT-ITC instrument and the data were processed with the Origin 7.0 software (MicroCal). Both the SpoIIQ and SpoIIIAH proteins were extensively dialyzed together in the same buffer to minimize thermal effects from differences in solutions components. In order to minimize artifactual heats of buffer ionization, the experiments were performed in sodium phosphate buffer (at pH 7.5 with 100 mM NaCl), which has a low heat of ionization (ΔH_{ion} = 0.9 kcal/mol at 25°C). Proteins were placed into the sample cell at a concentration of 15 µM, while proteins were loaded into the syringe at 150 µM. Each experiment consisted of an initial test injection of 5 µl followed by 28 injections of 10 µl into the sample cell at 25°C (29 total injections). Each injection was made over a 10 second interval and spaced 180 seconds apart to allow baseline re-equilibration. Throughout the titrations, the sample cell was stirred at 300 rpm. The heat associated with dilution of the injected protein was measured from the baseline at saturation and subtracted during data processing to correct the binding enthalpy for the heat of dilution.

Peptidoglycan co-sedimentation assay

B. subtilis was grown in 100 ml LB medium at 37°C to mid-expontential phase (OD_{600} = 0.5) and vegetative peptidoglycan was purified according to the protocol provided by David Popham. The culture was chilled in an ice bath for 5 minutes, centrifuged, and the cell pellet was resuspended in 2 ml cold water. The suspension was dripped into 50 ml boiling, stirring 4% SDS over a period of 1-2 minutes. Boiling was continued for another 30 minutes and water was added to maintain a volume of 50 ml. The solution was cooled to room temperature and centrifuged at 7,000 X g for 6 minutes at room temperature. Then it was washed 4 times with 20 ml water at 60°C. The pellet was resuspended in 1 ml 100mM Tris pH 7.4, 10 μg DNase, 50 μg RNase, 20 mM $MgSO_4$ and incubated at 37°C for 2 hours. 100 μl 1 mg/ml trypsin in 100 mM $CaCl_2$ was added and the solution was incubated at 37°C overnight. The peptidoglycan was 3 times with 1 ml water and resuspended in 1 ml water. 25 μl peptidoglycan and 15 μl of 100 mM Tris, 100 mM NaCl, 2 mM βME, pH 7.5 was added to 10 μl of 100 μM SpoIIQ43-283, lysozyme, or BSA (in 100 mM Tris, 100 mM NaCl, 2 mM βME, pH 7.5). The reactions were incubated on ice for 30 minutes and then centrifuged for 1 minute. The supernatant was collected and the pellet was resuspended in 50 μl 100 mM Tris, 100 mM NaCl, 2 mM βME, pH 7.5. Each fraction was analyzed by SDS-PAGE and Coomassie blue staining.

RESULTS

SpoIIIAH and SpoIIQ interact directly *in vitro*

To begin to understand the molecular basis of the SpoIIIAH-SpoIIQ interaction, we expressed and purified the extracellular domains of SpoIIIAH and SpoIIQ (SpoIIIAH25-218 and SpoIIQ43-283, respectively) as described in the Materials and Methods, and analyzed their interaction by gel filtration chromatography (Figures 3A and B). Elution of the proteins from the column was monitored by UV absorbance and subsequently confirmed by SDS-polyacrylamide gel electrophoresis (PAGE). Apparent molecular weights of the proteins were determined by comparing their elution volumes with those obtained for several standard proteins. SpoIIIAH25-218 eluted with an apparent molecular weight of 60 kDa. Whereas this protein has a predicted molecular weight of 21 kDa, its apparent molecular weight by SDS-PAGE is 32 kDA. Similarly, SpoIIQ43-283 eluted with an apparent molecular weight of 67 kDa, while its predicted and apparent molecular weight by SDS-PAGE are 26 and 35 kDa, respectively. Thus, both SpoIIIAH25-218 and SpoIIQ43-283 behaved as dimers in gel filtration chromatography. To determine the molecular weight of the protein-protein complex, SpoIIIAH25-218 and SpoIIQ43-283 were mixed and analyzed by gel filtration chromatography. The SpoIIIAH25-218 - SpoIIQ43-283 complex eluted with an apparent molecular weight of 150 kDa, slightly larger than the sum of the molecular weights observed for the individual proteins. Therefore, SpoIIIAH25-218 and SpoIIQ43-283 formed a heterotetrameric complex, a dimer of dimers, in gel filtration chromatography.

To confirm the stoichiometry of the SpoIIIAH25-218 - SpoIIQ43-283 complex observed by gel filtration chromatography, we analyzed the complex by isothermal titration calorimetry (Figure 3C). This experiment allowed direct measurements of the protein complex in solution. The observed stoichiometry (n) was approximately 1.0. In addition to stoichiometry, we also measured an apparent binding constant (K_a) and enthalpy of about 5 X 10^6 M^{-1} (K_d = 2 X 10^{-7} M) and -38 kcal/mol, respectively. To gain insight into the mechanism of SpoIIIAH-SpoIIQ complex formation, we calculated the Gibbs free energy change ($\Delta G = - RT \ln K_a$ = -9 kcal/mol) and entropy ($-T\Delta S = \Delta G - \Delta H$ = 29 kcal/mol) of the protein-protein interaction. As indicated by the favorable enthalpy and unfavorable entropy, the complex appears to be driven by polar interactions and may involve conformation changes in one or both proteins.

YscJ domain of SpoIIIAH interacts with SpoIIQ

The combination of gel filtration chromatography and isothermal titration calorimetry was used to assess which portions of SpoIIIAH extracellular domain were necessary and sufficient for the interaction with SpoIIQ. First, we tested whether the N-terminal region which lacks predicted secondary structure (residues 25-89) was necessary for the interaction. To do so, we purified SpoIIIAH90-218 and analyzed its interaction with SpoIIQ43-283 by gel filtration chromatography (Figure 4A). SpoIIIAH90-218 interacted with SpoIIQ43-283. Analysis of these proteins by isothermal titration calorimetry indicated that the stoichiometry and binding affinity were indistinguishable from those observed with the full-length SpoIIIAH25-218 (Table 4).

Therefore, the unstructured N-terminal region of SpoIIIAH was dispensable for the interaction with SpoIIQ.

Next, we tested whether the YscJ domain (residues 132-218) was sufficient for the interaction with SpoIIQ. We purified SpoIIIAH132-218 and analyzed its interaction with SpoIIQ43-283 by gel filtration chromatography (Figure 4B). SpoIIIAH132-218 interacted with SpoIIQ43-283, indicating that the YscJ domain was sufficient for the interaction. The isothermal titration calorimetry data, however, showed a 4-fold reduction in the binding affinity of SpoIIIAH132-218 compared to the SpoIIIAH25-218 (Table 4). Therefore, while the YscJ domain is sufficient for the interaction with SpoIIQ, the adjacent N-terminal region also contributes to the interaction.

LytM domain of SpoIIQ is sufficient for the interaction with SpoIIIAH

In parallel with the experiments described above, we determined which regions of the SpoIIQ extracellular domain were necessary and sufficient for the SpoIIIAH. To test whether the LytM domain (residues 89-220) was sufficient for the formation of the SpoIIIAH-SpoIIQ complex, we purified a truncated SpoIIQ (SpoIIQ73-220) that lacked the N- and C-terminal extensions and analyzed its interaction with SpoIIIAH25-218 (Figures 5A and B). We chose Gly73 at the N-terminus of this truncation because it is the site of SpoIVB-dependent proteolysis *in vivo* (8), which suggests that this region may not be stably folded into the predicted LytM domain. SpoIIQ73-220 interacted with SpoIIIAH25-218 in gel filtration chromatography and the binding affinity measured by isothermal titration calorimetry was only reduced 2.75-fold compared to full-length

SpoIIQ43-283 (Table 5). Thus, the LytM domain was sufficient and both extensions were dispensable for the interaction with SpoIIIAH.

To test whether the complete LytM domain was necessary for the formation of the complex, we analyzed the interaction of two truncated proteins, SpoIIQ114-220 and SpoIIQ73-208, lacking either N- or C-terminal portions of the LytM domain, respectively (Figure 5A, C, and D). Both proteins were abundantly expressed, soluble and eluted as discrete peaks in gel filtration chromatography, suggesting that they were stably folded. Neither SpoIIQ114-220 nor SpoIIQ73-208 interacted with SpoIIIAH25-218 by gel filtration chromatography, indicating that both loops are necessary for the complex to form. Consistent with these data, we did not detect binding of either protein to SpoIIIAH25-218 by isothermal titration chromatography (Table 5). Thus, the complete LytM domain is necessary for the interaction with SpoIIIAH. Together with data from the SpoIIIAH truncations, these results suggest that the YscJ and LytM domains mediate the formation of the SpoIIIAH-SpoIIQ complex.

Typically, LytM proteins bind and hydrolyze peptidoglycan. So we tested whether SpoIIQ was able to bind peptidoglycan. To this end, we used a simple sedimentation assay to test whether the SpoIIQ extracellular domain (SpoIIQ43-283) would bind peptidoglycan, purified from vegetative *B. subtilis* (Figure 5E). After co-incubation and centrifugation, proteins that bind peptidoglycan should be found in the pellet, while those that do not bind should remain in the supernatant. SpoIIQ43-283 was observed in the supernatant. To confirm that binding can be detected under these conditions, we tested two control proteins. The positive control protein lysozyme (a

peptidoglycan hydrolase) was found in the pellet, while the negative control protein bovine serum albumin (BSA) was found in the supernatant. Therefore, SpoIIQ does not bind to vegetative *B. subtilis* peptidoglycan.

Extracellular domain of SpoIIIAG does not interact with the SpoIIIAH-SpoIIQ complex

SpoIIIAG is a component of one of the protein sub-complexes that localizes to the mother cell-forespore interface (11). It is an integral membrane protein with an N-terminal transmembrane segment and a predicted C-terminal extracellular domain. Using the HHpred server (26), we and others noticed this extracellular domain also shares weak similarity with the YscJ-FliF family proteins (Figures 6A and 7) (7, 11, 19). Since the localization of a CFP-SpoIIIAG fusion protein to the mother cell-forespore interface is dependent on SpoIIQ (11), it was proposed that SpoIIIAG may interact with SpoIIQ, as SpoIIIAH does. This would be consistent with the YscJ-LytM module in the SpoIIIAH-SpoIIQ complex. To test whether SpoIIIAG interacts with SpoIIQ, we purified the extracellular domain of SpoIIIAG (SpoIIIAG51-229) and analyzed its interaction with SpoIIQ43-283 by gel filtration chromatography (Figure 6B). SpoIIIAG51-229 did not interact with SpoIIQ43-283. Since CFP-SpoIIIAG localization is also dependent on SpoIIIAH (11), we tested whether SpoIIIAG51-229 interacted with SpoIIIAH25-218 (Figure 6C). Once again we were unable to detect an interaction by gel filtration chromatography. We were also unable to detect an interaction between SpoIIIAG51-229 and the SpoIIIAH25-218 - SpoIIQ43-283 complex (Figure 6D).

DISCUSSION

In this study, we demonstrated that the purified, unmodified SpoIIIAH and SpoIIQ extracellular domains directly interact *in vitro*. We measured an apparent dissociation constant of 2 X 10^{-7} M. By comparison, the dissociation constants measured for homomeric eukaryotic cell adhesion proteins such as junction adhesion molecules (JAMs) and cadherins were approximately 10^{-4} to 10^{-5} M (2, 4, 16). The dissociation constants measured for heteromeric cell adhesion proteins such as integrin-laminin and P-selectin-PSGL1 were 10^{-7} to 10^{-8} M (14, 18). Thus, the binding affinity of the SpoIIIAH-SpoIIQ complex is within the range reported for other cell-cell junctions. Furthermore, we showed that the C-terminal YscJ domain was sufficient for the interaction with SpoIIQ. We also showed that the LytM domain is necessary and sufficient for interaction with SpoIIIAH *in vitro*. Thus, the LytM domain provides the positional cue, which when recognized by the YscJ domain, dictates the localization of several important mother cell proteins to the mother cell-forespore interface.

A direct interaction between SpoIIIAH and SpoIIQ was proposed based on several prior experiments using tagged proteins from cell lysates. GFP-SpoIIQ co-immunoprecipitated from a detergent-solubilized lysate of sporulating *B. subtilis* cells with FLAG-tagged SpoIIIAH (5). The transmembrane segments of both proteins were shown to be dispensable for the interaction when a nontagged SpoIIQ extracellular domain was pulled-down from an *E. coli* lysate with a GST-tagged SpoIIIAH extracellular domain (10).

Consistent with our results indicating that the LytM domain was necessary for the interaction with SpoIIIAH *in vitro*, Camp and Losick (6) showed that a truncation of the C-terminal 100 residues of SpoIIQ, leaving residues 1-183, blocked the localization of GFP-SpoIIIAH to the cell-cell interface. This truncation is expected to disrupt the SpoIIQ LytM domain (residues 89-220). They also showed that an internal LytM deletion (202-216), expected to disrupt the LytM domain, prevented GFP-SpoIIIAH localization to the interface. In contrast, a truncation of the C-terminal 50 residues, which removes a portion of the C-terminal extension and preserves the LytM domain, produced a functional protein (SpoIIQ1-233) that anchored SpoIIIAH at the interface.

While LytM proteins are known to bind and hydrolyze peptidoglycan, they may also possess the capacity for protein-protein interactions. Although the precise molecular details of the SpoIIIAH-SpoIIQ interaction remain unclear, it is tempting to speculate that YscJ recognition occurs in the LytM central groove. In the structure of latent *S. aureus* lysostaphin, its inhibitory N-terminal segment binds within the LytM groove, making contacts with the loops the form the walls that line it. If SpoIIIAH binds to SpoIIQ in a similar manner, then these loops would be necessary for the interaction. In support of this model, our truncations which are predicted to disrupt one of these walls disrupted the interaction of SpoIIQ with SpoIIIAH. SpoIIQ also has an insertion of a predicted α-helix (residues 100-108) in the first loop of its LytM domain that may be involved in recognition of the YscJ domain. This protein-binding mode may be common among degenerate LytM proteins. Uehara et al. recently showed that the amidases that mediate *E. coli* daughter cell separation are controlled by degenerate LytM proteins (30).

Although the mechanism is unclear, it was proposed to involve a protein-protein interaction. It will be interesting to find out whether the protein-binding mode of latent lysostaphin is adapted for partner protein recognition in degenerate LytM proteins.

Peptidoglycan-binding is another possible function of LytM domain of SpoIIQ. The mother cell-forespore interface is a site where peptidoglycan remodeling occurs (1, 20, 21). Forespore engulfment is initiated by septal PG hydrolysis and migration of the mother cell membrane around the forespore is thought to be promoted by new peptidoglycan synthesis at the cell-cell interface. While the SpoIIQ extracellular domain did not bind to vegetative peptidoglycan in our co-sedimentation assay, it is possible that it binds to a modified peptidoglycan (or muropeptides) found only at the cell-cell interface.

This study begins to elucidate how the mother cell founder protein SpoIIIAH recognizes the cell-cell interface. We currently know very little, however, about the mechanisms by which the SpoIIIAH-SpoIIQ complex anchors the three mother cell protein sub-complexes (SpoIIM-SpoIIP-SpoIID, SpoIIIAB-SpoIIIAC-SpoIIIAD-SpoIIIAE-SpoIIIAF-SpoIIIAG, and SpoIVFA-SpoIVFA-BofA) at this location. Although SpoIIIAH and SpoIIQ are necessary for the localization of CFP-SpoIIIAG to the mother cell-forespore interface (11), we were unable to detect an interaction of the extracellular domain with SpoIIIAH, SpoIIQ, or the SpoIIIAH-SpoIIQ complex *in vitro*. Doan et al. (11) reported that neither SpoIIIAH nor SpoIIQ co-immunoprecipitated with SpoIIIAG from a detergent-solubilized lysate of sporulating *B. subtilis* cells. However, SpoIIIAG co-immunoprecipitated with FLAG-tagged SpoIIIAH from a lysate of sporulating *B.*

subtilis cells prepared by mechanical disruption in the absence of a detergent. One possible explanation for these results is that the transmembrane segments of SpoIIIAG and SpoIIAH interact (directly or indirectly) in the plane of the mother cell membrane. This idea is consistent with the apparent detergent-sensitivity of the interaction (direct or indirect) between SpoIIIAG and the SpoIIQ-SpoIIIAH complex. Another possibility is that SpoIIIAG interacts with another protein at the cell-cell interface. The putative SpoIIIAG YcsJ domain has a 55-amino-acid segment, with four predicted β-strands, inserted between the first and second β-strands of the core three-stranded β-sheet (Figure 6A). Interestingly, this loop is unstructured and likely surface-exposed in the EscJ structure (31). Therefore, this flexible, surface-exposed loop may specify a protein-protein interaction by the SpoIIIAG.

ACKNOWLEDGEMENTS

We thank Christine Dunham for help with gel filtration chromatography, Graeme Conn for assistance with ITC, and David Popham for providing the peptidoglycan purification protocol. We also thank Kyle Frantz, Gordon Churchward, Phil Rather, Bill Shafer, Christine Dunham and Graeme Conn for constructive comments on the manuscript. This work was supported by National Institute of General Medical Sciences Public Health Services Grant GM54395.

FIGURES

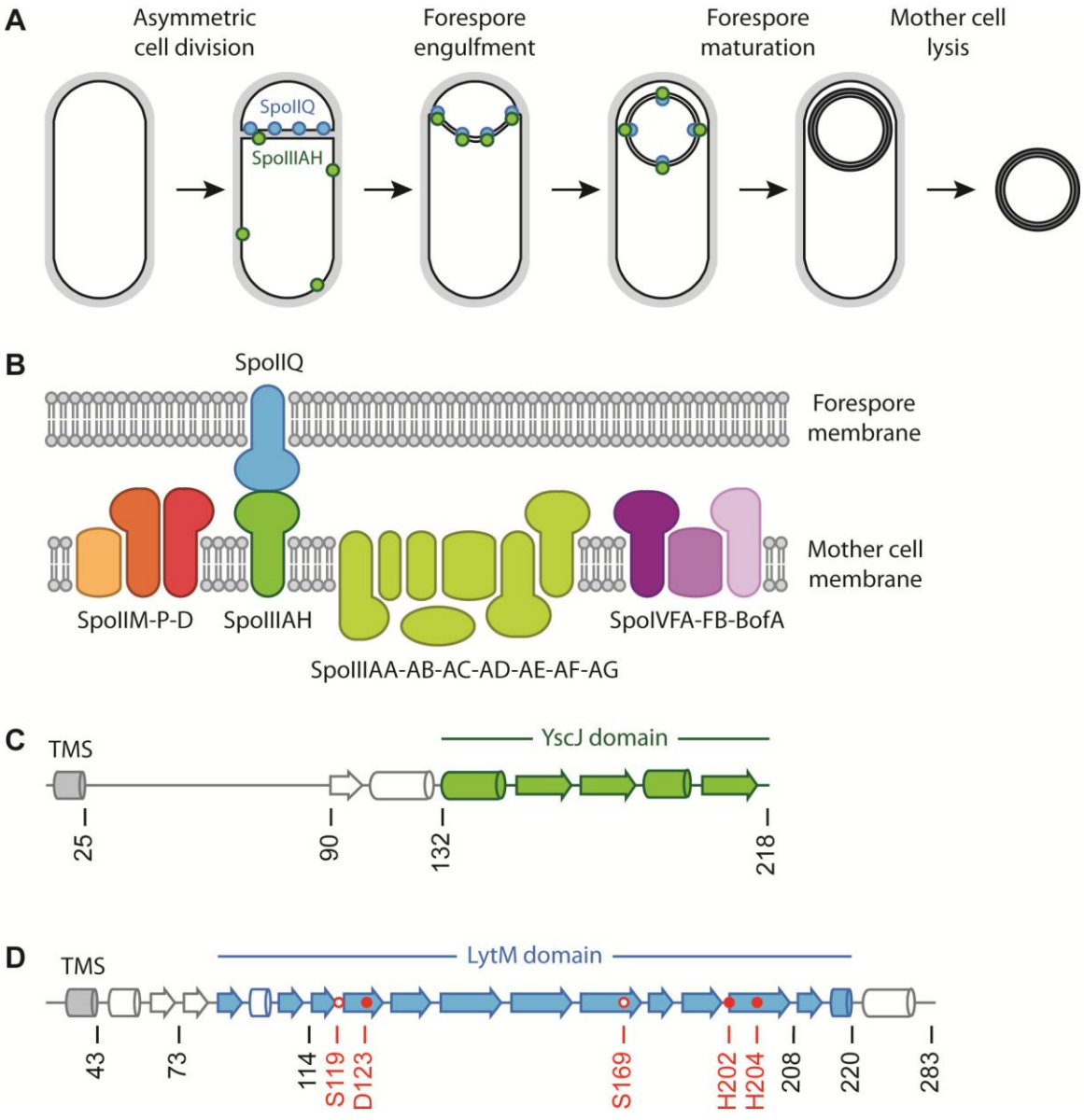

Figure 1. Cartoon representation of the SpoIIIAH-SpoIIQ complex. (A) Subcellular localization of SpoIIIAH (filled green circles) and SpoIIQ (filled blue circles) during each of the morphological stages of sporulation. (B) Three protein sub-complexes anchored at the mother cell-forespore interface, at least in part, by the SpoIIIAH-SpoIIQ complex. (C)

Linear representation of predicted SpoIIIAH secondary structure. α-helices and β-strands are shown as cylinders and arrows, respectively. The YscJ domain is shown in filled green objects with the adjacent N-terminal β-strand and α-helix in empty gray, and transmembrane segment (TMS) in filled gray. (D) Linear representation of predicted SpoIIQ secondary structure. The LytM domain is shown in filled blue objects with the predicted α-helical insertion in empty blue, N- and C-terminal extensions in empty gray, and TMS in filled gray. Residues at the N- and C-termini of truncated proteins are indicated in black. Zn^{2+} ligands and catalytic residues are indicated in red. Filled circles show the position of conserved residues while empty circles show non-conserved (degenerate) residues.

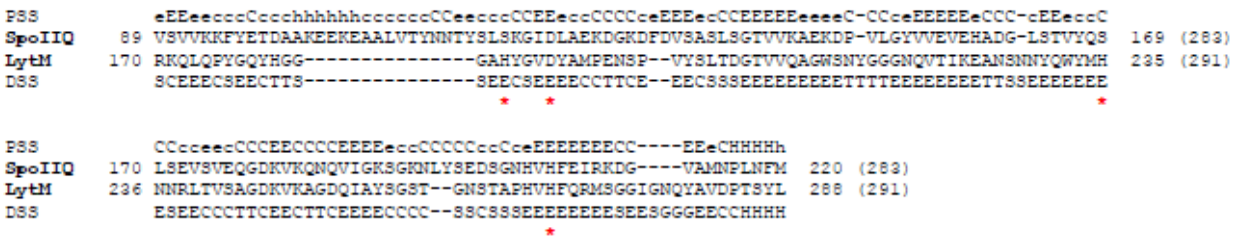

Figure 2. Sequence alignment of SpoIIQ and *S. aureus* LytM (1QWY) based on HHpred. Predicted secondary structure (PSS) and determined secondary structure (DSS) are shown above SpoIIQ and below LytM, respectively. For the PSS, H stands for α-helix, E means β-strand, and C signifies a coil or loop. For DSS, H, E, and C are the same as PSS. S is a bend, T a turn, and G a 3_{10}-helix. LytM active site residues are indicated with red asterisks.

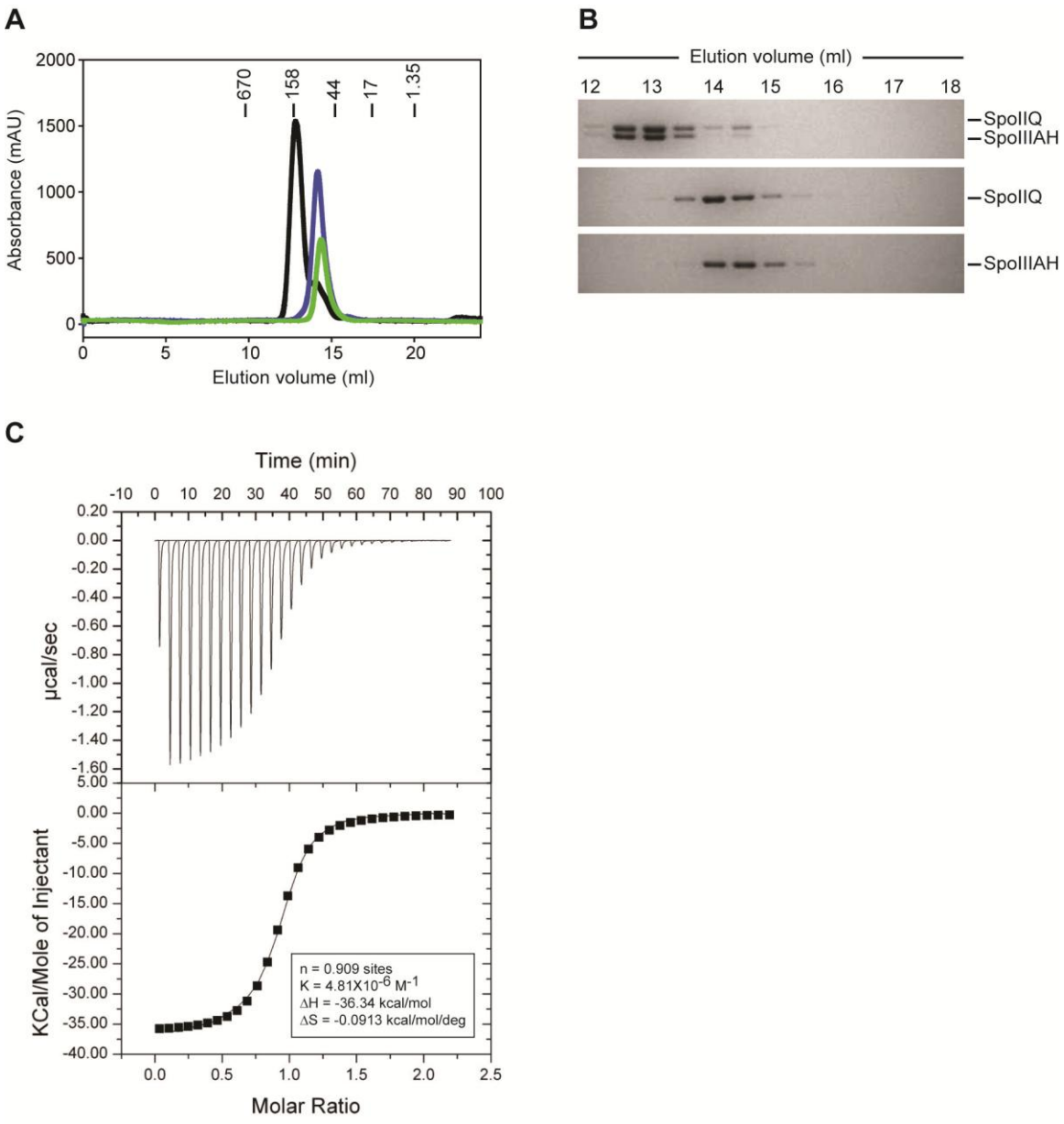

Figure 3. Biochemical analysis of the SpoIIIAH-SpoIIQ complex. (A) Gel filtration chromatography of the mixture of SpoIIIAH25-218 and SpoIIQ43-283 (black line), SpoIIIAH25-218 alone (green line), and SpoIIQ34-283 alone (blue line). Protein elution is shown by graphing UV absorbance (230 nm) versus elution volume. Indicated above the curves are the elution volumes and molecular weights (kDa) of the standard proteins.

(B) SDS-polyacrylamide gel electrophoresis (PAGE) analyses of the elution fractions from the gel filtration chromatography in Figure 2A. Coomassie blue-stained SDS-PAGE gels are shown. (C) Isothermal titration calorimetry of the interaction of SpoIIIAH25-218 (sample cell) and SpoIIQ43-283 (syringe). The top graph shows the raw data, and the bottom graph shows the normalized integration data.

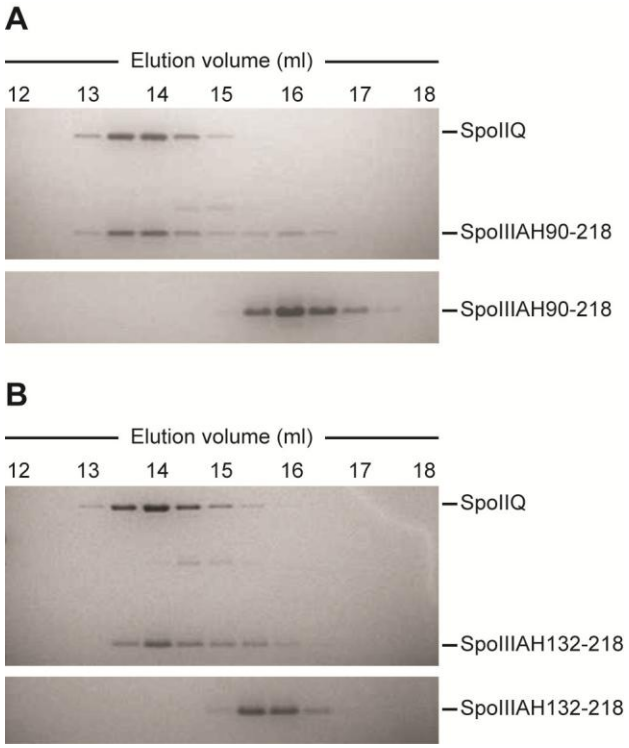

Figure 4. Gel filtration chromatography of the interaction of and SpoIIQ43-283 and truncated SpoIIIAH proteins. (A) Coomassie blue-stained SDS-PAGE of the mixture of SpoIIQ43-283 and SpoIIIAH90-218 (top panel), and SpoIIIAH90-218 alone (bottom panel). (B) Coomassie blue-stained SDS-PAGE of the mixture of SpoIIQ43-283 and SpoIIIAH132-218 (top panel), and SpoIIIAH132-218 alone (bottom panel).

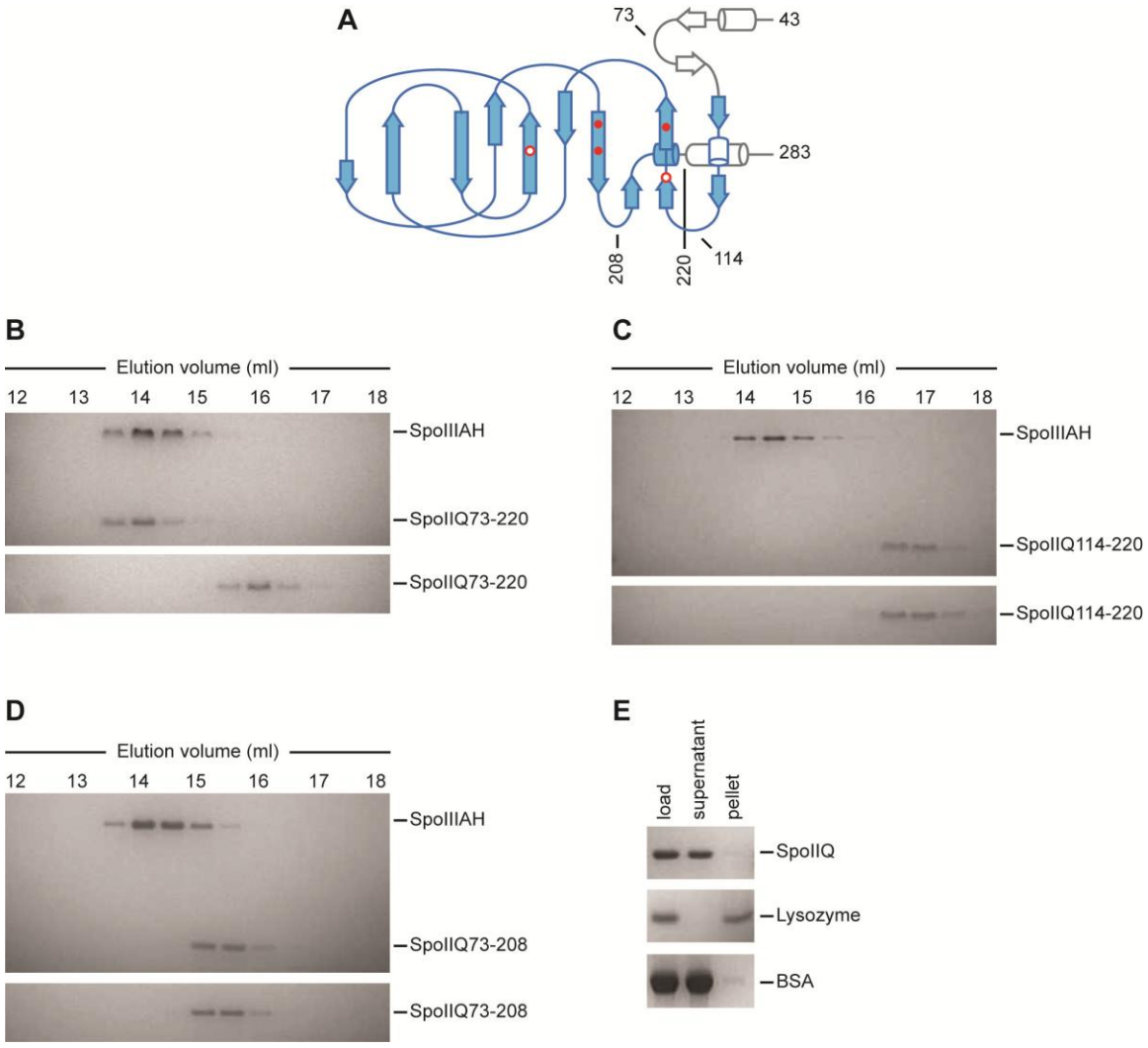

Figure 5. Gel filtration chromatography of the interaction of and SpoIIIAH25-218 and truncated SpoIIQ proteins. (A) Cartoon representation of the predicted tertiary structure of the SpoIIQ extracellular domain emphasizing the organization of the core β-sheet of the LytM domain (filled blue objects). α-helices and β-strands are shown as cylinders and arrows, respectively. The predicted α-helical insertion is shown in empty blue, and N- and C-terminal extensions in empty gray. Residues at the N- and C-termini of truncated proteins are indicated in black. Filled circles show the position of conserved

active site residues while empty circles show non-conserved (degenerate) residues. (B-D) Gel filtration chromatography of the interaction of SpoIIIAH25-218 and truncated versions of SpoIIQ proteins (SpoIIQ73-220, Figure 4B), (SpoIIQ114-200, Figure 4C), and (SpoIIQ73-208, Figure 4D). Shown are Coomassie blue-stained SDS-PAGE analyses of the elution fractions from the gel filtration chromatography of the mixtures of SpoIIIAH25-218 and truncated SpoIIQ proteins (top panel), and truncated SpoIIQ proteins alone (bottom panel). (E) Peptidoglycan co-sedimentation with SpoIIQ43-283, lysozyme, or bovine serum albumin (BSA). Peptidoglycan was added to each protein, incubated and centrifuged as described in the Materials and Methods. Coomassie blue-stained SDS-PAGE analysis of the sedimentation fractions is shown.

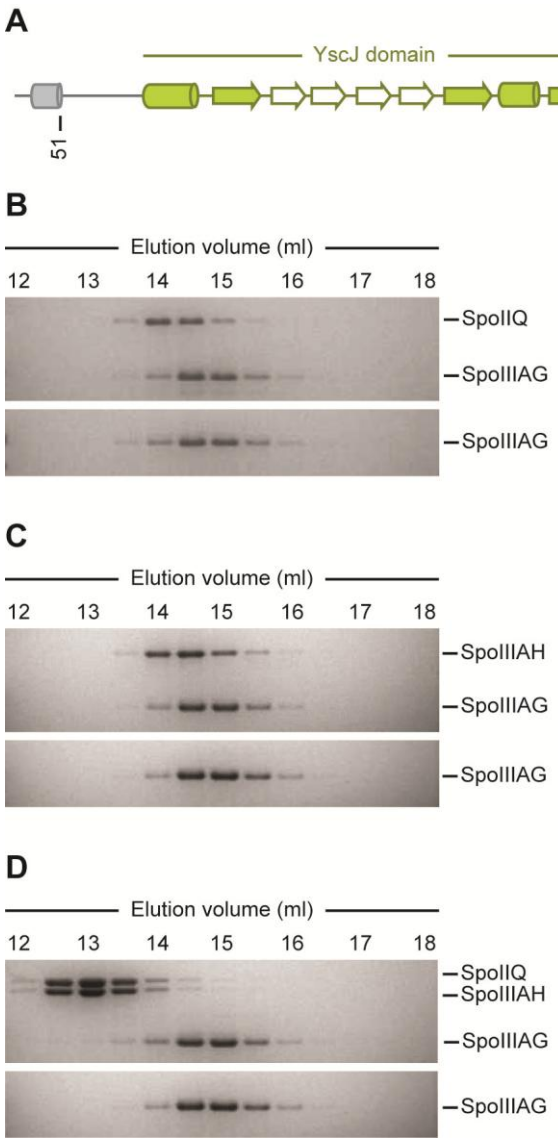

Figure 6. Gel filtration chromatography of the interaction of and SpoIIIAG51-229 with SpoIIIAH25-218, SpoIIQ43-283, or the SpoIIIAH25-218 - SpoIIQ43-283 complex. (A) Cartoon representation of the predicted SpoIIIAG secondary structure. α-helices and β-strands are shown as cylinders and arrows, respectively. The predicted YscJ domain is shown in filled light green objects with the predicted four β-strand insertion in empty light green. Residues at the N- and C-termini of the protein are indicated in black. Gel

filtration chromatography of the interaction of SpoIIIAG51-229 and SpoIIQ43-283 (B), SpoIIIAH25-218 (C), and the SpoIIQ43-283 – SpoIIIAH25-218 complex (D). Shown are Coomassie blue-stained SDS-PAGE analyses of the elution fractions from the gel filtration chromatography.

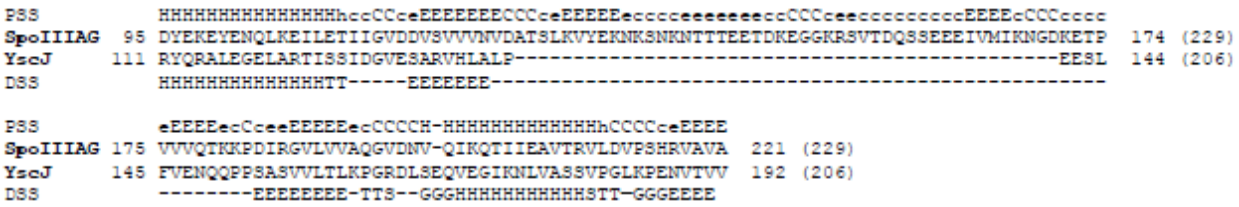

Figure 7. HHpred sequence alignment of SpoIIIAG and YscJ-FliF family (PF01514). Predicted secondary structure (PSS) and determined secondary structure (DSS) are shown above SpoIIIAG and below YscJ-FliF, respectively. For the PSS, H stands for α-helix, E means β-strand, and C signifies a coil or loop. For DSS, H,E, and C are the same as PSS. S is a bend, T a turn, and G a 3_{10}-helix.

TABLES

Table 1. Oligonucleotide primers

Primer	Sequence
spoIIIAHF5	GGAATTCCATATGTCGCCGGAAAGCAAAAACG
spoIIIAHrevBamHI	CACACACAGGATCCTTTAGCGGGCTTTTTTCCCTCATTC
spoIIIAHF10	GGAATTCCATATGGATGCAACAGCCAAGGAGAAAAGC
spoIIIAHF12	GGAATTCCATATGGCCAGTGAAAAAGGAACTGTTGTTACG
spoIIIAGF5	GGAATTCCATATGTCTTCACCTGAGAAAACTGAAAACG
spoIIIAHR6	CGGGATCCTTATGAATCCTCCTTTATTTTTTTAGGGG
spoIIQF13	GGAATTCATTAATCAATCAGTATCAAATGATGAGGTAAAGGATC
spoIIQR14	CGGGATCCTTAAGACTGTTCAGTGTCTTCTGTTGTG
spoIIQF17	GGAATTCCATATGGGAAAGTCAATGGAAAATGTCGC
spoIIQF15	GGAATTCCATATGAACACGTACAGCCTAAGCAAAGG
spoIIQR16	CGGGATCCTTACATAAAGTTTAACGGATTCATTGCAACC
spoIIQR19	CGGGATCCTTATGCACGGATTTCAAAGTGCACGTG

Table 2. Plasmids

Plasmid	Description	Reference
pET14b	pBR322 derivative with T7 promoter followed by N-terminal His-tag, thrombin site and three cloning sites	Novagen
pJM212	pET14b spoIIIAH25-218	This study
pJM244	pET14b spoIIIAH132-218	This study
pJM252	pET14b spoIIIAH90-218	This study
pJM243	pET14b spoIIQ43-283	This study
pJM250	pET14b spoIIQ73-220	This study
pJM246	pET14b spoIIQ114-220	This study
pJM253	pET14b spoIIQ73-208	This study

Table 3. Bacterial strains

Strain	Genotype	Reference
BL21 Star (DE3)	F– *omp*T *hsd*SB(rB–, mB–) *gal dcm rne*131 (DE3)	Invitrogen
JME97	BL21 Star (DE3) pJM212	This study
JME106	BL21 Star (DE3) pJM244	This study
JME114	BL21 Star (DE3) pJM252	This study
JME104	BL21 Star (DE3) pJM242	This study
JME105	BL21 Star (DE3) pJM243	This study
JME112	BL21 Star (DE3) pJM250	This study
JME108	BL21 Star (DE3) pJM246	This study
JME116	BL21 Star (DE3) pJM253	This study

Table 4. Thermodynamic parameters determined by ITC for the interaction of truncated SpoIIIAH proteins (syringe) and SpoIIQ43-283 (sample cell)[a]

Ligand	n	K_d (M)	ΔG^b (kcal mol^{-1})	ΔH (kcal mol^{-1})	$-T\Delta S^b$ (kcal mol^{-1})
SpoIIIAH25-218	0.934	1.96×10^{-7}	-9.15	-40.4	31.2
SpoIIIAH90-218	1.06	1.93×10^{-7}	-9.16	-35.7	26.6
SpoIIIAH132-218	0.966	7.81×10^{-7}	-8.33	-20.8	12.5

[a] Values are for 25 mM sodium phosphate buffer, 100 mM NaCl, pH 7.5 at 25 °C.

[b] Calculated from $\Delta G = RT \ln K_d = \Delta H - T\Delta S$, where R is the gas constant (1.987 cal K^{-1} mol^{-1}) and T is temperature in degrees K.

Table 5. Thermodynamic parameters determined by ITC for the interaction of truncated SpoIIQ proteins (syringe) and SpoIIIAH25-218 (sample cell)[a]

Ligand	n	K_d (M)	ΔG^b (kcal mol^{-1})	ΔH (kcal mol^{-1})	$-T\Delta S^b$ (kcal mol^{-1})
SpoIIQ43-283	0.909	2.08×10^{-7}	-9.12	-36.3	27.2
SpoIIQ73-220	1.13	5.78×10^{-7}	-8.51	-44.8	36.3
SpoIIQ114-220	ND	ND		ND	
SpoIIQ73-208	ND	ND		ND	

[a] Values are for 25 mM sodium phosphate buffer, 100 mM NaCl, pH 7.5 at 25 °C.

[b] Calculated from $\Delta G = RT \ln K_d = \Delta H - T\Delta S$, where R is the gas constant (1.987 cal K^{-1} mol^{-1}) and T is temperature in degrees K. ND indicates that binding was not detected and values were not determined.

REFERENCES

1. **Abanes-De Mello, A., Y. L. Sun, S. Aung, and K. Pogliano.** 2002. A cytoskeleton-like role for the bacterial cell wall during engulfment of the Bacillus subtilis forespore. Genes Dev **16:**3253-3264.

2. **Alattia, J. R., J. B. Ames, T. Porumb, K. I. Tong, Y. M. Heng, P. Ottensmeyer, C. M. Kay, and M. Ikura.** 1997. Lateral self-assembly of E-cadherin directed by cooperative calcium binding. FEBS Lett **417:**405-408.

3. **Aung, S., J. Shum, A. Abanes-De Mello, D. H. Broder, J. Fredlund-Gutierrez, S. Chiba, and K. Pogliano.** 2007. Dual localization pathways for the engulfment proteins during Bacillus subtilis sporulation. Mol Microbiol **65:**1534-1546.

4. **Baumgartner, W., P. Hinterdorfer, W. Ness, A. Raab, D. Vestweber, H. Schindler, and D. Drenckhahn.** 2000. Cadherin interaction probed by atomic force microscopy. Proc Natl Acad Sci U S A **97:**4005-4010.

5. **Blaylock, B., X. Jiang, A. Rubio, C. P. Moran, Jr., and K. Pogliano.** 2004. Zipper-like interaction between proteins in adjacent daughter cells mediates protein localization. Genes Dev **18:**2916-2928.

6. **Camp, A. H., and R. Losick.** 2009. A feeding tube model for activation of a cell-specific transcription factor during sporulation in Bacillus subtilis. Genes Dev **23:**1014-1024.

7. **Camp, A. H., and R. Losick.** 2008. A novel pathway of intercellular signalling in Bacillus subtilis involves a protein with similarity to a component of type III secretion channels. Mol Microbiol **69:**402-417.

8. **Chiba, S., K. Coleman, and K. Pogliano.** 2007. Impact of membrane fusion and proteolysis on SpoIIQ dynamics and interaction with SpoIIIAH. J Biol Chem **282:**2576-2586.

9. **Cohen, D. N., Y. Y. Sham, G. D. Haugstad, Y. Xiang, M. G. Rossmann, D. L. Anderson, and D. L. Popham.** 2009. Shared catalysis in virus entry and bacterial cell wall depolymerization. J Mol Biol **387:**607-618.

10. **Doan, T., K. A. Marquis, and D. Z. Rudner.** 2005. Subcellular localization of a sporulation membrane protein is achieved through a network of interactions along and across the septum. Mol Microbiol **55:**1767-1781.

11. **Doan, T., C. Morlot, J. Meisner, M. Serrano, A. O. Henriques, C. P. Moran, Jr., and D. Z. Rudner.** 2009. Novel secretion apparatus maintains spore integrity and developmental gene expression in Bacillus subtilis. PLoS Genet **5:**e1000566.

12. **Firczuk, M., and M. Bochtler.** 2007. Folds and activities of peptidoglycan amidases. FEMS Microbiol Rev **31:**676-691.

13. **Firczuk, M., A. Mucha, and M. Bochtler.** 2005. Crystal structures of active LytM. J Mol Biol **354:**578-590.

14. **Gonzalez, A. M., M. Gonzales, G. S. Herron, U. Nagavarapu, S. B. Hopkinson, D. Tsuruta, and J. C. Jones.** 2002. Complex interactions between the laminin alpha 4 subunit and integrins regulate endothelial cell behavior in vitro and angiogenesis in vivo. Proc Natl Acad Sci U S A **99:**16075-16080.

15. **Kimbrough, T. G., and S. I. Miller.** 2002. Assembly of the type III secretion needle complex of Salmonella typhimurium. Microbes Infect **4:**75-82.

16. **Kirchner, E., K. M. Guglielmi, H. M. Strauss, T. S. Dermody, and T. Stehle.** 2008. Structure of reovirus sigma1 in complex with its receptor junctional adhesion molecule-A. PLoS Pathog **4:**e1000235.

17. **Londono-Vallejo, J. A., C. Frehel, and P. Stragier.** 1997. SpoIIQ, a forespore-expressed gene required for engulfment in Bacillus subtilis. Mol Microbiol **24:**29-39.

18. **Mehta, P., R. D. Cummings, and R. P. McEver.** 1998. Affinity and kinetic analysis of P-selectin binding to P-selectin glycoprotein ligand-1. J Biol Chem **273:**32506-32513.

19. **Meisner, J., X. Wang, M. Serrano, A. O. Henriques, and C. P. Moran, Jr.** 2008. A channel connecting the mother cell and forespore during bacterial endospore formation. Proc Natl Acad Sci U S A **105:**15100-15105.

20. **Meyer, P., J. Gutierrez, K. Pogliano, and J. Dworkin.** 2010. Cell wall synthesis is necessary for membrane dynamics during sporulation of Bacillus subtilis. Mol Microbiol **76:**956-970.

21. **Morlot, C., T. Uehara, K. A. Marquis, T. G. Bernhardt, and D. Z. Rudner.** 2010. A highly coordinated cell wall degradation machine governs spore morphogenesis in Bacillus subtilis. Genes Dev **24:**411-422.

22. **Odintsov, S. G., I. Sabala, M. Marcyjaniak, and M. Bochtler.** 2004. Latent LytM at 1.3A resolution. J Mol Biol **335:**775-785.

23. **Rudner, D. Z., and R. Losick.** 2010. Protein subcellular localization in bacteria. Cold Spring Harb Perspect Biol **2:**a000307.

24. **Rudner, D. Z., and R. Losick.** 2002. A sporulation membrane protein tethers the pro-sigmaK processing enzyme to its inhibitor and dictates its subcellular localization. Genes Dev **16:**1007-1018.

25. **Shapiro, L., H. H. McAdams, and R. Losick.** 2009. Why and how bacteria localize proteins. Science **326:**1225-1228.

26. **Soding, J.** 2005. Protein homology detection by HMM-HMM comparison. Bioinformatics **21:**951-960.

27. **Spreter, T., C. K. Yip, S. Sanowar, I. Andre, T. G. Kimbrough, M. Vuckovic, R. A. Pfuetzner, W. Deng, A. C. Yu, B. B. Finlay, D. Baker, S. I. Miller, and N. C. Strynadka.** 2009. A conserved structural motif mediates formation of the periplasmic rings in the type III secretion system. Nat Struct Mol Biol **16:**468-476.

28. **Sun, Y. L., M. D. Sharp, and K. Pogliano.** 2000. A dispensable role for forespore-specific gene expression in engulfment of the forespore during sporulation of Bacillus subtilis. J Bacteriol **182:**2919-2927.

29. **Suzuki, H., K. Yonekura, K. Murata, T. Hirai, K. Oosawa, and K. Namba.** 1998. A structural feature in the central channel of the bacterial flagellar FliF ring complex is implicated in type III protein export. J Struct Biol **124:**104-114.

30. **Uehara, T., K. R. Parzych, T. Dinh, and T. G. Bernhardt.** 2010. Daughter cell separation is controlled by cytokinetic ring-activated cell wall hydrolysis. EMBO J **29:**1412-1422.

31. **Yip, C. K., B. B. Finlay, and N. C. Strynadka.** 2005. Structural characterization of a type III secretion system filament protein in complex with its chaperone. Nat Struct Mol Biol **12:**75-81.

CHAPTER 4. SpoIIIAA is a secretion superfamily ATPase

The data presented in this chapter were published in the following manuscript:

Doan, T., C. Morlot, J. Meisner, M. Serrano, A.O. Serrano, C.P. Moran, Jr, and D.Z. Rudner. 2009. Novel secretion apparatus maintains forespore integrity and developmental gene expression in Bacillus subtilis. PLoS Genet **5:**e1000566.

T.D., C.M., J.M., C.P.M, and D.Z.R. designed the experiments. T.D., C.M., and J.M. performed the experiments. T.D., C.M., and D.Z.R. wrote the manuscript.

INTRODUCTION

We and others proposed that σ^G activation is triggered by a signal which is transmitted from the mother cell to the forespore by a novel secretion system comprised of the eight SpoIIIA proteins (SpoIIIAA, SpoIIIAB, SpoIIIAC, SpoIIIAD, SpoIIIAE, SpoIIIAF, SpoIIIAG, and SpoIIIAH) and SpoIIQ (3, 4, 6, 8). SpoIIIAH shares remote homology with the ring-forming proteins that serve as structural scaffolds for the assembly of type III protein secretion systems. Because the extracellular domains of both SpoIIIAH and SpoIIQ are accessible to modification by an enzyme produced in the forespore, we hypothesized that these proteins form a channel that connects the mother cell and forespore (8). Neither protein, however, is accessible to modification when the enzyme is produced in the mother cell. By analogy with type III secretion systems, we further hypothesized that SpoIIIAH serves as a scaffold for the assembly of a specialized secretion system composed of the other SpoIIIA proteins. Consistent with this hypothesis, the other SpoIIIA proteins show limited similarity with components of several different types of secretion systems (8). Although the components of these different types of secretion systems vary, they each contain an ATP hydrolase (ATPase) that provides the energy necessary for protein secretion.

The secretion superfamily ATPases are involved in bacterial type II secretion, type IV pilus biogenesis, type IV secretion, DNA uptake and archaeal flagellar biogenesis (5, 10, 11). These ATPases are composed of two domains: the N-terminal domain (NTD) and C-terminal domain (CTD) (13, 14, 19, 20). The NTD is divided into two sub-domains: N1 and N2. The N2 sub-domain consists of a six-stranded antiparallel

β-sheet with one face that packs against the CTD and two α-helices located on the opposite face. The CTD is also divided into two sub-domains: C1 and C2. The C1 sub-domain consists of a central six-stranded β-sheet with three α-helices on one side and four on the other. The C1 sub-domain contains 4 characteristic sequence motifs: Walker A (P-loop nucleotide binding motif), atypical Walker B, Asp and His boxes (12). Secretion superfamily ATPases also contain a pair of conserved arginines, the dual arginine fingers, in the N2 subdomain that form an intra-subunit clamp in the ATP-bound form (19). Secretion superfamily ATPases form an asymmetric hexamer with a mixture of subunits in open and closed conformations (19). The open form facilitates ATP binding. Binding to the ATP γ-phosphate and Mg^{2+} drives the open to closed transition by increasing N2-C1 subdomain interactions, converting binding energy into a conformational change. The closed form hydrolyzes ATP. After ATP hydrolysis, ATP γ-phosphate release destabilizes the interaction with one of the dual arginine fingers and triggers the closed to open conformational change (19). A universal "push-n-pull" mechanism to couple ATP binding and hydrolysis to mechanical work was proposed.

The results presented here argue that SpoIIIAA is a secretion superfamily ATPase. The HHpred server detected homology between SpoIIIAA and several secretion superfamily ATPases. Both the core structural features and characteristic sequence motifs are conserved in SpoIIIAA orthologs. We show that the conserved amino acid residues are necessary for SpoIIIAA function. Presumably SpoIIIAA provides the energy necessary to transmit the signal that activates σ^G. Whether this signal is a secreted protein, or other macromolecule, remains unclear.

MATERIALS AND METHODS

Bioinformatics

The *B. subtilis* SpoIIIAA amino acid sequences was submitted to the HHpred server for protein homology detection and structure prediction (16). HHpred performed a maximum of eight PSI-BLAST iterations to build an alignment from the input sequence and then searched the Protein Data Bank (PDB) and PfamA multiple sequence alignment databases. The secondary of the input sequence was predicted by PSIPRED and compared to the database sequences to improve sensitivity and alignment quality (15). MODELLER was used to calculate a comparative structural model based on the HHpred alignment (7). The sequences of selected spore-forming bacteria were aligned using the ClustalW multiple sequence alignment program (17).

General bacterial methods

B. subtilis strains were grown in Luria broth (LB) and sporulation was induced by nutrient exhaustion in Difco sporulation medium (DSM) at 37 °C with aeration. Genetic competence was developed and transformations were performed as described previously (1). Transformants were selected on LB agar plates containing 1 μg/ml erythromycin or 5 μg/ml chloramphenicol. *Escherichia coli* transformants were grown in LB containing 100 μg/ml ampicillin.

Plasmid and strain construction

A *B. subtilis* strain containing an in-frame deletion in *spoIIIAA* was provided by Richard Losick (Harvard University). Complementation strains were constructed by

transforming the in-frame deletion strains with integration vectors carrying cloned *spoIIIAA* alleles. The cloned alleles were integrated into the chromosome at the *thrC* locus by double crossover recombination. The *PsspE-lacZ* reporter gene fusions were introduced in these strains by double crossover recombination at the *amyE* locus.

The wild-type *spoIIIAA* gene was cloned from *B. subtilis* strain JH642 chromosomal DNA by polymerase chain reaction (PCR). The oligonucleotide primers used for cloning are listed in Table 1. The cloned gene included the upstream spoIIIA promoter, and *BamHI* or *EcoRI* restriction sites at each end. The fragment and integration vector pDG1664 were cut with the restriction enzymes, purified, and ligated. One Shot Top10 chemically competent *E. coli* cells (Invitrogen) were transformed with the ligated plasmid and transformants were selected on LB agar containing 100 μg/ml ampicillin. Plasmid was purified from the transformants and confirmed by DNA sequencing. Finally, *B. subtilis* strains containing the in-frame deletions transformed with these plasmids were selected on LB containing 1 μg/ml erythromycin.

The *sspE* promoter was amplified by PCR from chromosomal DNA. The fragment contained *BamHI* or *EcoRI* restriction sites at each end. The fragment was ligated into integration vector pDG1661 and the resulting plasmid was purified as described above. *B. subtilis* transformants were selected on LB containing 5 μg/ml chloramphenicol. The plasmids and strain used in this work are shown in Tables 2 and 3, respectively.

Sporulation test

B. subtilis strains were grown in DSM at 37°C for 48 hours. 500 ml of each culture was heated at 80°C for 10 minutes. Then heated and non-heated cultures were serially diluted (10-fold) in LB. 100 ml of each dilution was spread on LB agar at incubated at 37°C overnight. Colonies were counted and the numbers of heat-resistant spores and total cells per ml of the DSM culture were calculated. The sporulation efficiency is the number of heat-resistant spores per total cells.

β-galactosidase assay

Strains containing P_{sspE}-*lacZ* reporter gene fusions were grown in DSM at 37°C and OD_{600} was measured hourly. 1 ml of each culture was collected hourly after the end of exponential phase (the onset of sporulation) and pelleted cells in a microcentrifuge. Pellets were washed in 500 μl 25 mM Tris, pH 7.4 and stored at -80°C. Cell pellets were thawed and resuspended in 640 μl Z buffer (60 mM Na_2HPO_4-$7H_2O$, 40 mM NaH_2PO_4, 10 mM KCl, 1 mM $MgSO_4$-$7H_20$, 50 mM βME, pH 7.0). Then 16 μl of lysozyme (2.5 mg/ml in Z buffer) was added, and the solutions were vortexed briefly and incubated at 37°C for 5 minutes. 8 μl of 10% Triton X100 was added, and each solution was vortexed briefly and stored on ice. Cell extracts were pre-warmed at 30°C for 2-5 minutes. 200 μl of *o*-nitrophenyl-β-D-galactoside (4 mg/ml in Z buffer) was added to each solution and incubated at 30°C for 5 minutes. The reactions were stopped by adding 400 μl of 1 M Na_2CO_3. The solutions were centrifuged for 5 minutes and the absorbance at 420 nm was measured. β-galactosidase activity was represented in Miller units (9) and calculated by the following formula: $(1000 \times A_{420})/(\text{reaction time (minutes)} \times OD_{600})$.

RESULTS

SpoIIIAA is homologous to secretion superfamily ATPases

SpoIIIAA is a cytoplasmic protein which is reported to share similarity with AAA+ (ATPases associated with various cellular activities) proteins (2). To further characterize the homologous relationships of SpoIIIAA, we submitted its protein sequence to the HHpred server for homology detection and structure prediction (16). HHpred returned significant hits to secretion superfamily ATPases (PF00437). Figure 1 shows a sequence alignment of SpoIIIAA and an archaeal type II secretion system protein GspE. SpoIIIAA contains the core N2-C1 sub-domains, including the four characteristic sequence motifs and dual arginine fingers. These sequences are conserved among SpoIIIAA orthologs from diverse endospore-forming bacteria (Figure 2). It also has an extended N-terminal α-helix instead of an N1 sub-domain and lacks a C2 sub-domain. Figure 3 compares the sub-domain composition of three secretion superfamily ATPases: type II secretion system protein GspE, type IV pilus assembly protein PilT, and type IV secretion system protein VirB11. Each of the three types of proteins shares the core N2-C1 sub-domains. Both PilT and VirB11 have an α-helix instead of an N1 sub-domain, and VirB11 lacks a C2 sub-domain. Therefore, the sub-domain composition of SpoIIIAA most closely resembles that of VirB11. However, SpoIIIAA lacks the C1 sub-domain α8-α9 insertion which is characteristic of VirB11 proteins (20).

Characteristic secretion ATPase sequence motifs are necessary for SpoIIIAA function during sporulation.

Each secretion superfamily ATPase sequence motif contains conserved residues that are necessary for protein function (12). The lysine of the Walker A box and the aspartate of the Walker B box are necessary for ATP binding and hydrolysis, respectively. The aspartate of the Asp box and the histidine of the His box are also necessary for function. A mutant containing an in-frame deletion in *spoIIIAA* is unable to produce heat-resistant endospores, due to an inability to activate σ^G in the forespore. This mutant phenotype was restored (or complemented) when a wild-type *spoIIIAA* allele integrated at the *thrC* locus. To determine whether the secretion superfamily ATPase sequence motifs are necessary for SpoIIIAA function, we tested the ability of mutant alleles to complement the *spoIIIAA* deletion. Alleles with mutations of key residues in Walker A (K149R), Walker B (E225Q), Asp (E180Q), and His (H250Y) boxes failed to complement the sporulation defect of the *spoIIIAA* deletion (Table 1).

Based on the sequence alignment of SpoIIIAA and *Archaeoglobus fulgidus* GspE (afGspE), the dual arginine fingers of SpoIIIAA appear to be the arginines at positions 89 and 107. The multiple sequence alignment of SpoIIIAA orthologs shows that R89 is conserved but R107 is not. Instead, the nearby arginine at position 115 is conserved among each of the orthologs examined. To determine whether these residues were necessary for SpoIIIAA function, we tested the ability of mutant alleles to complement the *spoIIIAA* deletion. The R107A mutant complemented the *spoIIIAA* deletion, while those with the R89A or R115A mutations failed to complement. Thus, SpoIIIAA appears

to contain the one of the two dual arginine fingers. To pursue the possibility that R115 is the other arginine finger, we used submitted the HHpred alignment of SpoIIIAA and afGspE to the MODELLER program (7). MODELLER constructed a comparative structural model of SpoIIIAA using the afGspE structure as a template (Figure 4). R89 and R107 reside in the N2 subdomain in an appropriate position to stabilize the closing of the N2 subdomain by interacting with ATP in the C1 subdomain active site. Rather than residing in the N2 subdomain, R115 is located in the loop that separates the N2 and C1 subdomains. The position of R115 outside the N2 subdomain is inconsistent with the function of the dual arginine fingers. Because it is predicted to be exposed on the surface of the C1 subdomain, R115 may stabilize the intersubunit interactions common among secretion superfamily ATPases.

Sporulation defect of *spoIIIAA* mutants is due to an inability to activate σ^G

To determine if the sporulation defect of these mutants was due to an inability to signal the activation of σ^G in the forespore, we measured the β-galactosidase activity in strains containing a σ^G-dependent transcriptional reporter gene fusion (P_{sspE}-*lacZ*) integrated at the *amyE* locus. While the wild-type allele restored σ^G activity to the *spoIIIAA* deletion, none of the mutant alleles showed σ^G activity (Figure 5). Thus, the sporulation defect of these mutants was a consequence of an inability to signal the activation of σ^G. The strain bearing the wild-type allele exhibited an unexpected delay in the onset of σ^G activity. We cannot explain this delay but it does not reduce the sporulation efficiency of the strain. It is possible that the genetic separation of the *spoIIIAA* gene from the other *spoIIIA* genes may account for this delay. Perhaps the

cotranscription of the *spoIIIA* genes promotes the assembly of the subsequently cotranslated proteins into the multi-protein complexes thought to control the activation of σ^G.

Functionally important residues are conserved among orthologous SpoIIIAA

The C1 subdomains are well conserved among SpoIIIAA orthologs from diverse endospore-forming bacteria. The N1 and N2 subdomains are more divergent. The variation in these domains may be due to homotypic interactions with integral membrane partner proteins. To test this hypothesis, we assessed the ability of *spoIIIAA* orthologs to complement the *B. subtilis spoIIIAA* deletion (Table 5). The *spoIIIAA* genes from *B. amyloliquefacians*, *B. licheniformis* and *Geobacillus kaustophilus* are 77%, 65%, and 56% identical (87%, 82%, and 75% similar) to *B. subtilis*, respectively. Surprisingly, each the orthologs complemented the *B. subtilis spoIIIAA* mutant. While the sequences of the N1 and N2 subdomains are somewhat divergent, the important residues are conserved across these orthologs.

DISCUSSION

In this study, we identified a homologous relationship between SpoIIIAA and the secretion superfamily ATPases (PF00437). Because the conserved secretion superfamily ATPase residues are necessary for SpoIIIAA function, we propose that SpoIIIAA functions as a secretion superfamily ATPase. This superfamily includes proteins involved in type II protein secretion, type IV pilus assembly, These ATPase are thought to couple domain movements to ATP binding and hydrolysis. These domain

movements may be transmitted to integral membrane protein complexes (19). Conformational changes in these membrane protein complexes promote either protein secretion or filament assembly. By analogy, SpoIIIAA may interact with and promote conformational changes in one or more of the integral membrane SpoIIIA proteins. Although no such interactions have been identified, SpoIIIAB and SpoIIIAF are attractive candidates. These membrane proteins have predicted cytoplasmic domains which share weak similarity with the membrane proteins that serve as docking platforms for the ATPases in type II and type III secretion systems, respectively. Because the variable N1 subdomains (or extended α-helices) of secretion superfamily ATPases are thought to specify interactions with the docking platform proteins, the N-terminal extended α-helix of SpoIIIAA may interact with SpoIIIAB or SpoIIIAF. Although the N-terminal α-helices of diverse spore-forming bacteria are relatively divergent, we showed that SpoIIIAA from *B. amyloliquefacians*, *B. licheniformis*, and *Geobacillus kaustophilus* function in place of the *B. subtilis* protein. Therefore, the important residues, including those that may specify interactions with the putative membrane docking protein, are conserved among these orthologs.

We and others have proposed that the SpoIIIA proteins and SpoIIQ form a secretion system that translocates its substrate from the mother cell to the forespore, where it promotes σ^G activity. The identity of the substrate, however, remains unknown. Camp and Losick showed that *spoIIIA* and *spoIIQ* are necessary for the activity of a heterologous RNA polymerase (T7 bacteriophage) in the forespore (3). They hypothesized that the secretion system functions as a feeding tube, supplying the

forespore with a small molecule needed for general biosynthetic activity. Doan and colleagues reported that *spoIIIA* and *spoIIQ* are also necessary to maintain the integrity of the forespore following the completion of engulfment, i.e. the forespore membranes collapsed in their absence (6). The conserved SpoIIIAA ATPase residues were also necessary for forespore integrity. The authors suggested that the secretion system moves a small molecule into the forespore, maintaining its metabolic potential.

Membrane collapse can be caused by osmotic pressure when the external solute concentration (water potential) greatly exceeds the internal solute concentration of the cell. To prevent such catastrophe, bacteria generally import or synthesize osmolytes (18). This strategy may explain the function of putative secretion system. In addition to osmolyte accumulation, the rigid cell walls that surround bacteria also play important roles in preventing membrane collapse. During the transition from forespore engulfment to forespore maturation, the germ cell wall is synthesized in the inner membrane space between the inner and outer forespore membranes. This germ cell wall serves as the template for vegetative cell wall synthesis following spore germination. It may also oppose the osmotic pressure to which the forespore is subjected following engulfment. Consistent with the maintenance of forespore integrity, it is possible that the secretion system promotes germ cell wall synthesis. Because the germ cell wall is thought to be synthesized on the inner forespore membrane, the secretion system may translocate cell wall precursors, called muropeptides, from the mother cell to the forespore. Although identifying the substrate of the proposed secretion system presents a difficult challenge, it will undoubtedly illuminate a poorly understood morphological transition.

FIGURES

Figure 1. Sequence alignment of SpoIIIAA and archaeal secretion superfamily ATPase GspE (*Archaeoglobus fulgidus*). Walker A (teal), Asp (green), Walker B (purple) and His (gold) boxes are shaded. Dual arginine fingers (gray) are also shaded. Conserved secretion ATPase residues are marked with red asterisks. Predicted (SpoIIIAA) and determined (afGspE) secondary structure is shown above the alignment. α-helices are represented as cylinders and β-strands as arrows.

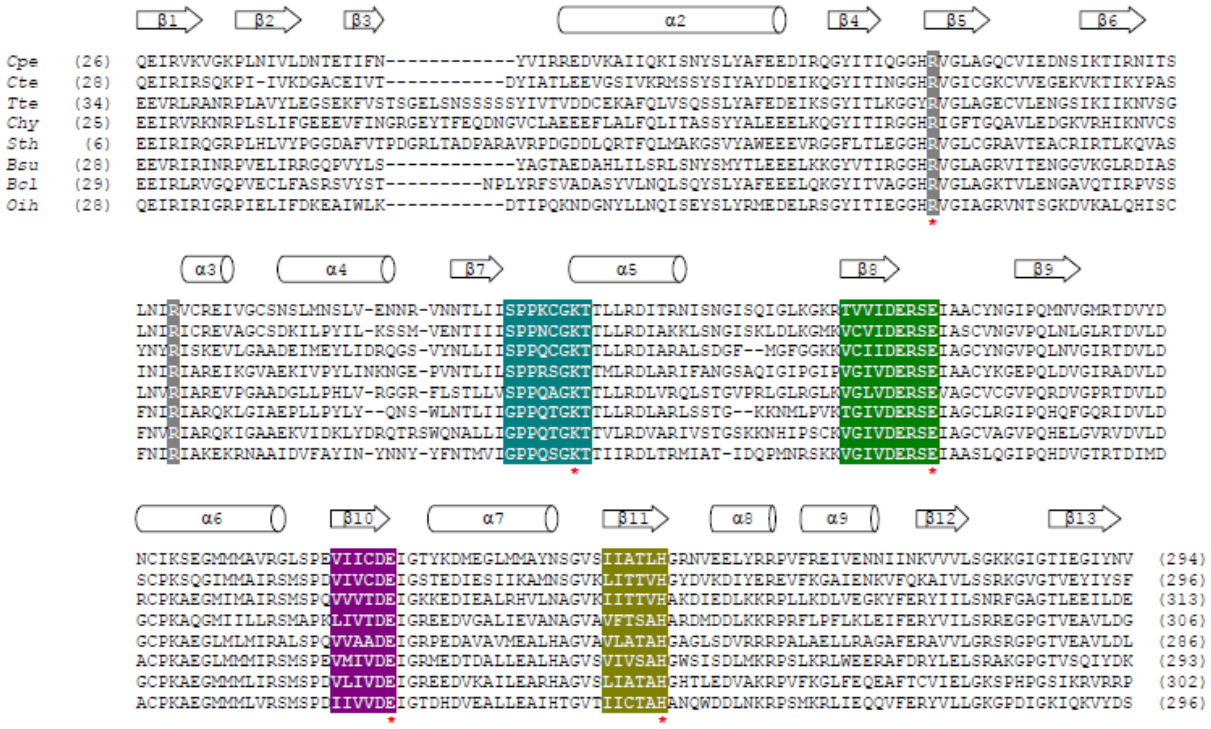

Figure 2. Multiple sequence alignment of N2-C1 sub-domains from SpoIIIAA orthologs. *Clostridium perfringens* (*Cpe*), *Clostridium tetani* (*Cte*), *Thermoanaerobacter tengcongensis* (*Tte*), *Carboxydothermus hydrogenoformans* (*Chy*), *Symbiobacterium thermophilum* (*Sth*), *Bacillus subtilis* (*Bsu*), *Bacillus clausii* (*Bcl*), and *Oceanobacillus iheyensis* (*Ohi*) are shown. The Walker A (teal), Asp (green), Walker B (purple) and His (gold) boxes are shaded. The putative dual arginine fingers (gray) are also shaded. Conserved secretion ATPase residues are marked with red asterisks. Predicted secondary structure is shown above the alignment. α-helices are represented as cylinders and β-strands as arrows.

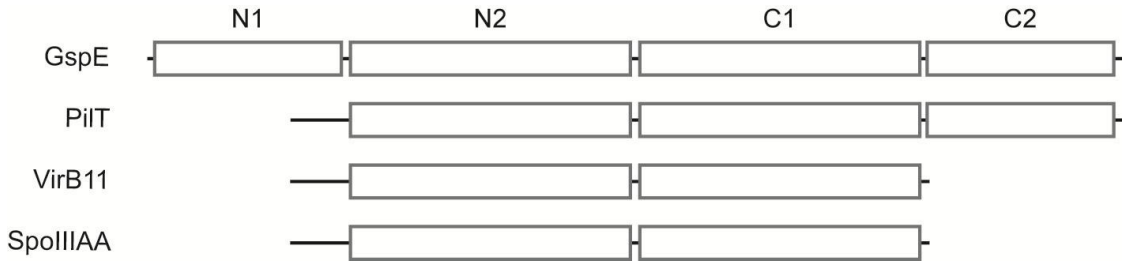

Figure 3. Subdomain composition of GspE, PilT, VirB11, and SpoIIIAA. N1, N2, C1, and C2 subdomains are shown. PilT, VirB11, and SpoIIIAA have an N-terminal α-helix instead of an N1 subdomain. VirB11 and SpoIIIAA lack a C2 subdomain.

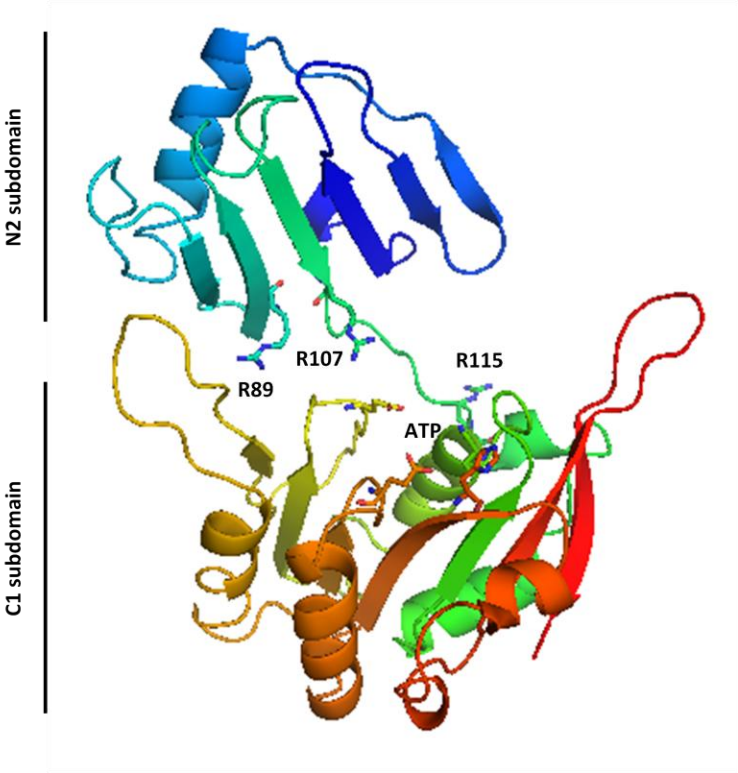

Figure 4. Comparative structural model of the SpoIIIAA N2-C1 subdomains using afGspE as the template. The protein is colored as a spectrum from blue at the N-terminus (residue 20) to red at the C-terminus (residue 292). The N2 and C1 subdomains are labeled to the left of the structural model. The C1 subdomain active site residues K149, E180, E225, and H250 are represented as sticks and the approximate position where ATP binds is labeled. The putative dual arginine finger residues (R89, R107, and R115) are also represented as sticks and labeled.

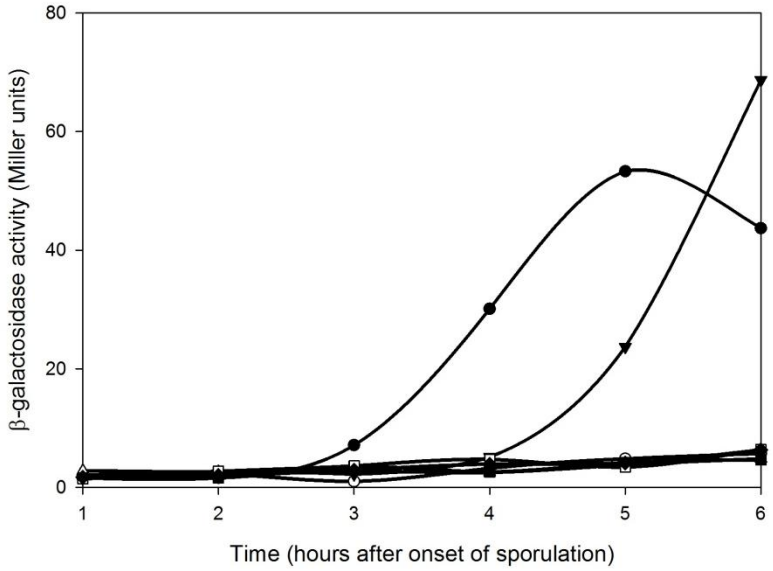

Figure 5. Effects of *spoIIIAA* mutations on σ^G activity. β-galactosidase activity in strains containing P_{sspE}-*lacZ* during sporulation. Shown are wild-type (filled circles), *spoIIIAA* deletion (empty circles), and *spoIIIAA* deletion with wild-type (filled triangles) or mutant *spoIIIAA* alleles (K149R empty triangles, E180Q filled squares, E225Q empty squares, and H250Y filled diamonds). Lysates were prepared hourly after the onset of sporulation.

TABLES

Table 1. Oligonucleotide primers

Primer	Sequence
PspoIIIAF1	CGGGATCCGTTCTTTGTGAATGAAGGCGACACAC
spoIIIAAR1	CCCAAGCTTTCAGCATGTTTTCACGCCCGTC
spoIIIAAR89AF1	ATCAGAGGCGGCCACGCAGTCGGACTGGCGGGCAG
spoIIIAAR89AF2	GCCCGCCAGTCCGACTGCGTGGCCGCCTCTGATCG
spoIIIAAR107AF1	GAGGTGTGAAAGGCCTCGCTGACATCGCATCTTTTAATATACG
spoIIIAAR107AF2	GTATATTAAAAGATGCGATGTCAGCGAGGCCTTTCACACCTCC
spoIIIAAR115AF1	CATCGCATCTTTTAATATAGCAATTGCCCGGCAAAAGCTGG
spoIIIAAR115AF2	CAGCTTTTGCCGGGCAATTGCTATATTAAAAGATGCGATGTC
spoIIIAAK149RF1	GCCCCAAACCGGCCGAACAACACTTCTCCGGGAC
spoIIIAAK149RF2	GGAGAAGTGTTGTTCGGCCGGTTTGGGGCGGTC
spoIIIAAE180QF1	TCGTCGATGAACGGTCACAAATTGCCGGATGTCTTCG
spoIIIAAE180QF2	AGACATCCGGCAATTTGTGACCGTTCATCGACGATCC
spoIIIAAE225QF1	GATGATTGTCGATCAGATCGGGCGTATGGAAGATACAG
spoIIIAAE225QF2	CATACGCCCGATCTGATCGACAATCATCACCTCAG
spoIIIAAH250YF1	GTAATCGTATCGGCGTACGGCTGGAGTATATCCGAC
spoIIIAAH250YF2	CGGATATACTCCAGCCGTACGCCGATACGATTACTG
PsspEF1	AACATCGTCATTAACTATGCACGCAGC
PsspER2	CGGGATCCACGGTCATTAGAATGTGCAGGTGATCG
P1spoIIIAR3	ATCTCATTCAACAGAGCCTCCTCCTTTCTACC
spoIIIAABamF1	GGAGGCTCTGTTGAATGAGATTACAGAGGTTCTCC
spoIIIAABamF2	GGAATTCTCAGCATGTCATCACGCTTTC
PspoIIIAR2	TGTGGTGCAACAGAGCCTCCTCCTTTCTACC
spoIIIAABliF1	GGAGGCTCTGTTGCACCACATCACAGAGATTCTC
spoIIIAABliF2	GGAATTCTCAGCATGATAACATCCTCTTTGC
P1spoIIIAR4	ACCGCTTCCAACAGAGCCTCCTCCTTTCTACC
spoIIIAAGkaF1	GAGGCTCTGTTGGAAGCGGTGTGGGGAATTTTG
spoIIIAAGkaF2	GGAATTCTCATCGATGGACCACCGCC

Table 2. Plasmids

Plasmid	Description/relevant genotype	Source
pDG1664	Integration of cloned gene and erythromycin-resistance cassette into *thrC* locus	Bacillus Genetic Stock Center
pJM70	pDG1664 *PspoIIIA1-spoIIIAA*	This study
pJM188	pDG1664 *PspoIIIA1-spoIIIAA-R89A*	This study
pJM189	pDG1664 *PspoIIIA1-spoIIIAA-R107A*	This study
pJM202	pDG1664 *PspoIIIA1-spoIIIAA-R115A*	This study
pJM106	pDG1664 *PspoIIIA1-spoIIIAA-K149R*	This study
pJM107	pDG1664 *PspoIIIA1-spoIIIAA-E180Q*	This study
pJM108	pDG1664 *PspoIIIA1-spoIIIAA-E225Q*	This study
pJM109	pDG1664 *PspoIIIA1-spoIIIAA-H250Y*	This study
pDG1661	Integration of reporter gene fusion and chloramphenicol-resistance cassette into *amyE* locus	Bacillus Genetic Stock Center
pJM63	pDG1661 *PsspE-lacZ*	This study
pJM196	pDG1664 $PspoIIIA1_{Bsu}$-$spoIIIAA_{Bam}$	This study
pJM195	pDG1664 $PspoIIIA1_{Bsu}$-$spoIIIAA_{Bli}$	This study
pJM203	pDG1664 $PspoIIIA1_{Bsu}$-$spoIIIAA_{Gka}$	This study

Table 3. Bacterial strains

Strain	Relevant genotype	Source
JH642	*trpC2 pheA1* (wild-type)	J. Hoch
RL2042	*ΔspoIIIAA*	R. Losick
JMB105	*ΔspoIIIAA thrC::P1spoIIIA-spoIIIAA*	This study
JMB368	*ΔspoIIIAA thrC::P1spoIIIA-spoIIIAA-R89A*	This study
JMB396	*ΔspoIIIAA thrC::P1spoIIIA-spoIIIAA-R107A*	This study
JMB407	*ΔspoIIIAA thrC::P1spoIIIA-spoIIIAA-R115A*	This study
JMB171	*ΔspoIIIAA thrC::P1spoIIIA-spoIIIAA-K149R*	This study
JMB172	*ΔspoIIIAA thrC::P1spoIIIA-spoIIIAA-E180Q*	This study
JMB173	*ΔspoIIIAA thrC::P1spoIIIA-spoIIIAA-E225Q*	This study
JMB174	*ΔspoIIIAA thrC::P1spoIIIA-spoIIIAA-H250Y*	This study
JMB291	*amyE::PsspE-lacZ*	This study
JMB292	*ΔspoIIIAA amyE::PsspE-lacZ*	This study
JMB293	*ΔspoIIIAA thrC::P1spoIIIA-spoIIIAA amyE::PsspE-lacZ*	This study
JMB295	*ΔspoIIIAA thrC::P1spoIIIA-spoIIIAA-K149R amyE::PsspE-lacZ*	This study
JMB296	*ΔspoIIIAA thrC::P1spoIIIA-spoIIIAA-E180Q amyE::PsspE-lacZ*	This study
JMB297	*ΔspoIIIAA thrC::P1spoIIIA-spoIIIAA-E225Q amyE::PsspE-lacZ*	This study
JMB298	*ΔspoIIIAA thrC::P1spoIIIA-spoIIIAA-H250Y amyE::PsspE-lacZ*	This study
JMB388	*ΔspoIIIAA thrC::P1spoIIIA*$_{Bsu}$*-spoIIIAA*$_{Bam}$	This study
JMB387	*ΔspoIIIAA thrC::P1spoIIIA*$_{Bsu}$*-spoIIIAA*$_{Bli}$	This study
JMB408	*ΔspoIIIAA thrC::P1spoIIIA*$_{Bsu}$*-spoIIIAA*$_{Gka}$	This study

Table 4. Complementation of *spoIIIAA* deletion by wild-type and mutant alleles

Relevant genotype	Sporulation efficiency
Wild-type	0.76
ΔspoIIIAA	2.8 X 10^{-6}
ΔspoIIIAA thrC::PspoIIIA1-spoIIIAA	0.65
ΔspoIIIAA thrC::PspoIIIA1-spoIIIAA-R89A	6.8 X 10^{-5}
ΔspoIIIAA thrC::PspoIIIA1-spoIIIAA-R107A	1.0
ΔspoIIIAA thrC::PspoIIIA1-spoIIIAA-R115A	3.3 X 10^{-5}
ΔspoIIIAA thrC::PspoIIIA1-spoIIIAA-K149R	7.0 X 10^{-6}
ΔspoIIIAA thrC::PspoIIIA1-spoIIIAA-E180Q	1.2 X 10^{-5}
ΔspoIIIAA thrC::PspoIIIA1-spoIIIAA-E225Q	6.0 X 10^{-6}
ΔspoIIIAA thrC::PspoIIIA1-spoIIIAA-H250Y	3.1 X 10^{-6}

Table 5. Complementation of *spoIIIAA* deletion by orthologous alleles

Relevant genotype	Sporulation efficiency
ΔspoIIIAA thrC::PspoIIIA1$_{Bsu}$ spoIIIAA$_{Bam}$	0.92
ΔspoIIIAA thrC::PspoIIIA1$_{Bsu}$ spoIIIAA$_{Bli}$	1.0
ΔspoIIIAA thrC::PspoIIIA1$_{Bsu}$ spoIIIAA$_{Gka}$	0.85

REFERENCES

1. **Anagnostopoulos, C., and J. Spizizen.** 1961. Requirements for Transformation in Bacillus Subtilis. J Bacteriol **81:**741-746.

2. **Blaylock, B., X. Jiang, A. Rubio, C. P. Moran, Jr., and K. Pogliano.** 2004. Zipper-like interaction between proteins in adjacent daughter cells mediates protein localization. Genes Dev **18:**2916-2928.

3. **Camp, A. H., and R. Losick.** 2009. A feeding tube model for activation of a cell-specific transcription factor during sporulation in Bacillus subtilis. Genes Dev **23:**1014-1024.

4. **Camp, A. H., and R. Losick.** 2008. A novel pathway of intercellular signalling in Bacillus subtilis involves a protein with similarity to a component of type III secretion channels. Mol Microbiol **69:**402-417.

5. **Craig, L., M. E. Pique, and J. A. Tainer.** 2004. Type IV pilus structure and bacterial pathogenicity. Nat Rev Microbiol **2:**363-378.

6. **Doan, T., C. Morlot, J. Meisner, M. Serrano, A. O. Henriques, C. P. Moran, Jr., and D. Z. Rudner.** 2009. Novel secretion apparatus maintains spore integrity and developmental gene expression in Bacillus subtilis. PLoS Genet **5:**e1000566.

7. **Eswar, N., B. Webb, M. A. Marti-Renom, M. S. Madhusudhan, D. Eramian, M. Y. Shen, U. Pieper, and A. Sali.** 2006. Comparative protein structure modeling using Modeller. Curr Protoc Bioinformatics **Chapter 5:**Unit 5 6.

8. **Meisner, J., X. Wang, M. Serrano, A. O. Henriques, and C. P. Moran, Jr.** 2008. A channel connecting the mother cell and forespore during bacterial endospore formation. Proc Natl Acad Sci U S A **105:**15100-15105.

9. **Miller, J.** 1972. Experiments in Molecular Genetics. Cold Spring Harbor Laboratory, Cold Spring Harbor, NY.

10. **Peabody, C. R., Y. J. Chung, M. R. Yen, D. Vidal-Ingigliardi, A. P. Pugsley, and M. H. Saier, Jr.** 2003. Type II protein secretion and its relationship to bacterial type IV pili and archaeal flagella. Microbiology **149:**3051-3072.

11. **Planet, P. J., S. C. Kachlany, R. DeSalle, and D. H. Figurski.** 2001. Phylogeny of genes for secretion NTPases: identification of the widespread tadA subfamily and development of a diagnostic key for gene classification. Proc Natl Acad Sci U S A **98:**2503-2508.

12. **Possot, O., and A. P. Pugsley.** 1994. Molecular characterization of PulE, a protein required for pullulanase secretion. Mol Microbiol **12:**287-299.

13. **Robien, M. A., B. E. Krumm, M. Sandkvist, and W. G. Hol.** 2003. Crystal structure of the extracellular protein secretion NTPase EpsE of Vibrio cholerae. J Mol Biol **333:**657-674.

14. **Satyshur, K. A., G. A. Worzalla, L. S. Meyer, E. K. Heiniger, K. G. Aukema, A. M. Misic, and K. T. Forest.** 2007. Crystal structures of the pilus retraction motor PilT suggest large domain movements and subunit cooperation drive motility. Structure **15:**363-376.

15. **Soding, J.** 2005. Protein homology detection by HMM-HMM comparison. Bioinformatics **21:**951-960.

16. **Soding, J., A. Biegert, and A. N. Lupas.** 2005. The HHpred interactive server for protein homology detection and structure prediction. Nucleic Acids Res **33:**W244-248.

17. **Thompson, J. D., D. G. Higgins, and T. J. Gibson.** 1994. CLUSTAL W: improving the sensitivity of progressive multiple sequence alignment through sequence weighting, position-specific gap penalties and weight matrix choice. Nucleic Acids Res **22:**4673-4680.

18. **Wood, J. M.** 1999. Osmosensing by bacteria: signals and membrane-based sensors. Microbiol Mol Biol Rev **63:**230-262.

19. **Yamagata, A., and J. A. Tainer.** 2007. Hexameric structures of the archaeal secretion ATPase GspE and implications for a universal secretion mechanism. EMBO J **26:**878-890.

20. **Yeo, H. J., S. N. Savvides, A. B. Herr, E. Lanka, and G. Waksman.** 2000. Crystal structure of the hexameric traffic ATPase of the Helicobacter pylori type IV secretion system. Mol Cell **6:**1461-1472.

CHAPTER 5. Bioinformatics analysis and site-directed mutagenesis of SpoIIIAB, SpoIIIAC, SpoIIIAD, and SpoIIIAE

INTRODUCTION

The SpoIIIA proteins are proposed to assemble into an integral membrane complex, constituting a novel export apparatus that moves an unidentified substrate from the mother cell to the forespore (2, 3, 5, 9). SpoIIIAH recognizes the mother cell-forespore interface, by interacting with the forespore protein SpoIIQ, and is hypothesized to serve as a structural scaffold for the assembly of the putative export apparatus. This hypothesis is based on the observation that SpoIIIAH shares similarity with the ring-forming protein of the type III export apparatus. The type III export apparatus consists of six integral membrane proteins which are thought to assemble within the central channel of the ring (4, 8). Two of these six proteins have N-terminal transmembrane segments (TMS) and C-terminal cytoplasmic domains which interact with a cytoplasmic protein complex, including an ATP hydrolase. The other four integral membrane proteins contain several TMS and lack significant cytoplasmic domains. Although some interactions among these proteins are established, their functions are not understood.

While biochemical data suggest that SpoIIIAB, SpoIIIAC, SpoIIIAD, SpoIIIAE, SpoIIIAF, and SpoIIIAG form an integral membrane complex (5), essentially nothing is known about the function of these proteins. To begin to understand their functions, we performed bioinformatics analyses to predict the membrane topologies of the proteins and identify conserved residues. Then, we determined whether alleles with mutations in these conserved residues complemented the sporulation defects of in-frame deletions of

the corresponding gene. These complementation analyses allowed us to determine which residues were necessary for function.

MATERIALS AND METHODS

Bioinformatics

The *B. subtilis* SpoIIIAB, SpoIIIAC, SpoIIIAD, and SpoIIIAE amino acid sequences were analyzed by the MEMSAT, TMHMM, TOPPRED, TMPRED, and HMMTOP programs and the membrane topology of each protein was predicted (6, 7, 16, 18, 19). The amino acid sequences were also submitted to the HHpred server for protein homology detection and structure prediction (14, 15). The sequences of selected spore-forming bacteria were aligned using the multiple sequence alignment program ClustalW (17).

General bacterial methods

B. subtilis strains, derivatives of laboratory strain JH642, were grown in Luria broth (LB) and sporulation was induced by nutrient exhaustion in Difco sporulation medium (DSM) at 37 °C with aeration. Genetic competence was developed and transformations were performed as described previously (1). Transformants were selected on LB agar plates containing 1 μg/ml erythromycin. *Escherichia coli* transformants were grown in LB containing 100 μg/ml ampicillin.

Plasmid and strain construction

B. subtilis strains containing in-frame deletions in *spoIIIAB*, *spoIIIAC-spoIIIAD*, and *spoIIIAE* were provided by Richard Losick (Harvard University). Complementation

strains were constructed by transforming the in-frame deletion strains with integration vectors carrying a cloned allele. Following double cross-over recombination, the cloned alleles were integrated into the chromosome at the *thrC* locus.

Each wild-type gene was cloned from *B. subtilis* chromosomal DNA by polymerase chain reaction (PCR). The oligonucleotide primers used for cloning are listed in Table 1. Each of the cloned gene was fused downstream of a cloned *spoIIIA* promoter by overlapping PCR. The resulting DNA fragments consisted of the *spoIIIA* promoter and transcriptional start site fused to the ribosome binding site and open reading frame from the cloned genes, with *BamHI*, *HindIII*, or *EcoRI* restriction sites at each end. The fragments and integration vector pDG1664 were cut with the appropriate restriction enzymes, purified, and ligated. One Shot Top10 chemically competent *E. coli* cells (Invitrogen) were transformed with the ligated plasmids and transformants were selected on LB agar containing 100 μg/ml ampicillin. Plasmids were purified from the transformants and confirmed by DNA sequencing. Finally, *B. subtilis* strains containing the in-frame deletions were transformed with these plasmids. The plasmids and strain used in this work are shown in Tables 2 and 3.

Site-directed mutagenesis

Mutations were introduced into the plasmids using the QuikChange site-directed mutagenesis kit (Stratagene). The following PCR conditions were used: one step at 95 °C for 1 minute; 18 cycles of 95 °C for 30 seconds, 55 °C for 1 minute, and 68 °C for 6 minute; and a final extension step at 68 °C for 10 minutes. 1 μl of each QuikChange reaction was cut with DpnI restriction enzyme at 37 °C for 1 hour. One Shot Top10

chemically competent *E. coli* cells were transformed with 2.5 μl of each reaction and transformants were selected on LB agar containing 100 μg/ml ampicillin. Plasmids were purified from the transformants and confirmed by DNA sequencing. *B. subtilis* strains containing the in-frame deletions were transformed with these plasmids.

Sporulation test

B. subtilis strains were grown in DSM at 37 °C for 48 hours. 500 ml of each culture was heated at 80 °C for 10 minutes. Then heated and non-heated cultures were serially diluted (10-fold) in LB. 100 ml of each dilution was spread on LB agar at incubated at 37 °C overnight. Colonies were counted and the numbers of heat-resistant spores and total cells per ml of the DSM culture were calculated. The sporulation efficiency is the number of heat-resistant spores per total cells.

RESULTS AND DISCUSSION

Predicted membrane topology of SpoIIIAB, SpoIIIAC, SpoIIIAD, and SpoIIIAE

Using five prediction methods, the membrane topology of a set of 60 *E. coli* inner membrane proteins could be predicted with high reliability by a "majority-vote" approach (10). To start to explore the functions of SpoIIIAB, SpoIIIAC, SpoIIIAD, and SpoIIIAE, we analyzed their amino acid sequences with five different prediction programs and assessed whether a majority-vote could be used to predict the membrane topology of each protein (Table 4). Using MEMSTAT, TMHMM, TOPPRED, TMPRED, and HMMTOP (6, 7, 16, 18, 19), only SpoIIIAC and SpoIIIAD can be reliably predicted by a majority-vote. SpoIIIAC has two transmembrane segments (TMS) with both

termini in the cytoplasm, while SpoIIIAD had four TMS with both termini outside the cell. SpoIIIAB has an N-terminal TMS, an approximately 130 amino acid cytoplasmic domain, and a hydrophobic C-terminus. There is disagreement among the predictions about whether the C-terminus contains a TMS. There is also disagreement about the number of TMS (either seven or eight) and membrane topology of SpoIIIAE.

Site-directed mutagenesis of SpoIIIAB

SpoIIIAB is a predicted integral membrane protein with a central cytoplasmic domain which is probably flanked by N- and C-terminal TMS (Figure 1). The HHpred server detected remote homology between the predicted cytoplasmic domain (residues 25-150) and the type II secretion protein GspF (PF00482). This protein is part of the integral membrane docking platform for the GspE ATPase (11). Reasoning that important residues would be conserved among orthologs, we generated multiple sequence alignments of proteins from diverse spore-forming bacteria and searched for conserved residues. We identified several conserved residues in SpoIIIAB orthologs (Figure 1). To determine whether these residues are necessary for SpoIIIAB function, we tested the ability of five different mutant alleles to complement the sporulation defect of an in-frame deletion in *spoIIIAB* (Table 5). The mutant phenotype was complemented when a wild-type allele was integrated at the *thrC* locus. Alleles containing Y48A or L53A mutations, however, failed to complement. Therefore, residues Y48 and L53 are necessary for SpoIIIAB function. We cannot eliminate the possibly that these residues are necessary for the stability of the protein.

Because the SpoIIIAB forms a complex with SpoIIIAD, SpoIIIAE, SpoIIIAF, and SpoIIIAG *in vivo* (5), we considered the possibility that Y48 and L53 are necessary for interactions of SpoIIIAB with other SpoIIIA proteins. If these mutants are defective because they disrupt such interactions, then we may be able to identify mutations in the other *spoIIIA* genes that suppress the mutant phenotype by restoring a protein-protein interaction. To attempt to identify suppressor mutations, we spread the Y48A and L53A mutants on sporulation medium containing the chemical mutagen, ethyl methane sulfonate (EMS), and waited for colonies to form. Only cells that acquire a mutation that suppresses the sporulation defect of the parental mutants can form colonies. Unfortunately, we were unable to isolate any mutants with extragenic suppressor mutations in other *spoIIIA* genes. In the case of the L53A mutant, we isolated six intragenic suppressor (pseudorevertant) mutants. Each of these six suppressors contained the same A53V mutation in *spoIIIAB*. This pseudorevertant mutation from alanine to valine restores the physiochemical properties of the wild-type leucine. A large, hydrophobic residue must be important at position 53 of SpoIIIAB.

Site-directed mutagenesis of SpoIIIAC and SpoIIIAD

SpoIIIAC and SpoIIIAD are both predicted polytopic integral membrane proteins. SpoIIIAC has two predicted transmembrane segments, while SpoIIIAD has four (Figures 2 and 3). Neither proteins displays sequence similarity with proteins of known function. As described above, we identified several conserved residues in SpoIIIAC and SpoIIIAD orthologs (Figures 2 and 3) and tested the ability of mutant *spoIIIAC-spoIIIAD* alleles to complement the sporulation defect of an in-frame deletion in

spoIIIAC-spoIIIAD (Table 6). While the wild-type *spoIIIAC-spoIIIAD* integrated at the *thrC* locus complemented the mutant phenotype, the *spoIIIAC-spoIIIAD-K75A* mutant did not complement. Therefore, the residue K75 is necessary for SpoIIIAD function or stability. Interestingly, this residue is located in the middle of a transmembrane segment (TMS3). Because of it positive charge, K75 would not be stably partitioned into the hydrophobic membrane. It would have to be neutralized by an electrostatic interaction with a residue in another transmembrane segment, from either SpoIIIAD itself or an interacting protein. Alternatively, it could reside in an aqueous central pore. Therefore, the K75A mutation may prevent a protein-protein interaction between SpoIIIAD and another SpoIIIA protein or disrupt the architecture of a central pore.

Site-directed mutagenesis of SpoIIIAE

SpoIIIAE is a polytopic integral membrane protein with seven or eight predicted transmembrane segments and a cleavable N-terminal signal peptide which, through the activities of the Sec translocon and the membrane protein insertase SpoIIIJ, facilitates its membrane insertion (3, 12). SpoIIIAE residues 200-350 show limited sequence similarity with various transporter proteins. This region of consists of 2 transmembrane segments (TMS4 and TMS5), an approximately 50 residue hydrophilic loop, and 2 more transmembrane segments (TMS6 and TMS7). In transporter proteins this hydrophilic loop, called the reentrant pore loop, folds into the central pore formed by the transmembrane segments (20). These reentrant pore loops are important determinants of transporter function and selectively (13). The putative SpoIIIAE reentrant pore loop (residues 270-315) contains several residues which are conserved among the orthologs

from diverse spore-forming bacteria. To determine whether these residues are necessary for SpoIIIAE function, we tested the ability of six different mutant alleles to complement the sporulation defect of an in-frame *spoIIIAE* deletion (Table 7). Each of the mutants we tested (D275A, R208A, T281A K283A, D299A, and S308A) complemented the phenotype of the *spoIIIAE* deletion. Therefore, none of the residues are necessary for function. A mutant allele containing a deletion of the central region of the loop (residues 273-309) failed to complement, indicating that the loop is necessary for SpoIIIAE function or stability.

We also tested whether twelve other conserved residues located elsewhere in the protein were necessary for function (Table 7). Mutations in residues F131 (loop TMS1-TMS2), F156 (TMS2), or K333 (TMS6) failed to fully complement the *spoIIIAE* deletion. The sporulation defects associated with these mutants were mild; an approximately 10-50 fold reduction in sporulation efficiency was observed with these mutants compared to the wild-type. Therefore, these residues may be contribute to SpoIIIAE but are not completely necessary for it.

Finally, we constructed a mutant spoIIIAE allele which lacked cysteines, i.e. a Cys-less mutant. A Cys-less mutant is an important tool for biochemical and structural characterization of transporter proteins. The residues that line the aqueous central pore can be identified by measuring the reactivity of cysteines engineered at various positions throughout the protein to membrane-impermeable, thiol-reactive compounds. The organization of transmembrane segments can be determined by identifying pairs of engineered cysteines that can be oxidized to form disulfide bonds or cross-linked with

homobifunctional, thiol-reactive compounds. Alleles with mutations in any of the three native SpoIIIAE cysteines (C121, C325, or C359) complemented the *spoIIIAE* deletion, indicating that none of them are necessary for SpoIIIAE function (Table 7). Furthermore, a Cys-less allele (C121A, C325A, and C359A) was almost fully functional, showing a 2-fold reduction in sporulation efficiency compared to wild-type (Table 7). Thus, this Cys-less spoIIIAE allele should be amenable to the biochemical and structural analyses used to study transporter proteins.

FIGURES

Figure 1. Multiple sequence alignment of SpoIIIAB orthologs. *Bacillus subtilis* (*Bsu*), *Bacillus clausii* (*Bcl*), *Oceanobacillus iheyensis* (*Ohi*), *Thermoanaerobacter tengcongensis* (*Tte*), *Symbiobacterium thermophilum* (*Sth*), *Clostridium tetani* (*Cte*), *Carboxydothermus hydrogenoformans* (*Chy*), and *Clostridium perfringens* (*Cpe*) are shown. Predicted secondary structure is shown above the alignment with α-helices represented as cylinders and transmembrane segments (TMS) shaded gray. Conserved residues are marked with red asterisks below the alignment.

Figure 2. Multiple sequence alignment of SpoIIIAC orthologs. *Bacillus subtilis* (*Bsu*), *Bacillus clausii* (*Bcl*), *Oceanobacillus iheyensis* (*Ohi*), *Clostridium perfringens* (*Cpe*), *Symbiobacterium thermophilum* (*Sth*), *Carboxydothermus hydrogenoformans* (*Chy*), and *Thermoanaerobacter tengcongensis* (*Tte*), and *Clostridium acetobutylicum* (*Cac*) are shown. Predicted transmembrane segments (TMS) are shown as gray cylinders above the alignment. Conserved residues are marked with red asterisks below the alignment.

Figure 3. Multiple sequence alignment of SpoIIIAD orthologs. *Bacillus subtilis* (*Bsu*), *Bacillus clausii* (*Bcl*), *Carboxydothermus hydrogenoformans* (*Chy*), *Oceanobacillus iheyensis* (*Ohi*), *Symbiobacterium thermophilum* (*Sth*), *Clostridium acetobutylicum* (*Cac*), *Thermoanaerobacter tengcongensis* (*Tte*), and *Clostridium perfringens* (*Cpe*) are shown. Predicted transmembrane segments (TMS) are shown above the alignment and represented as gray cylinders. Conserved residues are marked with red asterisks below the alignment.

Figure 4. Multiple sequence alignment of SpoIIIAE orthologs. *Bacillus subtilis* (*Bsu*), *Bacillus clausii* (*Bcl*), *Symbiobacterium thermophilum* (*Sth*), *Thermoanaerobacter tengcongensis* (*Tte*), and *Clostridium perfringens* (*Cpe*) are shown. Predicted transmembrane segments

(TMS) are shown as gray cylinders above the alignment. Conserved residues are marked with red asterisks below the alignment.

TABLES

Table 1. Oligonucleotide primers

Primer	Sequence
PspoIIIAF1	CGGGATCCGTTCTTTGTGAATGAAGGCGACACAC
PspoIIIAR3	GCTTCAGCATCAGAGCCTCCTCCTTTCTACC
spoIIIABF1	GGAGGCTCTGATGCTGAAGCTGCTGGGCG
spoIIIABR2	GGAATTCTCCCCTCACGTTTACATCAATAGAAGAATGAG
spoIIIABR28AF1	AAGATTTATACAGAAGCACCGCGGCAAATCCGCCAGCTG
spoIIIABR28AR2	CTGGCGGATTTGCCGCGGTGCTTCTGTATAAATCTTCGC
spoIIIABY48AF1	AGGCTGAAATCATGGCAGGCCATACACCGCTTCATACTG
spoIIIABY48AR2	TGAAGCGGTGTATGGCCTGCCATGATTTCAGCCTCGAG
spoIIIABL53AF1	GTACGGCCATACACCGGCTCATACTGCTTCACAGC
spoIIIABL53AR2	TGAAGCAGTATGAGCCGGTGTATGGCCGTACATGATTTCAG
spoIIIABL132AF1	CAGCAAAAGCACATCAAGGCGGCGCTGACACATTTGG
spoIIIAB L132AR2	CCAAATGTGTCAGCGCCGCCTTGATGTGCTTTTGCTG
spoIIIABK153AF1	GTCGCCACGATTGTAGATGACGCATTTAAAAAGATAAAAGCTGTG
spoIIIABK153AR2	ACAGCTTTTATCTTTTTAAATGCGTCATCTACAATCGTGGCGACC
PspoIIIAR4	GTCTACTCCCATCAGAGCCTCCTCCTTTCTACC
spoIIIACF1	GGAGGCTCTGATGGGAGTAGACGTGAATGTCATATTTCAAATCG
spoIIIADR2	CCCAAGCTTTCCTTTCGGTTATGACATAGAAGGTATAAGTCC
spoIIIACK30AF1	ATTGGATCAGATGGGCGCAAAAGAATATGCTCAGTGGGTGACG
spoIIIACK30AR2	CACCCACTGAGCATATTCTTTTGCGCCCATCTGATCCAATCTCG
spoIIIACK31AF1	ATTGGATCAGATGGGCGCAAAAGAATATGCTCAGTGGGTGACG
spoIIIACK31AR2	CACCCACTGAGCATATTCTTTTGCGCCCATCTGATCCAATATCG
spoIIIACE32AF1	ATTGGATCAGATGGGCAAGGCGGAATATGCTCAGTGGGTGACG
spoIIIACE32AR2	CACCCACTGAGCATATTCCGCCTTGCCCATCTGATCCAATATCG
spoIIIACL56AF1	GTCGCCACGATTGTAGATGACGCATTTAAAAAGATAAAAGCTGTG
spoIIIACL56AR2	ACAGCTTTTATCTTTTTAGCGTCATCTACAATCGTGGCGACC
spoIIIACK61AF1	GACCTATTTAAAAAGATAGCAGCTGTGTTTTTATTCCAAGGATAGG
spoIIIACK61AR2	CCTATCCTTGGAATAAAAACACAGCTGCTATCTTTTTAAATAGGTC
spoIIIADY69AF1	GCAAATGTCAACATGGTCGCTGTTGAAACCATTTTAAAGATTATCG
spoIIIADY69AR2	CGATAATCTTTAAAATGGTTTCAACAGCGACCATGTTGACATTTGC
spoIIIADT72AF1	GTCAACATGGTCTATGTTGAAGCAATTTTAAAGATTATCGGAATCG
spoIIIADT72AR2	CGATTCCGATAATCTTTAAAATTGCTTCAACATAGACCATGTTGAC

spoIIIADK75AF1	CTATGTTGAAACCATTTTAGCAATTATCGGAATCGCCTATATTGCTG
spoIIIADK75AR2	CAATATAGGCGATTCCGATAATTGCTAAAATGGTTTCAACATAGACC
spoIIIADD92AF1	ACAGCTCACAAAAGCAGCCGGTCAAGGAGCCATCG
spoIIIADD92AR2	ATGGCTCCTTGACCGGCTGCTTTTGTGAGCTGTGC
spoIIIADE103AF1	ATCGCCTCGAAAATAGCGTTGGCGGGGAAAATTTTAATACTC
spoIIIADE103AR2	GTATTAAAATTTTCCCCGCCAACGCTATTTTCGAGGCGATGG
PspoIIIA1R2	GAAAGCGCTTCAACAGAGCCTCCTCCTTTCTACC
spoIIIAEF1	GGAGGCTCTGTTGAAGCGCTTTCAATGGGTTTTGC
spoIIIAER2	CCCAAGCTTTTATTTGCCTGCCTCCTTCATTTCATCATC
spoIIIAEK109AF1	CTTGCCAACGGAGCGCTGCTGGGCACATTGATTTTGC
spoIIIAEK109AR2	AAAATCAATGTGCCCAGCAGCGCTCCGTTGGCAAGCAC
spoIIIAEQ125AF1	CACGATTTTTTGCGTCATTCTGGCGCTTTTGCAAAATGCTTTTCAGC
spoIIIAEQ125AR2	TGAAAAGCATTTTGCAAAAGCGCCAGAATGACGCAAAAAATCGTGAG
spoIIIAEF131AF1	CAGCTTTTGCAAAATGCTGCTCAGCAAAGCACCGTCAGTAAGGTC
spoIIIAEF131AR2	CTTACTGACGGTGCTTTGCTGAGCAGCATTTTGCAAAAGCTGCAG
spoIIIAEY145AF1	TAAGGTCGCTTACTCAATTGTGGCCATGGTGCTGATTATCCTTGC
spoIIIAEY145AR2	AAGGATAATCAGCACCATGGCCACAATTGAGTAAGCGACCTTACTG
spoIIIAEF156AF1	GATTATCCTTGCGCTTAATAGCGCTCATGTGGCAATTAACTATGC
spoIIIAEF156AR2	CATAGTTAATTGCCACATGAGCGCTATTAAGCGCAAGGATAATCAG
spoIIIAEH157AF1	TTGCGCTTAATAGCTTTGCTGTGGCAATTAACTATGCAACTGAGG
spoIIIAEH157AR2	TCAGTTGCATAGTTAATTGCCACAGCAAAGCTATTAAGCGCAAGG
spoIIIAES193AF1	TTCCTCAGGCGGAGCTGTAGCTGCTGCCTTCTTTCATCCTG
spoIIIAES193AR2	GATGAAAGAAGGCAGCAGCTACAGCTCCGCCTGAGGAAGC
spoIIIAEQ213AF1	ATGAACACGAGCGGTCTCTTGATTGCGAATATCGTCATGC
spoIIIAEQ213AR2	TGACGATATTCGCAATCAAGAGACCGCTCGTGTTCATCAG
spoIIIAER246AF1	AGCTGGCTAACCTGCTCGCAAATATCGCCATCGGAGC
spoIIIAER246AR2	TCCGATGGCGATATTTGCGAGCAGGTTAGCCAGCTGC
spoIIIAED275AF1	TCAGCTGCAGTGACAGCAGGCATTACGCTCAGGAC
spoIIIAED275AR2	CTGAGCGTAATGCCTGCTGTCACTGCAGCTGACG
spoIIIAER280AF1	GTGACAGACGGCATTACGCTCGCGACGGCTAAATTTATAACCG
spoIIIAER280AR2	GTTATAAATTTAGCCGTCGCGAGCGTAATGCCGTCTGTCACTG
spoIIIAET281AF1	GACGGCATTACGCTCAGGGCAGCTAAATTTATAACCG
spoIIIAET281AR2	GTTATAAATTTAGCTGCCCTGAGCGTAATGCCGTCTGTC
spoIIIAEK283AF1	ACGCTCAGGACGGCTGCATTTATAACCGGAAATTTTATTCCTGTG
spoIIIAEK283AR2	GGAATAAAATTTCCGGTTATAAATGCAGCCGTCCTGAGCGTAATGC

spoIIIAED299AF1	TTGGCCGAATGTTTACAGCTGCAACAGATACAGTAATCAGC
spoIIIAED299AR2	TGATTACTGTATCTGTTGCAGCTGTAAACATTCGGCCAAGC
spoIIIAES308AF1	ACAGTAATCAGCGCCGCATTACTGCTGAAAAATACGGTAGG
spoIIIAES308AR2	ACCGTATTTTTCAGCAGTAATGCGGCGCTGATTACTGTATCTG
spoIIIAE207-309F1	AGCGTCAGCTGCACTGCTGAAAAATACGGTAGG
spoIIIAE207-309R2	CGTATTTTTCAGCAGTGCAGCTGACGCTCCCTG
spoIIIAEK312AF1	GCGCCTCTTTACTGCTGGCAAATACGGTAGGGATTCTCG
spoIIIAEK312AR2	AGAATCCCTACCGTATTTGCCAGCAGTAAAGAGGCGCTG
spoIIIAEK333AF1	GCATTTCCGGCAATCGCAGTGCTTTCCCTCGCTTTTATTTATAAGCTG
spoIIIAEK333AR2	AAGCGAGGGAAAGCACTGCGATTGCCGGAAATGCCGCAATACAG
spoIIIAEQ349AF1	AGCCGCGATTCTTGCGCCGCTAGGAGGCGGGCCCGTC
spoIIIAEQ349AR2	CCCGCCTCCTAGCGGCGCAAGAATCGCGGCTGCCAGC
spoIIIAEC121AF1	TGCTCACGATTTTTTCGGTCATTCTGCAGCTTTTGCAAAATGC
spoIIIAEC121AR2	AGCTGCAGAATGACCGAAAAAATCGTGAGCAAAATCAATGTG
spoIIIAEC325AF1	GTGTCGCTATTTTGATCTCGATTGCGGCATTTCCGGCA
spoIIIAEC325AR2	GGAAATGCCGCAATCGAGATCAAAATAGCGACACCGAG
spoIIIAEC359AF1	GCCCGTCATCACCTCGCTCGACGTCATCAGC
spoIIIAEC359AR2	ATGACGTCGAGCGAGGTGATGACGGGCCCGCCT

Table 2. Plasmids

Strain	Relevant genotype	Source
pDG1664	Integration of cloned gene and erythromycin-resistance cassette into *thrC* locus	Bacillus Genetic Stock Center
pJM84	pDG1664 *spoIIIAB*	This study
pJM91	pDG1664 *spoIIIAB-R28A*	This study
pJM92	pDG1664 *spoIIIAB-Y48A*	This study
pJM110	pDG1664 *spoIIIAB-L53A*	This study
pJM111	pDG1664 *spoIIIAB-L132A*	This study
pJM93	pDG1664 *spoIIIAB-K153A*	This study
pJM85	pDG1664 *spoIIIAC-AD*	This study
pJM94	pDG1664 *spoIIIAC-K30A-AD*	This study
pJM95	pDG1664 *spoIIIAC-K31A-AD*	This study
pJM96	pDG1664 *spoIIIAC-E32A-AD*	This study
pJM112	pDG1664 *spoIIIAC-L56A-AD*	This study
pJM113	pDG1664 *spoIIIAC-K61A-AD*	This study
pJM114	pDG1664 *spoIIIAC-AD-Y69A*	This study
pJM115	pDG1664 *spoIIIAC-AD-T72A*	This study
pJM97	pDG1664 *spoIIIAC-AD-K75A*	This study
pJM98	pDG1664 *spoIIIAC-AD-D92A*	This study
pJM99	pDG1664 *spoIIIAC-AD-E103A*	This study
pJM71	pDG1664 *spoIIIAE*	This study
pJM141	pDG1664 *spoIIIAE-K109A*	This study
pJM157	pDG1664 *spoIIIAE-Q125A*	This study
pJM165	pDG1664 *spoIIIAE-F131A*	This study
pJM158	pDG1664 *spoIIIAE-Y145A*	This study
pJM166	pDG1664 *spoIIIAE-F156A*	This study
pJM142	pDG1664 *spoIIIAE-H157A*	This study
pJM159	pDG1664 *spoIIIAE-S193A*	This study
pJM160	pDG1664 *spoIIIAE-Q213A*	This study
pJM143	pDG1664 *spoIIIAE-R246A*	This study
pJM116	pDG1664 *spoIIIAE-D275A*	This study
pJM167	pDG1664 *spoIIIAE-R280A*	This study
pJM117	pDG1664 *spoIIIAE-T281A*	This study
pJM118	pDG1664 *spoIIIAE-K283A*	This study

pJM180	pDG1664 *spoIIIAE-D299A*	This study
pJM119	pDG1664 *spoIIIAE-S308A*	This study
pJM178	pDG1664 *spoIIIAEΔ273-309*	This study
pJM120	pDG1664 *spoIIIAE-K312A*	This study
pJM144	pDG1664 *spoIIIAE-K333A*	This study
pJM169	pDG1664 *spoIIIAE-Q349A*	This study
pJM132	pDG1664 *spoIIIAE-C121S*	This study
pJM133	pDG1664 *spoIIIAE-C325S*	This study
pJM134	pDG1664 *spoIIIAE-C359S*	This study
pJM146	pDG1664 *spoIIIAE-C121S-C325S-C359S (Cys-less)*	This study

Table 3. Bacterial strains

Strain	Relevant genotype	Source
JH642	Wild-type	J. Hoch
RL2043	*ΔspoIIIAB*	R. Losick
JMB115	*ΔspoIIIAB thrC::PspoIIIA1-spoIIIAB*	This study
JMB128	*ΔspoIIIAB thrC::PspoIIIA1-spoIIIAB-R28A*	This study
JMB129	*ΔspoIIIAB thrC::PspoIIIA1-spoIIIAB-Y48A*	This study
JMB156	*ΔspoIIIAB thrC::PspoIIIA1-spoIIIAB-L53A*	This study
JMB157	*ΔspoIIIAB thrC::PspoIIIA1-spoIIIAB-L132A*	This study
JMB130	*ΔspoIIIAB thrC::PspoIIIA1-spoIIIAB-K153A*	This study
RL2044	*ΔspoIIIAC-AD*	R. Losick
JMB116	*ΔspoIIIAC-AD thrC::PspoIIIA1-spoIIIAC-AD*	This study
JMB131	*ΔspoIIIAC-AD thrC::PspoIIIA1-spoIIIAC-K30A-AD*	This study
JMB132	*ΔspoIIIAC-AD thrC::PspoIIIA1-spoIIIAC-K31A-AD*	This study
JMB133	*ΔspoIIIAC-AD thrC::PspoIIIA1-spoIIIAC-E32A-AD*	This study
JMB158	*ΔspoIIIAC-AD thrC::PspoIIIA1-spoIIIAC-L56A-AD*	This study
JMB159	*ΔspoIIIAC-AD thrC::PspoIIIA1-spoIIIAC-K61A-AD*	This study
JMB160	*ΔspoIIIAC-AD thrC::PspoIIIA1-spoIIIAC-AD-Y69A*	This study
JMB161	*ΔspoIIIAC-AD thrC::PspoIIIA1-spoIIIAC-AD-T72A*	This study
JMB134	*ΔspoIIIAC-AD thrC::PspoIIIA1-spoIIIAC-AD-K75A*	This study
JMB135	*ΔspoIIIAC-AD thrC::PspoIIIA1-spoIIIAC-AD-D92A*	This study
JMB136	*ΔspoIIIAC-AD thrC::PspoIIIA1-spoIIIAC-AD-E103A*	This study
RL2040	*ΔspoIIIAE*	R. Losick
JMB103	*ΔspoIIIAE thrC::PspoIIIA1-spoIIIAE*	This study
JMB213	*ΔspoIIIAE thrC::PspoIIIA1-spoIIIAE-K109A*	This study
JMB254	*ΔspoIIIAE thrC::PspoIIIA1-spoIIIAE-Q125A*	This study
JMB300	*ΔspoIIIAE thrC::PspoIIIA1-spoIIIAE-F131A*	This study
JMB255	*ΔspoIIIAE thrC::PspoIIIA1-spoIIIAE-Y145A*	This study
JMB301	*ΔspoIIIAE thrC::PspoIIIA1-spoIIIAE-F156A*	This study
JMB214	*ΔspoIIIAE thrC::PspoIIIA1-spoIIIAE-H157A*	This study
JMB256	*ΔspoIIIAE thrC::PspoIIIA1-spoIIIAE-S193A*	This study
JMB257	*ΔspoIIIAE thrC::PspoIIIA1-spoIIIAE-Q213A*	This study
JMB215	*ΔspoIIIAE thrC::PspoIIIA1-spoIIIAE-R246A*	This study
JMB162	*ΔspoIIIAE thrC::PspoIIIA1-spoIIIAE-D275A*	This study
JMB302	*ΔspoIIIAE thrC::PspoIIIA1-spoIIIAE-R280A*	This study

JMB163	*ΔspoIIIAE thrC::PspoIIIA1-spoIIIAE-T281A*	This study
JMB164	*ΔspoIIIAE thrC::PspoIIIA1-spoIIIAE-K283A*	This study
JMB303	*ΔspoIIIAE thrC::PspoIIIA1-spoIIIAE-D299A*	This study
JMB165	*ΔspoIIIAE thrC::PspoIIIA1-spoIIIAE-S308A*	This study
JMB343	*ΔspoIIIAE thrC::PspoIIIA1-spoIIIAEΔ273-309*	This study
JMB166	*ΔspoIIIAE thrC::PspoIIIA1-spoIIIAE-K312A*	This study
JMB216	*ΔspoIIIAE thrC::PspoIIIA1-spoIIIAE-K333A*	This study
JMB304	*ΔspoIIIAE thrC::PspoIIIA1-spoIIIAE-Q349A*	This study
JMB205	*ΔspoIIIAE thrC::PspoIIIA1-spoIIIAE-C121S*	This study
JMB206	*ΔspoIIIAE thrC::PspoIIIA1-spoIIIAE-C325S*	This study
JMB207	*ΔspoIIIAE thrC::PspoIIIA1-spoIIIAE-C359S*	This study
JMB217	*ΔspoIIIAE thrC::PspoIIIA1-spoIIIAE-C121S-C325S-C359S (Cys-less)*	This study

Table 4. Predicted transmembrane segments of SpoIIIAB, SpoIIIAC, SpoIIIAD, and SpoIIIAE

Protein	MEMSAT	TMHMM	TopPred	TMpred	HMMTOP
SpoIIIAB	(out) 8-25	none	(out) 1-21, 151-171	(in) 1-19, 154-171	(out) 4-20, 154-170
SpoIIIAC	(in) 7-25, 36-53	(in) 7-24, 34-53	(in) 5-25, 33-53	(in) 7-25, 33-53	(in) 7-25, 36-53
SpoIIIAD	(out) 7-23, 30-46, 67-83, 108-126	(out) 5-22, 29-50, 65-87, 108-130	(out) 3-23, 27-47, 106-126	(out) 5-22, 29-46, 67-83, 108-126	(out) 5-22, 29-46, 59-83, 108-132
SpoIIIAE	(in) 110-127, 139-160, 173-197, 215-232, 248-266, 317-339, 367-391	(in) 104-126, 141-160, 173-195, 210-232, 244-266, 317-339, 367-389	(in) 4-24, 108-128, 139-159, 169-189, 214-234, 248-268, 313-333, 343-363, 370-390	(out) 4-22, 110-128, 139-160, 173-197, 212-232, 248-266, 314-332, 326-363, 366-385	(in) 104-127, 140-164, 171-195, 208-232, 249-273, 304-327, 334-358, 367-391

Table 5. Complementation of *spoIIIAB* deletion by mutant *spoIIIAB* alleles

Relevant genotype	Sporulation efficiency
Wild-type	0.76
ΔspoIIIAB	1.3×10^{-5}
ΔspoIIIAB thrC::spoIIIAB	0.87
ΔspoIIIAB thrC::spoIIIAB-R28A	0.91
ΔspoIIIAB thrC::spoIIIAB-Y48A	3.6×10^{-4}
ΔspoIIIAB thrC::spoIIIAB-L53A	5.7×10^{-5}
ΔspoIIIAB thrC::spoIIIAB-L132A	0.058
ΔspoIIIAB thrC::spoIIIAB-K153A	0.69

Table 6. Complementation of *spoIIIAC-spoIIIAD* deletion by mutant *spoIIIAC-spoIIIAD* alleles

Relevant genotype	Sporulation efficiency
Wild-type	0.76
ΔspoIIIAC-AD	8.3 X 10^{-5}
ΔspoIIIAC-AD thrC::spoIIIAC-AD	0.86
ΔspoIIIAC-AD thrC::spoIIIAC-K30A-AD	1.0
ΔspoIIIAC-AD thrC::spoIIIAC-K31A-AD	0.85
ΔspoIIIAC-AD thrC::spoIIIAC-E32A-AD	0.96
ΔspoIIIAC-AD thrC::spoIIIAC-L56A-AD	0.54
ΔspoIIIAC-AD thrC::spoIIIAC-K61A-AD	0.077
ΔspoIIIAC-AD thrC::spoIIIAC-AD-Y69A	0.96
ΔspoIIIAC-AD thrC::spoIIIAC-AD-T72A	1.0
ΔspoIIIAC-AD thrC::spoIIIAC-AD-K75A	4.8 X 10^{-5}
ΔspoIIIAC-AD thrC::spoIIIAC-AD-D92A	0.85
ΔspoIIIAC-AD thrC::spoIIIAC-AD-E103A	0.68

Table 7. Complementation of *spoIIIAE* deletion by mutant *spoIIIAE* alleles

Relevant genotype	Sporulation efficiency
Wild-type	0.74
ΔspoIIIAE	4.0×10^{-5}
ΔspoIIIAE thrC::spoIIIAE	0.87
ΔspoIIIAE thrC::spoIIIAE-K109A	0.83
ΔspoIIIAE thrC::spoIIIAE-Q125A	0.76
ΔspoIIIAE thrC::spoIIIAE-F131A	0.012
ΔspoIIIAE thrC::spoIIIAE-Y145A	1.0
ΔspoIIIAE thrC::spoIIIAE-F156A	0.054
ΔspoIIIAE thrC::spoIIIAE-H157A	1.0
ΔspoIIIAE thrC::spoIIIAE-S193A	0.98
ΔspoIIIAE thrC::spoIIIAE-Q213A	0.48
ΔspoIIIAE thrC::spoIIIAE-R246A	1.0
ΔspoIIIAE thrC::spoIIIAE-D275A	0.74
ΔspoIIIAE thrC::spoIIIAE-R280A	0.52
ΔspoIIIAE thrC::spoIIIAE-T281A	1.0
ΔspoIIIAE thrC::spoIIIAE-K283A	0.88
ΔspoIIIAE thrC::spoIIIAE-D299A	0.79
ΔspoIIIAE thrC::spoIIIAE-S308A	0.84
ΔspoIIIAE thrC::spoIIIAEΔ273-309	1.4×10^{-6}
ΔspoIIIAE thrC::spoIIIAE-K312A	0.86
ΔspoIIIAE thrC::spoIIIAE-K333A	0.026
ΔspoIIIAE thrC::spoIIIAE-Q349A	0.85
ΔspoIIIAE thrC::spoIIIAE-C121S	0.76
ΔspoIIIAE thrC::spoIIIAE-C325S	0.64
ΔspoIIIAE thrC::spoIIIAE-C359S	0.78
ΔspoIIIAE thrC::spoIIIAE-C121S-C325S-C359S (Cys-less)	0.40

REFERENCES

1. **Anagnostopoulos, C., and J. Spizizen.** 1961. Requirements for Transformation in Bacillus Subtilis. J Bacteriol **81:**741-746.

2. **Camp, A. H., and R. Losick.** 2009. A feeding tube model for activation of a cell-specific transcription factor during sporulation in Bacillus subtilis. Genes Dev **23:**1014-1024.

3. **Camp, A. H., and R. Losick.** 2008. A novel pathway of intercellular signalling in Bacillus subtilis involves a protein with similarity to a component of type III secretion channels. Mol Microbiol **69:**402-417.

4. **Cornelis, G. R.** 2006. The type III secretion injectisome. Nat Rev Microbiol **4:**811-825.

5. **Doan, T., C. Morlot, J. Meisner, M. Serrano, A. O. Henriques, C. P. Moran, Jr., and D. Z. Rudner.** 2009. Novel secretion apparatus maintains spore integrity and developmental gene expression in Bacillus subtilis. PLoS Genet **5:**e1000566.

6. **Hofmann, K., and W. Stoffel.** 1993. TMbase - A database of membrane spanning proteins segments. Biol Chem Hoppe-Seyler **374:**166.

7. **Jones, D. T., W. R. Taylor, and J. M. Thornton.** 1994. A model recognition approach to the prediction of all-helical membrane protein structure and topology. Biochemistry **33:**3038-3049.

8. **Macnab, R. M.** 2003. How bacteria assemble flagella. Annu Rev Microbiol **57:**77-100.

9. **Meisner, J., X. Wang, M. Serrano, A. O. Henriques, and C. P. Moran, Jr.** 2008. A channel connecting the mother cell and forespore during bacterial endospore formation. Proc Natl Acad Sci U S A **105:**15100-15105.

10. **Nilsson, J., B. Persson, and G. von Heijne.** 2000. Consensus predictions of membrane protein topology. FEBS Lett **486:**267-269.

11. **Py, B., L. Loiseau, and F. Barras.** 2001. An inner membrane platform in the type II secretion machinery of Gram-negative bacteria. EMBO Rep **2:**244-248.

12. **Serrano, M., F. Vieira, C. P. Moran, Jr., and A. O. Henriques.** 2008. Processing of a membrane protein required for cell-to-cell signaling during endospore formation in Bacillus subtilis. J Bacteriol **190:**7786-7796.

13. **Sobczak, I., and J. S. Lolkema.** 2005. Structural and mechanistic diversity of secondary transporters. Curr Opin Microbiol **8:**161-167.

14. **Soding, J.** 2005. Protein homology detection by HMM-HMM comparison. Bioinformatics **21:**951-960.

15. **Soding, J., A. Biegert, and A. N. Lupas.** 2005. The HHpred interactive server for protein homology detection and structure prediction. Nucleic Acids Res **33:**W244-248.

16. **Sonnhammer, E. L., G. von Heijne, and A. Krogh.** 1998. A hidden Markov model for predicting transmembrane helices in protein sequences. Proc Int Conf Intell Syst Mol Biol **6:**175-182.

17. **Thompson, J. D., D. G. Higgins, and T. J. Gibson.** 1994. CLUSTAL W: improving the sensitivity of progressive multiple sequence alignment through

sequence weighting, position-specific gap penalties and weight matrix choice. Nucleic Acids Res **22:**4673-4680.

18. **Tusnady, G. E., and I. Simon.** 1998. Principles governing amino acid composition of integral membrane proteins: application to topology prediction. J Mol Biol **283:**489-506.

19. **von Heijne, G.** 1992. Membrane protein structure prediction. Hydrophobicity analysis and the positive-inside rule. J Mol Biol **225:**487-494.

20. **Yernool, D., O. Boudker, Y. Jin, and E. Gouaux.** 2004. Structure of a glutamate transporter homologue from Pyrococcus horikoshii. Nature **431:**811-818.

CHAPTER 6. General Discussion

The data presented here support a new model for understanding the mechanisms that control late forespore transcription and the transition from forespore engulfment to forespore maturation. During forespore engulfment, the mother cell protein integral SpoIIIAH recognizes the mother cell-forespore interface by interacting with the degenerate LytM domain of the forespore integral membrane protein SpoIIQ (1, 6). Once anchored at the mother cell-forespore interface, the YscJ domain of SpoIIIAH drives the formation of a channel that connects the mother cell and forespore (3, 7). This channel then anchors other mother cell integral membrane protein subcomplexes at the cell-cell interface. One of these subcomplexes, consisting of SpoIIIAB, SpoIIIAC, SpoIIIAD, SpoIIIAE, SpoIIIAF, and SpoIIIAG (4), assembles within the channel and functions as an export apparatus which moves its as yet unidentified substrate from the mother cell to the forespore. SpoIIIAA converts the chemical energy of ATP hydrolysis into conformational changes in the integral membrane components which drive movement of the substrate through the exporter. This exported substrate then activates σ^G which controls late forespore gene expression and the transition to forespore engulfment.

While this model is attractive in many respects, it also generates several unanswered questions. The exporter model is based on the observation that SpoIIIAH is remotely homologous to the ring-forming proteins which serve as the structural scaffold for the assembly of the type III export apparatus (3, 7). We and others provided evidence

that support the exporter model (2-4, 7), but the structural basis of the model needs to be validated. In other words, an X-ray crystal structure of SpoIIIAH needs to be solved to confirm the presence of the ring-forming domain. Concomitant with our biochemical studies with SpoIIIAH and SpoIIQ, we attempted to crystallize the full-length proteins alone and in the complex. Although we screened hundreds of crystallization conditions, we were unable to grow protein crystals. One explanation for this problem is that each of the two proteins contains flexible regions that interfere with the symmetric packing of the proteins necessary for crystallization. Indeed, SpoIIIAH contains an N-terminal region that lacks predicted secondary structure, in addition to its putative ring-forming YscJ domain. SpoIIQ contains a central LytM domain flanked by N- and C-terminal extensions. Because each of these regions is dispensable for the formation of the SpoIIIAH-SpoIIQ complex, the truncated proteins that lack these regions (SpoIIIAH90-218 and SpoIIQ73-220) are excellent candidates for new crystallization trials.

In addition to validating the YscJ domain of SpoIIIAH, an X-ray crystal structure of the SpoIIIAH90-218 – SpoIIQ73-220 complex would also help explain the structural basis for SpoIIIAH-SpoIIQ recognition. One possibility is that SpoIIIAH recognizes SpoIIQ by interacting within the central groove of its LytM domain. In parallel with X-ray crystallography, the LytM groove model for SpoIIIAH-SpoIIQ recognition could be tested using chemical modification. If SpoIIIAH interacts with SpoIIQ within its LytM groove, then the accessibility to chemical modification of the residues that line the groove may be blocked by SpoIIIAH. Several methods chemically modify cysteine residues of proteins by reduction or alkylation. Because SpoIIQ is devoid of cysteine

residues, the accessibility of cysteines substitutions in the LytM groove could be determined. Free sulfhydryls, such as those of cysteine, can be measured with 5,5'-diothio-bis-(2-nitrobenzoic acid), also called Ellman's reagent (5). Because the LytM active site is located at one end of the central groove, the degenerate active site residues of SpoIIQ (S119 and S169) may be good candidates for cysteine substitution. Alanine substitutions at these positions did not affect the ability of SpoIIIAH to recognize SpoIIQ *in vivo*, indicating that neither residue is necessary for function (2). Cysteine substitutions should not cause any steric effects that might disrupt the complex as the side chains of serine and cysteine are similar in size. This biochemical approach can be used not only to test whether SpoIIIAH-SpoIIQ recognition occurs in the LytM groove, but also to probe any other protein-protein interface determined by X-ray crystallography.

Another unanswered question about the exporter model is how the other SpoIIIA proteins interact with the SpoIIIAH-SpoIIQ complex. The structure of the SpoIIIAH-SpoIIQ complex would guide the study of how these proteins interact with the complex. Presumably one or more of these proteins interact with the protein surfaces that are accessible in the complex. Directed mutations of these surfaces may disrupt the protein-protein interactions and reduce the ability of the mutant proteins to support efficient sporulation. If so, such mutants could be used to isolate extragenic suppressors which may identify proteins that directly interact with the SpoIIIAH-SpoIIQ complex. As described earlier, many of the SpoIIIA proteins are integral membrane proteins which lack extracellular domains capable of interacting with the SpoIIIAH-SpoIIQ

complex. Only SpoIIIAG contains a predicted extracellular domain, but this domain does not interact with the SpoIIIAH extracellular domain, the SpoIIQ extracellular domain, or the complex (6). One possibility is that the SpoIIIA subcomplex interacts with the transmembrane segment (TMS) of SpoIIIAH. If this were the case, then replacing the native TMS of SpoIIIAH with one from an unrelated protein would disrupt the interaction. The localization of a GFP-tagged SpoIIIAG to the mother cell-forespore interface is disrupted by an in-frame deletion of *spoIIIAH* (4). If the native TMS is necessary for the interaction with SpoIIIAG, then the chimeric *spoIIIAH* would not complement the localization defect of the *spoIIIAH* deletion. Furthermore, mutations in either the unrelated TMS of the chimera or the interacting protein would restore the interaction and localization of SpoIIIAG. Such suppressor mutations could be isolated if they restore the sporulation efficiency of the strain. Ultimately, this approach may aid in understanding the assembly of the SpoIIIA proteins, as well as the other protein subcomplexes anchored at the mother cell-forespore interface.

The most difficult question about the exporter model is the identity of the exported substrate. Reasonable arguments can be made to support the translocation of a metabolite or polypeptide. The metabolite substrate model is supported by the observation that the SpoIIIAH-SpoIIQ complex is necessary for σ^G, prolonged σ^F (in a *sigG* mutant), and even T7 polymerase activity in the forespore (2). This suggests that the exported substrate is necessary to maintain the metabolic capacity of the forespore, rather than to specifically activate σ^G. The SpoIIIAH-SpoIIQ complex is also necessary to maintain the integrity of forespore, further supporting the metabolite substrate model

(4). While the general effects of the SpoIIIAH-SpoIIQ complex can be interpreted to support this model, they are not inconsistent with a polypeptide substrate model. For example, any essential enzyme which becomes limiting in the forespore could be the translocated substrate. If the substrate is an essential enzyme, this would explain why genetic screens have failed to identify the gene which encodes the substrate. Genetics screens may also miss the gene if it encoded a small peptide. Furthermore, bioinformatics analysis of the SpoIIIA proteins indicates similarities to components of several protein export systems. Finally, while these models describe a substrate which is exported from the mother cell to the forespore, the substrate may instead be moved from the forespore to the mother cell. Consistent with the general effects of the SpoIIIAH-SpoIIQ complex, the substrate may accumulate, become detrimental to the forespore, and need to be removed. A description of the nature of substrate, including the direction of its movement, will be critical to understanding how the transition from forespore engulfment to forespore maturation is controlled.

The exporter model explains how forespore engulfment is necessary for the functions of the SpoIIIA proteins and SpoIIQ, but it does not describe how these functions are coordinated with the completion of engulfment. Prior to the onset of engulfment, the septal peptidoglycan which separates the mother cell and forespore prevents the formation of the SpoIIIAH-SpoIIQ complex. When engulfment begins this peptidoglycan is removed, allowing the formation of the complex and assembly of the other SpoIIIA proteins (1). Once assembled at the mother cell-forespore, the putative exporter would translocate its substrate and activate late forespore transcription. This

model does not describe a strict separation of morphological events. There may be an unanticipated overlap between forespore engulfment and forespore maturation, whereby maturation begins before engulfment is completed. The continued study of this protein junction will yield valuable insights into the mechanisms by which bacterial cell differentiation is controlled.

REFERENCES

1. **Blaylock, B., X. Jiang, A. Rubio, C. P. Moran, Jr., and K. Pogliano.** 2004. Zipper-like interaction between proteins in adjacent daughter cells mediates protein localization. Genes Dev **18:**2916-2928.
2. **Camp, A. H., and R. Losick.** 2009. A feeding tube model for activation of a cell-specific transcription factor during sporulation in Bacillus subtilis. Genes Dev **23:**1014-1024.
3. **Camp, A. H., and R. Losick.** 2008. A novel pathway of intercellular signalling in Bacillus subtilis involves a protein with similarity to a component of type III secretion channels. Mol Microbiol **69:**402-417.
4. **Doan, T., C. Morlot, J. Meisner, M. Serrano, A. O. Henriques, C. P. Moran, Jr., and D. Z. Rudner.** 2009. Novel secretion apparatus maintains spore integrity and developmental gene expression in Bacillus subtilis. PLoS Genet **5:**e1000566.
5. **Ellman, G. L.** 1959. Tissue sulfhydryl groups. Arch Biochem Biophys **82:**70-77.
6. **Meisner, J., and C. P. Moran, Jr.** 2010. A LytM domain dictates the localization of proteins to the mother cell-forespore interface during bacterial endospore formation. J Bacteriol.
7. **Meisner, J., X. Wang, M. Serrano, A. O. Henriques, and C. P. Moran, Jr.** 2008. A channel connecting the mother cell and forespore during bacterial endospore formation. Proc Natl Acad Sci U S A **105:**15100-15105.